Potential applications of confocal Raman spectroscopy in ophthalmology

Potential applications of confocal Raman spectroscopy in ophthalmology

ISBN 90 5278 263 6

Layout en druk: Datawyse | Universitaire Pers Maastricht

Potential applications of confocal Raman spectroscopy in ophthalmology

Proefschrift

ter verkrijging van de graad van doctor
aan de Universiteit Maastricht,
op gezag van de Rector Magnificus,
Prof. dr A.C. Nieuwenhuijzen Kruseman,
volgens het besluit van het College van Decanen,
in het openbaar te verdedigen
op vrijdag 17 december 1999 om 10.00 uur

door

Noël Jozef Catharinus Bauer
geboren op 11 november 1968 te Heerlen

UM
UNIVERSITAIRE PERS MAASTRICHT

Promotores

Prof. dr F. Hendrikse
Prof. dr W.F. March (University of Texas Medical Branch, Galveston, Texas)

Co-promotoren

Dr. M. Motamedi (University of Texas Medical Branch, Galveston, Texas)
Dr. ir G.J. Puppels (Erasmus Universiteit Rotterdam)

Beoordelingscommissie

Prof. dr H.A.J. Struijker-Boudier (voorzitter)
Prof. dr W.Th. Hermens
Prof. dr A. Persoons (Universiteit van Leuven)
Prof. dr F. Spaans
Dr. ir D. Sterenborg (Erasmus Universiteit Rotterdam)

This work was performed at the ophthalmic division of the Biomedical Laser and Spectroscopy Program of the Department of Ophthalmology (Professor W.F. March, MD) at the University of Texas Medical Branch, Galveston, Texas, USA, and was sponsored in part by a grant from the Department of Energy (DOE-FG03-95ER61971), a Research to Prevent Blindness Development grant, and a Research to Prevent Blindness Unrestricted grant.

To my loving wife Elaine
and my son Brandon
In loving memory of my mother

Contents

CHAPTER 1

Introduction

General

The eye, as the sensory organ of vision, has a tissue composition optimal for its main function of transmission, refraction and detection of light.[1] Because of its function and delicate anatomy, the eye does not easily allow for invasive diagnostic procedures. Ophthalmology therefore has to its disposal a wide variety of non-invasive diagnostic techniques which by definition do not lead to additional cell damage of the ocular tissues or the regions around the eye.[2] Non-invasive procedures include non-contact or remote sensing techniques (i.e. fundoscopy, refractometry, keratometry, slitlamp biomicroscopy, specular microscopy, optical coherent tomography, fluorophotometry), contact or marginally invasive techniques (i.e. ultrasonography, tonometry, pachymetry), and parainvasive techniques, in which a non-invasive observation in the eye is performed after an invasive procedure elsewhere (i.e. fluorescein angiography, indocyanine green angiography).[2] The aforementioned techniques lack the ability to provide specific information on the biochemical properties of ocular tissues. Biochemical information, however, is of clinical importance, since numerous physiological and pathological processes and therapeutic as well as diagnostic interventions have significant effects on the biochemical composition of the eye.[3]

The biochemistry of the eye can be influenced by physiological, degenerative, metabolic, inflammatory, toxicological, and neoplastic processes, as well as through iatrogenic interventions, such as topical drug application.

Corneal hydration control is an example of a physiological process involving biochemical changes. The water content of the corneal stroma is actively regulated by means of the endothelial pumpmechanism, and this is crucial for the transparency of the cornea.[4,5] Corneal dystrophies are characterized by functional and morphologic abnormalities resulting in progressive corneal opacification, which can lead to loss of vision. Many forms of corneal dystrophy have been described, and can be classified as epithelial, stromal, or endothelial.[6] Prevention of vision loss needs early and accurate diagnosis of the disease state, including corneal thickness measurements and slitlamp examination.[7] The various different corneal dystrophies suggest differences in the underlying pathology, possibly expressed in the biochemistry.

Cataractogenesis is a pathophysiological process of the crystalline lens, which involves biochemical changes that seem to be pathognomic for this degenerative disorder. Apart from the underlying causes, opacification occurs following disturbance of the ordered packing of the lens crystallins, induced by changes in hydration, aggregate formation of lens proteins, and vacuole formation within the lens fibers.[8] These morphologic changes need a quantitative measurement of the biochemical composition with high spatial resolution.

Metabolic disorders are usually systemic in nature and can possibly also manifest themselves through local ocular biochemical alterations. In uncontrolled insulin dependent diabetes mellitus (IDDM), the level of glucose in the aqueous humor correlates with that of the blood.[9,10] Many investigators have focussed on the non-invasive detection of glucose in the eye, with the objective of developing a real-time 'closed loop' system for control of the blood glucose level.[9,10,11]

A breakdown of the blood-aqueous barrier during inflammation of the eye (uveitis) involves elevated levels of cells and proteins in the aqueous humor and vitreous. Recently, a non-invasive Helium-Neon laser based cell- and flare meter was developed and applied clinically for diagnostic purposes of uveitis.[12] Although highly sensitive, no specific information about the proteins involved is obtained which could possibly be of additional value in the diagnosis and follow-up this diseased state.

Local ocular biochemical changes can also occur due to elevated levels of potentially toxic substances in the blood (i.e. excitatory amino-acids in inborn errors of metabolism, endotoxins) with initially no obvious detrimental effect to the eye, but which can potentially be detected utilizing a non-invasive technique for biochemical assessments in the aqueous humor.[13]

The detection of biochemical changes due to neoplastic alterations of tissues using tumor specific markers is applied in the diagnosis, treatment and follow-up of various cancers (prostate, breast, lung).[14] Although the overall incidence of ocular tumors is relatively low, neoplasia have been documented for all tissues in the eye (pigmented and nonpigmented epithelial, muscular, nervous, vascular, fibroadipose, connective, lymphoid and glandular tissues), and non-invasive biochemical analysis could provide the information needed for early diagnosis and treatment of the specific tumor.

Lastly, surgical interventions[15] and topical ocular drug delivery[16] can cause detectable biochemical changes, whether desirable or not. An impending corneal graft rejection after a penetrating keratoplasty (PKP) could be detected by assessing the water content of the cornea well in advance of clinically objective changes in the corneal morphology. Furthermore, it could be useful to assess the corneal uptake of a topical ocular drug in order to test its efficacy, or to assess whether or not the concentration of an intraocular depot drug (Ganciclovir implant) is still at a therapeutic level.

In the light of the aforementioned, it is worthwhile to perform qualitative and quantitative detection of ocular biochemical changes prior to therapeutic interventions and during follow-up of a disease. The application of a successful non-invasive biochemical analytical technique could also increase our understanding of normal physiological processes in the eye.[17] This is analog to the assessment of biochemical parameters in various readily accessible other tissues (blood, urine, feces, saliva).

Aim of the thesis

The aim of this thesis was to investigate the potential application of a novel optical sectioning technique utilizing Raman spectroscopy for non-contact biochemical assessments of (intra)ocular tissues and fluids of the intact eye under *in vivo* circumstances.

Theoretical aspects

Raman spectroscopy (RS) is a powerful optical technique for biochemical assessments, and utilizes the Raman phenomenon which occurs when light interacts with molecules. Incident light from a sample is mostly scattered elastically, i.e. without energy transfer between light and matter. Raman scattering on the other hand is the small fraction of light that is scattered inelastically due to the transfer of energy between photons of the incident light and molecules, on the molecular vibrational level. The change in photon energy (E) equals the change in molecular vibrational energy, which is inherently specific for the molecular bond involved, and results in a change in photon frequency ν, since $E=h\nu$ (h=Planck's constant). Utilizing spectroscopy these frequency changes are spatially resolved into a spectrum depicting Raman bands with a certain intensity and Raman (frequency) shift position (in wavenumber or cm^{-1}), over a certain wavenumber region. Each band can be assigned to a known molecular vibrational mode and spectral analysis provides qualitative and quantitative information on the molecular content and conformation.

Advantageous characteristics of RS include its inherent high specificity, the ability to assess solids, liquids and gases, and the remote sensing capability which reduces probing artifacts. On the other hand the low Raman yield (only 10^{-4} to 10^{-6} of the scattered light is Raman scattering) usually requires the use of high incident light energies for an adequate spectral signal-to-noise ratio. A typical Raman spectroscopy system consists of a monochromatic light source (a laser), focusing and collecting optics, a spectrometer, and a photon counting device. In

Chapter 2 a detailed outline of the principles and practice of Raman spectroscopy is given.

Practical aspects

Raman spectroscopy has been applied in the past in every aspect of biochemistry, from the biochemical characterization of nucleic acids and related compounds, amino-acids, polypeptides, proteins, lipids and cellular membranes, carbohydrates, and bacteria and viruses, to the application of Raman spectroscopy in biology and medicine for the study of cells, tissues and even whole organs.[18,19]

Applications of Raman spectroscopy in ophthalmology have mainly focused on the elucidation of the process of cataract formation,[20] although applications for biochemical analysis of the cornea[21], aqueous humor[13,17], vitreous humor[22], and the retinal pigments have also been suggested.[23] Most of these studies have been performed under *in vitro* conditions, because of significant limitations in the proposed RS systems for probing the intact eye *in vivo*.

First, the inherently weak Raman signals require tissue samples to be exposed to high doses of laser light for prolonged periods of time in order to achieve an adequate signal-to-noise ratio. Thus, light induced damage to the ocular tissues in general and the retina in specific is likely to occur, limiting safe application of RS in the living intact eye (see below).

Secondly, the heterogeneous nature of the ocular tissues can significantly contribute to the occurrence of strong fluorescence masking most of the Raman signals. This event is generally minimized through the use of thin tissue preparations which, apart from the likely occurrence of artifacts, excludes *in vivo* application of RS in the eye by definition.

Lastly, most of the proposed Raman spectroscopic techniques in ophthalmology usually lack adequate resolution in time, essential for reducing movement artifacts in living specimens, and spatial resolution, essential for optical sectioning through laminated ocular tissues. In the latter part of Chapter 2 the design considerations are outlined for a suitable Raman spectroscopy system for ophthalmic use *in vivo*.

Optical aspects

The key factors for the successful application of Raman spectroscopy for the non-invasive assessment of biochemical parameters in the eye are: adequate working distance (i.e. an objective lens capable of probing superficial as well as deeper ocular tissues in a non-contact manner), high sensitivity (high

signal-to-noise ratio spectra without interfering signals from nearby tissues), high specificity (inherent to Raman spectroscopy), adequate spatial resolution for optical sectioning, temporal resolution for rapid spectral acquisition, and safety. Chapter 3 describes the details and performance of such a system in the form of a laser confocal Raman spectroscopy (CRS) system. Spatial resolution and reduction of fluorescence interference was achieved using confocal optics (see Figure 1) effectively reducing light from out of focus places, thus increasing the signal-to-noise ratio, while decreasing the actual probing volume at the expense of the absolute Raman signal. Since interchangeable fiber-optics were used as the 'confocal pinhole', the thickness of the optical sections could be adjusted from 20-900 μm. High sensitivity was guaranteed by using a microscope objective lens both for focusing the laser light onto the sample as well as collecting it, in conjunction with a highly sensitive CCD-camera as a photon counting device. The microscope objective lens (LDMO) ensured an adequately long working distance of ~13 mm and a high numerical aperture (solid angle of acceptance) of NA=0.5. This lens could be moved along its optical axis without changing its focal distance, thus enabling axial probing of static objects, and permitted probing of the cornea, aqueous humor, the ocular lens, and the anterior vitreous humor, while projecting a large defocused spot onto the retina of ~2 cm in diameter, irrespective of the probing depth (0-11 mm) into the eye. This is depicted in graphical format in Figure 2. At a given power setting the defocused spotsize is safer than a focused spot. For example, a collimated light beam (NA=0) from a 1 mW laser will focus to a spotsize of ~15 μm, yielding a retinal irradiance of ~650 W/cm^2, while the same laser utilizing the high NA LDMO would yield a retinal irradiance of ~0.3 mW/cm^2. Since the reduction of light load was an important issue in this thesis, this system as a whole was designed with the eye on maximum signal collection, throughput and detection.

Although the proposed CRS system has various advantageous characteristics, as described, true non-invasive application of this novel optical technique for clinical diagnosis in the living eye will highly depend on its safety. This means that the exposure to laser light should not damage the ocular tissues. Since the ocular media are transparent to light with a wavelength between 400 and 1400 nm, retinal exposure becomes the limiting factor when using a visible lightsource (400-700 nm). Prolonged exposure of light to the retina can lead to either thermal or photochemical damage and is wavelength dependent. Below 500 nm predominantly photochemical damage occurs, as a result of the absorption of light in the photopigments and the retinal pigment epithelial layer (RPE). Above 600 nm mainly thermal damage ensues when the temperature increase is >20°C causing proteins to denature. Between 500 and 600 nm, thermally enhanced photochemical damage may occur. Thus, the retinal irradiance (in mW/cm^2) should stay within certain limits to guarantee retinal safety. For

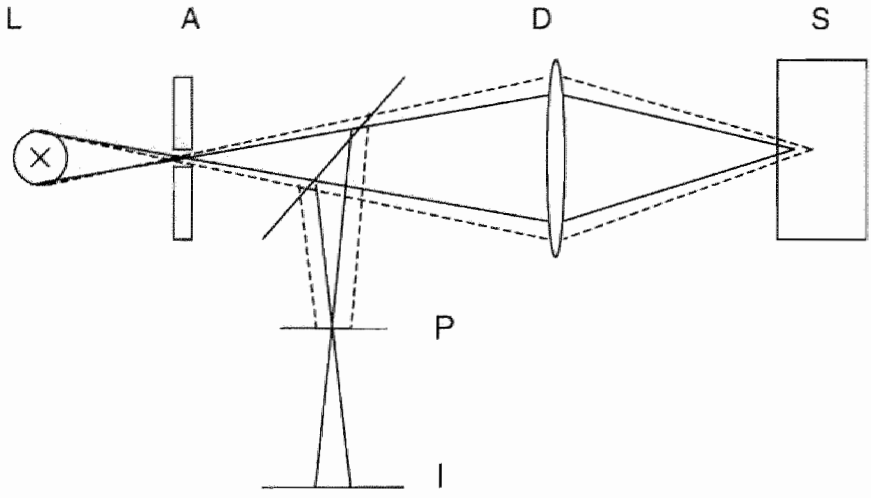

Figure 1. Principles of confocal optics. Light from out of focus places (dashed rays) are blocked by the pinhole (P) and are not imaged. L = light source, A = aperture, D = positive lens, S = sample, I = image plane.

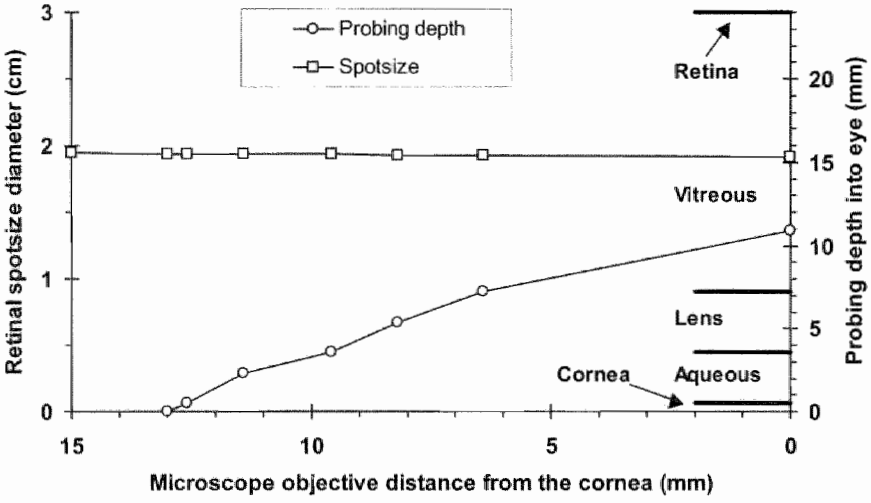

Figure 2. Relationship between the microscope objective distance (NA=0.5) from the cornea (0-13 mm) and both the retinal spotsize diameter as well as the probing depth into the eye (emmetropic non-accomodated Gullstrand-Littman model-eye with a pupil size larger than the diameter of the light-beam).

lasers these limits are given by the maximum permissible exposure (MPE) as set forth by the ANSI Standard for the Safe Use of Lasers.[24] These MPE-values are dependent on the wavelength, energy (J), exposure duration (s), and retinal spotsize diameter. In general, for continuous wave lasers at a given wavelength in the visible range, it can be stated that the longer the exposure time and the larger the retinal spotsize, the lower the maximum permissible retinal irradiance (in mW/cm^2). The latter dependence can be explained through the fact that in larger retinal spotsizes (>10 μm), the radial dissipation of heat becomes negligible, effectively decreasing the threshold for retinal damage (Figure 3). In Figure 4, the maximum permissible retinal irradiance for visible light as a function of both the exposure time as well as the retinal spotsize is depicted in graphical format. The retinal irradiance at the normal range of operation of the laser confocal Raman spectroscopy system (5-8 mW/cm^2) is also outlined. In addition to this, Table 1 depicts the retinal irradiances of various common lightsources as well as some frequently used ophthalmic equipment. It can be seen that the normal mode of operation of the CRS is in the blue light hazard range. However, high signal-to-noise ratio Raman spectra could be recorded utilizing the proposed confocal Raman spectroscopy technique at a significantly reduced light load when compared to other studies, thus yielding the possibility to perform *in-vivo* animal studies.

The applications

Chapter 4 provides an overview of the *in vivo* animal (pilot)studies performed and describes the potential applications of confocal Raman spectroscopy in ophthalmology. The following chapters will deal in more detail with these applications.

The application of confocal Raman spectroscopy for the non-contact assessment of the normal extent and distribution of corneal hydration in the anesthetized rabbit is discussed in Chapter 5. In Chapter 6, confocal Raman spectroscopy is utilized for the non-contact assessment of changes in corneal hydration following topical application of a dehydrating agent in two legally blind patients. Chapter 7 reports on the application of confocal Raman spectroscopy for the non-contact assessment of the drug transport into the cornea. The feasibility of CRS to perform remote temperature measurements in the eye is described in Chapter 8.

Lastly, the summary describes what has been accomplished with this project and contains suggestions for future improvements in order to increase the impact of Raman spectroscopy as a clinical diagnostic tool in ophthalmology. Although most studies have dealt with animal experiments, one of the consistent features was the minimization of the amount of light needed to obtain an

Figure 3. Heat transfer in the retina during irradiation with visible light. In a small spot (<10 µm diameter), [A], heat can dissipate in all directions. In larger spot sizes, [B], dissipation of heat in the radial direction becomes negligible, effectively decreasing the threshold level for thermal damage to the retina. I.e., if 10 mW/cm^2 would be the maximum safe irradiation level in situation [A], this would not be safe in situation [B].

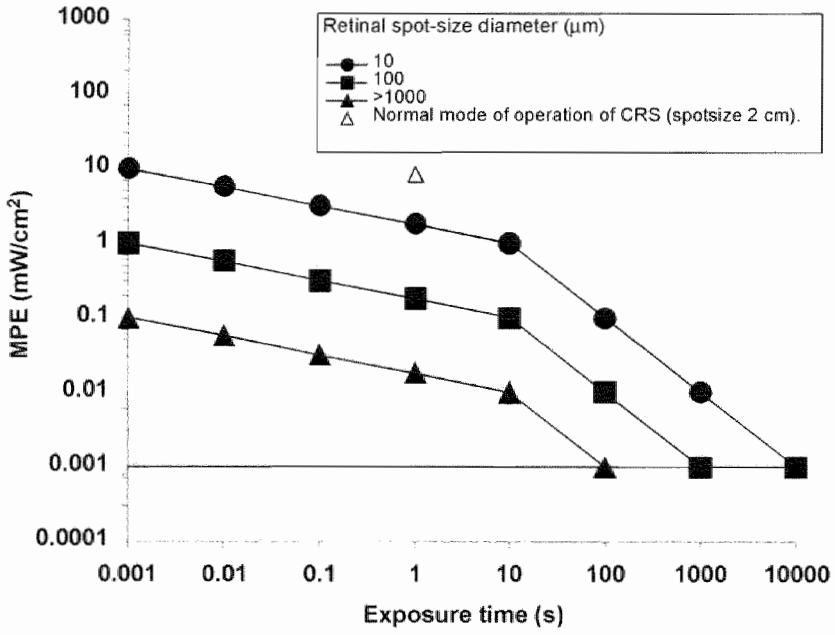

Figure 4. Maximum permissible retinal irradiance (MPE; mW/cm^2) to the retina of laser-light (400-550 nm) as a function of exposure time (s) and retinal spot-size diameter. Typical mode of operation of CRS (open triangle) is: 1 s. exposures with 25 mW on retinal spotsize of 3 cm^2. Horizontal line is the normal retinal irradiance caused by a TV-set or 1/10th the retinal irradiance of a candle.

Table 1. Retinal irradiance levels for continuous exposure to various lightsources.

Light source	Retinal irradiance (mW/cm^2)
Daylight (inside)	0.0001
TV	0.001
Daylight (outside)	0.001-0.1
Candle	0.01
Lightbulb	0.1
Blue light hazard	0.1-1000
Firework flash	1
The sun	10^4
1 mW laser	10^6
Overhead surgical lamps	24
Indirect ophthalmoscopy	70
Slit lamp biomicroscopy	210
Surgical operating microscope	460
Typical operating mode CRS*	~8

*Short expsosure (<10 s.).

acceptable signal, in order to increase the safety and applicability of this optical technique in the human eye. In future we expect to direct this research to a truly non-invasive Raman spectroscopy technique suitable for *in vivo* diagnostic purposes in patients suffering from eye diseases.

References

1. Forrester JV, Dick AD, McMenamin P, and Lee WR, Eds., Anatomy of the Eye. In: *The Eye; Basic Sciences in Practice*, Saunders, London (1996), pp. 13-86.
2. Masters BR, Ed., *Noninvasive Diagnostic Techniques in Ophthalmology*, Springer-Verlag, New-York (1990).
3. Berman ER, Ed., *Biochemistry of the Eye*, Plenum Press, New York (1991).
4. Davson H. The Hydration of the Cornea. *Biochem. J.* 1955; 59: pp. 24-28.
5. Maurice DM. The Cornea and Sclera. In: Davson H, Ed., *The Eye*, 3rd edition. Academic Press Inc., Orlando (1984), Vol 1b: pp. 1-158.
6. Kanski JJ. Disorders of the Cornea and Sclera. In: Kanski JJ, Ed., *Clinical Ophthalmology*, 1st edition. The C V Mosby Co., St. Louis (1984), pp. 5.1-5.34.
7. Polse KA, Brand RJ, Vastine DW, et al. Clinical Assessment of Corneal Hydration Control in Fuchs' Dystrophy. *Optom. Vis. Sci.* 1991; 68(11): pp. 831-841.
8. Forrester JV, Dick AD, McMenamin P, and Lee WR, Eds., Biochemistry. In: *The Eye; Basic Sciences in Practice*, Saunders, London (1996), pp. 180-182.

9. Rabinovitch B, March WF, and Adams RL. Noninvasive Glucose Monitoring of the Aqueous Humor of the Eye: Part I. Measurement of Very Small Optical Rotations. *Diabetes Care* 1982; 5: pp. 254-258.
10. March WF, Rabinovitch B, and Adams RL. Noninvasive Glucose Monitoring of the Aqueous Humor of the Eye: Part II. Animal Studies and the Scleral Lens. *Diabetes Care* 1982; 5: pp. 259.
11. Cameron BD, and Cote GL. Noninvasive Glucose Sensing utilizing a Digital Closed-loop Polarimetric Approach. *IEEE Transactions on Biomedical Engineering* 1997; 44(12): pp. 1221-1227.
12. Sawa M, Tsurimaki Y, Tsuru T, and Shimizu H. New Quantitative Method to Determine Protein Concentration and Cell Number in Aqueous *in vivo*. *Jpn. J. Ophthalmol.* 1988; 32: pp. 132-142.
13. Erckens RJ, Motamedi M, Wicksted JP, and March WF. Raman Spectroscopy for Non-Invasive Characterization of Ocular Tissue: Potential for Detection of Biological Molecules. *Journal of Raman Spectroscopy* 1997; 28: pp. 293-299.
14. Damjanov I. Cell, tissue and organ specific tumor markers: an overview. *Curr. Top. Path.* 1987; 77: pp. 367-384.
15. Dougherty PJ, Wellish KL, and Maloney K. Excimer Laser Ablation and Corneal Hydration. *Am. J. Ophth.* 1994; 118: pp. 169-176.
16. Lee VHL. Precorneal, Corneal, and Postcorneal Factors. In: Mitra AK, Ed., *Ophthalmic Drug Delivery Systems*. Marcel Dekker, New York (1993): pp. 59-81.
17. Wicksted JP, Erckens RJ, Motamedi M, and March WF. Raman Spectroscopy Studies of Metabolic Concentrations in Aqueous Solutions and Aqueous Humor Specimens. *Applied Spectroscopy* 1995; 49(7): pp. 987-993.
18. Puppels GJ. Confocal Raman Spectroscopy: a new look at cells and chromosomes. Thesis. University Twente, The Netherlands. 1991.
19. Ozaki Y. Medical Application of Raman Spectroscopy. *Applied Spectroscopy Reviews* 1988; 24(3&4): pp. 259-312.
20. Huizinga A, Bot ACC, de Mul FFM, Vrensen GFJM, and Greve J. Local Variation in Absolute Water Content of Human and Rabbit Eye Lenses Measured by Raman Microspectroscopy. *Exp. Eye Res.* 1989; 48: pp. 487-469.
21. Siew DCW, Clover GM, Cooney RP, and Wiggins PM. Micro-Raman Spectroscopic Study of Organ Cultured Corneae. *J Raman Spectroscopy* 1995; 26: pp. 3-8.
22. Sebag J, Nie S, Reiser K, Charles MA, and Yu N-T. Raman Spectroscopy of Human Vitreous in Proliferative Diabetic Retinopathy. *Invest. Ophthalmol. Vis. Sci.* 1994; 35: pp. 2976-2980.
23. Bernstein PS, Yoshida MD, Katz NB, McClane RW and Gellermann W. Raman Detection of Macular Carotenoid Pigments in Intact Human Retina. *Invest. Ophthalmol. Vis. Sci.*1998; 39:2003-2011.
24. ANSI Standard American National Standards Institute. Safe Use of Lasers. In: *ANSI Standard Z136.1*, Laser Institute of America, Orlando, 1993.

CHAPTER 2

Raman spectroscopy

Theory of Raman scattering

When light interacts with a material, this usually results in elastic (Rayleigh) scattering of the incident light, i.e. without the exchange of energy between photons and material (Figure 1). Raman scattering on the other hand is the result of an inelastic light scattering process, in which an exchange of energy between photons and molecules in the material occurs. A Raman scattered photon will therefore have an energy that is different from the energy of the incident photon. Since photon energy is linearly related to photon frequency (Appendix; Formulas 1-3) when monochromatic light is incident onto the material, the spectrum of the scattered light will show lines at frequencies different from that of the incident light. In a Stokes-Raman scattering process a specific amount of energy is transferred from the photon to the molecule, thereby exciting a molecular vibration in this molecule. The amount of energy that is transferred depends on the molecular vibration that is excited. Thus, the assessment of the frequencies of Raman scattered light can be utilized to identify specific molecular vibrations. In applied Raman spectroscopy a spectrometer is used to spatially resolve these frequencies into a spectrum of vibrational modes, the so-called Raman spectrum. The peak *position* of a particular Raman line is depicted as the difference between the incident light frequency and the Raman scatter frequency ($\nu_0 \pm \nu_{vib}$), and is independent of the irradiation wavelength used. Raman scattering can either be the result of acceptance or transfer of photon-energy by the molecule, hence a decrease or increase in scattered light frequency, respectively (Appendix; Formula 4 and 5). The former is commonly represented by the so-called "Stokes lines" of a Raman spectrum with a frequency of $\nu_0 - \nu_{vib}$, while the latter are the "anti-Stokes lines" ($\nu_0 + \nu_{vib}$) (Figure 2). At room temperature the amount of molecules in the unexcited vibrational state is higher than molecules in excited vibrational states (Appendix; Formula 6). Consequently, more molecules will accept energy rather than transfer energy. Thus, in a typical Raman spectrum the Stokes lines are significantly more pronounced than the anti-Stokes lines, and in general the latter are omitted from a Raman spectrum. The Raman scatter *intensity* is linearly dependent on the concentration of the species of molecules giving rise to the Raman line, the intensity of the incident light, the frequency of the scattered

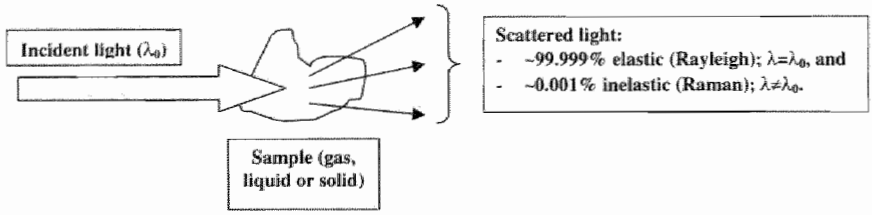

Figure 1. Elastic and inelastic (Raman) light scattering.

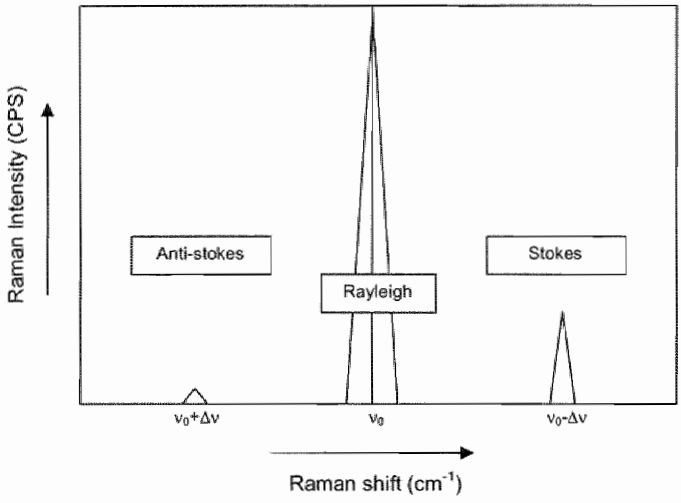

Figure 2. Principles of a Raman spectrum (see text voor details).

light to the fourth power and the molecular polarizability to the second power (Appendix; Formula 7).

Principles of applied Raman spectroscopy

In essence, Raman spectroscopy yields information on intramolecular chemical bonds and the interaction of molecules with their direct environment. Various advantageous characteristics make this technique suitable for biochemical analysis of biological media. The inherent specificity of Raman scattering yields the possibility to identify entire biomolecules at once. Furthermore, the *dynamics* of processes involving biochemical changes in living material can be

studied with time-resolved (nano- or even pico-second) Raman spectroscopy since Raman scattering occurs very fast (~10^{-16} s). In addition, the medium of interest in Raman spectroscopy can either be in gaseous, liquid, or solid form. Unlike infrared absorption spectroscopy Raman spectroscopy is not hampered by the presence of water, and the ability to assess biomolecules in aqueous solutions is not trivial since most of the biological media in living physiological systems contain water. Lastly, Raman spectroscopy systems yield the possibility for remote sensing and *in vivo* application since non-contact probing is possible with the use of (fiber)optics. All these characteristics make Raman spectroscopy a versatile and powerful biochemical analytical tool, and with the right system design this technique can be applied in various fields of medicine[3], including ophthalmology.

Raman spectroscopic techniques and systems

In general, all Raman spectroscopy systems consist of the same basic components: a (monochromatic) light-source, some auxiliary optics, a spectrometer, and a photon-counting device (Figure 3).

Because the intensity of Raman scattering is usually very weak (~10^{-4}-10^{-6} of the intensity of Rayleigh scattering), a light-source of sufficient intensity is needed in applied Raman spectroscopy. Furthermore, it is obvious that this light-source should be monochromatic in order to identify changes in scattering frequency (C.V. Raman used filtered sunlight).[1] With the introduction of the laser in the 1960's a wide variety of stable monochromatic light-sources of sufficient intensity and coherency have become available. The laser is now the light-source of choice in Raman spectroscopy. Because the Raman shift *position* is independent of the wavelength of the irradiating photons a multitude of different laser-wavelengths can be used, depending on the conditions necessary during the Raman scattering experiment. Ultraviolet (UV) is utilized in those cases where the use of visible light might lead to the occurrence of interfering fluorescence, and is applied in time-resolved UV resonance Raman scattering experiments.[4,5] Raman spectroscopy using infrared (IR) and near-infrared (NIR) wavelengths for excitation have found significant applications in for example the detection of cancers and pre-cancers.[6-9] The possibility to include tunable dye lasers (280-1500 nm) into a Raman spectroscopy system has allowed investigators to find the most suitable wavelength with regards to Raman yield and fluorescence reduction.[10,11] However, in general mostly visible laser sources are used of which the Argon and Krypton laser are the most universal.[12]

The auxiliary optics can be divided into two functional categories (although both categories are sometimes combined to perform both functions at the same

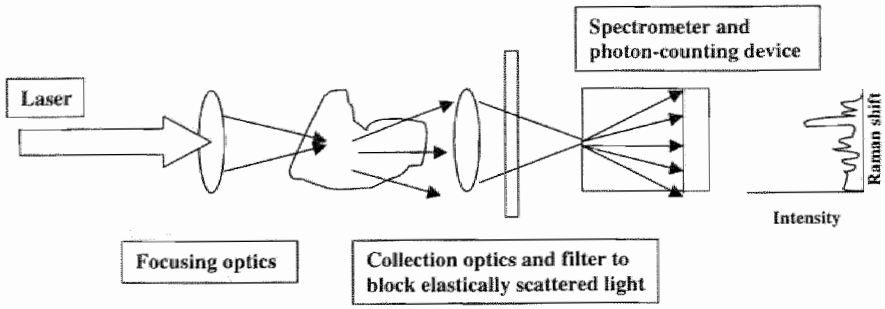

Figure 3. Basic Raman spectroscopy system.

time): optics to transfer and focus the irradiation light onto the sample, and optics to collect as much of the scattered light as possible while transferring only the Raman scattered portion to the detector-site, by blocking elastically scattered light. In both instances the use of fiber-optics is becoming increasingly popular.[13-15]

A spectrometer spatially disperses the incoming Raman scattered light like a prism, and effectively resolves this light into a spectrum of Raman frequencies. At the exit port of the spectrometer this spectrum is detected and recorded either sequentially by a single scanning photomultiplier tube (PMT), or in real-time by a multichannel detector, i.e. a charged coupled device (CCD) array.[16]

The Raman yield during a Raman spectroscopic experiment is determined by the aforementioned different components used as well as the sample itself. The absolute Raman intensity is directly proportional to the intensity of the incident laser light, the frequency of the scattered light to the fourth power (mostly with the same wavelength as the incident light), and the dipole polarizability of the molecules to the second power (Appendix; Formula 7). As mentioned before, the Raman intensity is also a function of the concentration of molecules in the sample of interest which yield the potential for quantitative biochemical analysis. Small probing volumes are sometimes necessary and can be achieved using high magnification microscope objectives.[17] The collection site of a Raman spectroscopy system should be optimized for maximum (Raman) light gathering power, and this can be achieved using a high numerical aperture (NA) objective at the site of the sample or by multiple collectors in the form of a multi-fiber.[14] In addition, the losses in the remaining optics (filters, focusing lenses, and spectrometer) should be kept at a minimum, while the actual photon counting device should obviously be sufficiently sensitive for the scattered frequencies.

Applications of Raman spectroscopy in biochemistry

Over the last 30 years, the interest in Raman spectroscopy (RS) has been advanced steadily as can be seen by the increasing amount of scientific publications on this topic during this period (Figure 4). Two technological developments clearly boosted the potential for applicability of Raman spectroscopy in biology and medicine: the introduction of the laser in the late 1960's, and the application of highly sensitive detectors in the visible range that started in the 1980's. However, it was the knowledge that the Raman signature of simple molecular bonds (i.e. O-H, C-H, S-H, N-H, S-S, C=C, C=O) could be used to explain the Raman features of larger and more complex biomolecules, that has contributed more significantly to the applicability of RS in biochemistry[2]. The fact that these so-called group-frequencies (see for example Table 1.3 in Ref. 19) are characterized by Raman-lines with highly consistent positions, regardless of the biochemical compound studied, has actually been the key factor in interpreting a Raman spectrum as being the 'blue-print' of a biomolecule with regards to its chemical composition (=primary structure), conformation (=secondary, tertiary, and quaternary structure) and environment. Thus, Raman spectroscopy has been applied in every aspect of biochemistry, from the biochemical characterization of nucleic acids and related compounds, amino-acids, polypeptides, proteins, lipids and cellular membranes, carbohydrates, and bacteria and viruses, to the Raman spectroscopic study of cells, tissues and even whole organs. The application of RS in biochemistry has always been in close relation with, if not the necessary stepping stone to, applications of RS in medicine, although *clinical* applications have been limited to the use of Raman spectroscopy in anesthesiology for the quality control of expired gases.[18] Since the scope of this thesis does not permit for a thorough discussion on all the applications of Raman spectroscopy in the field of analytical biochemistry, biology, and medicine, I would like to refer the reader to the abundance of excellent works that have been written about this subject,[2,19-23] and will focus on the applications of RS in ophthalmology in particular.

Applications of Raman spectroscopy in the eye

Biochemical characterization of proteins in general entails the assessment of the chemical signatures of the individual protein constituents, being the polypeptides and amino-acids, for which Raman spectroscopy is inherently suitable. Although specific signatures can be obtained from each biochemical, the assessment of the primary structure (i.e. the order in which the polypeptides appear and the sequence of amino-acids herein) is much more difficult to attain,

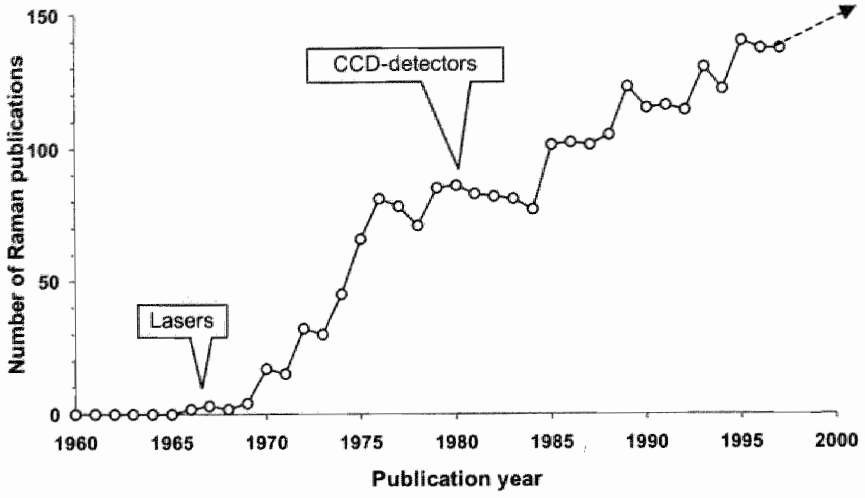

Figure 4. Number of new MEDLINE-publications on 'Raman' from 1960-1997. 'Lasers' and 'CCD-detectors' refer to the application of the laser and the CCD-detector in Raman spectroscopy systems, respectively.

and usually other biochemical assays have to complement the Raman spectroscopic findings. However, Raman spectroscopy offers valuable information on the conformational structure of proteins, which is almost equally important to their function as primary structure.[24,25] The secondary protein structure is determined by the shape of the protein backbone of amide-bonds, -O=C-N-H-. Both the amide-bonds and the shape of the protein backbone determine the position of the Raman-amide bands, which are denoted Amide I through VII, A and B. Amide-modes I and III are particularly Raman-active, and their signals are used to determine the conformation of the peptide in question. The Amide I Raman signal is the combined result of the vibrations of C=O (80%), C-N (10%), and N-H (10%). Its Raman band ranges from 1645-1680 cm^{-1}, depending on the conformation. The Amide III mode (range 1225-1310 cm^{-1}), which is much more difficult to interpret due to overlapping CH- and several amino-acid ring vibrations, involves C-N (40%), N-H (30%), CH_3-C (20%), and very little C=O vibrations. Since a protein is made up of many peptides, the Amide I and III modes of this protein in a Raman spectrum will be the result of the sum of all individual peptide bond vibrations. Thus, in order to determine the conformation of a *protein*, or rather peptide back-bone, it is custom to analyze both the Amide I as well as the Amide III mode. In an α-helix conformation the Amide I mode can be found at ~1645-1657 cm^{-1},

while the Amide III is at ~1260-1310 cm^{-1}. A β-sheet conformation has an Amide I mode at ~1665-1680 cm^{-1} and an Amide III at ~1225-1245 cm^{-1}. A random coil protein conformation is present when the Amide I mode is found at ~1660-1665 cm^{-1} while the Amide III mode is at ~1240-1250 cm^{-1}.[24]

The biochemical contents of the ocular media consist for a large part of water and proteins and are closely related to the normal function of these tissues (Table 1). Not only do proteins maintain the structural integrity of ocular tissues (i.e. collagen fibrils in the cornea), but certain non-structural proteins also perform specialized functions as hormones, enzymes, and neurotransmitters, or more importantly function in such a way that they permit optimal light transmission in the case of lens crystallins.[26,27] When normal function and physiology of these proteins is hampered by biochemical changes within the tissues various ocular pathologies may arise which might ultimately lead to vision loss or blindness. It has been the object of many investigations to try to identify these biochemical changes in order to decrease the occurrence of pathology by providing a basis for early diagnosis and therapy. Also Raman spectroscopy has been applied in the biochemical analysis of ocular tissues and has made significant contributions to the field of ocular biochemistry.

Applied Raman spectroscopy in ophthalmology has mainly focused on the elucidation of biochemical processes in the ocular lens in particular with regards to cataract formation, and a vast amount of publications are available in the literature.[28-71] This can be understood when considering the high incidence of cataract in the normal population and the potentially significant clinical importance of early diagnosis and treatment of this degenerative disorder.[27] In addition, the lens contains a high concentration of proteins yielding strong Raman signals, and human tissues are readily available. The ocular lens is a transparent medium composed of closely packed lens fiber cells which, upon maturation, specialize in producing the lens crystallins (α, β, and γ-types and subtypes, all in the β-pleated sheet conformation) that are embedded in a cytoskeletal matrix. Protein synthesis stops when the lens fiber cells are mature and anucleate. The lens has an epithelial layer for maintenance of the fluid and electrolyte transport, and is bordered by a lipid-containing semi-permeable capsule. The water content of the lens ranges from 68% in the nucleus to 80% at the periphery. Aging of the lens is accompanied by changes in macromolecular structure, protein and water content, morphologically characterized by disorganization of the lens fiber cells, and the formation of vacuoles and electron-dense bodies. Functional changes during lens aging include ion channel dysfunctions, and decrease in enzyme activity in the nucleus but not the cortex or epithelium. Vision loss in cataract is caused by decreased transmission of light as a result of a disruption in the ordered packing of the lens crystallins due to increased water accumulation in the lens, formation of high molecular weight protein aggregates

Table 1. Anatomy of the ocular media with respect to biochemistry and physiology (Adapted from Ref. 26).

Ocular tissue (thickness)	Biochemical content	Physiological function
Tear-film (45 μm)		
• Lipid layer	• Meibomian lipids	• Prevention of evaporation, and tear-spillover, and provides clear optical medium
• Aquous layer (60%)	• Water with soluble lactoferrin, lysozyme, and IgA	• Lubrication, equalizing optical imperfections of cornea, and bacteriostatic function.
• Mucus layer (30-40%)	• Mucin	• Tear-film stabilization
Cornea (~520 μm)		
• Epithelium (50-60 μm)	• Keratin-expressing cells; collagen Types IV, VII, IX, and XVI, and heparan sulfate (basal lamina)	• Barrier-function and light refraction
• Bowmans layer (8-12 μm)	• Collagen Type I, III and IV	• Elasticity and deformability
• Stroma (~450 μm)	• 80% water, structural fibrillar collagen Types I (~50%), V (10%), and III (~2%), structural non-fibrillar collagen Type VI (~35%), and ~5% glycosaminoglycans, all produced by the keratocytes	• Corneal structure and transparency
• Descemet layer (8-12 μm)	• Collagen Types V, VIII, IX, XII	• Strength and resistance to IOP.
• Endothelium (5-6 μm)	• Single endothelial cell-layer	• Water transport out of the stroma.
Anterior chamber (2-3 mm)		
• Aqueous humor	• Water (~100%) and glucose, lactate, ascorbate, albumin, transferrin, fibronectin, IgG, Na, K, HCO_3, Mg, Ca, Cl	• Intraocular pressure (IOP), and metabolism and transport
Lens (~4 mm)		
• Capsule (9-28 μm)	• Collagen Type IV and heparan sulfate	• Diffusion barrier
• Epithelium	• Single cell layer	• Maintenance of fluid and electrolyte balance
• Cortex and nucleus	• Water (68-80%) and cytoskeletal matrix embedded crystallins (α, β, and γ) produced by the lens fiber cells, which contain various mambrane proteins (ATP-ases, calpactin-1, *N*-cadherin)	• Lens structure and transparency (300-1400 nm)

and vacuole formation within the lens fibers. A multitude of biochemical factors are involved in the process of cataract formation, including increased protein cross-linking and aggregation, oxidation of amino-acids (tryptophan photolysis), decreases in the antioxidants and glutathione, increased proteolysis, loss of α- and γ-crystallins, and nonenzymatic glycation of lens proteins. The latter is possibly inhibited by the reducing action of glutathione on ascorbic acid.[26]

Raman spectroscopy of the ocular lens yields specific signals in both the lower as well as the higher Raman shift region as depicted in Figure 5 (for band assignments see Table 2). Clearly visible are Raman bands that can be assigned to the amino-acids tyrosine (Tyr: 644, 828, 857, 1175, 1208, and 1620 cm^{-1}), phenylalanine (Phe: 622, 1003, 1032, 1175, and 1610 cm^{-1}), and tryptophan (Trp: 756, 878, 1340, 1546, and 1581 cm^{-1}), some group-frequencies (C-C, C-N, CH, CH_2, and $-CO_2^-$), and the Amide modes I (at 1668 cm^{-1}) and III (at 1238 cm^{-1}), denoting the β-sheet conformation. The higher spectral region exhibits the aliphatic (at 2880, 2930, and 2960 cm^{-1}) and aromatic (3060 cm^{-1}) C-H vibrations of the lens proteins (crystallins), and the O-H vibrations of water (at 3230, 3390, and a shoulder at ~3550 cm^{-1}). The Raman intensity ratio I(3390)/I(2930) is in direct proportion to the relative hydration of the lens, and has been used in the past to spatially resolve the regional variations of water within the lens along the optical axis.[56,61] The local differences in Raman spectral features are quite obvious in the higher spectral region (Figure 5B), where it can be seen that the the water content is higher in the cortical than in the nuclear region of the lens, which is in agreement with earlier finds.

In 1975, Yu et al. were the first to publish their results on Raman spectroscopic investigations of the ocular lens proteins, and lay the basis for all future investigations on aging and cataract-formation in the lens.[28,29] Raman spectra of the lens crystallins (α, β1, β2, β3, and γ) and albuminoid showed that these compounds are mainly in the antiparallel β-pleaded sheet conformation. Furthermore, in the intact lens the amount of γ-crystallin was found to be higher in the nucleus while the α-crystallin amount increased from the nucleus to the cortical region of the lens. They also found that lens opacification does not necessarily entail oxidation of sulfhydryl or involve conformational changes, since heat denaturation does not result in an altered SH content or a change in β-sheet conformation.[29] Opacification might rather be the result of macromolecular rearrangement causing large refractive index differences. Experimental proof of latter suggestion was given by Schachar and Solin and later by Ondruska and Hanson.[30,31] Former authors showed a remarkable similarity in lens protein macro-structure (lens fiber cross-section) and micro-structure (the β-sheet conformation), and concluded that cortical cataracts are the result of fluctuations in the orientational order or lens proteins.[30]

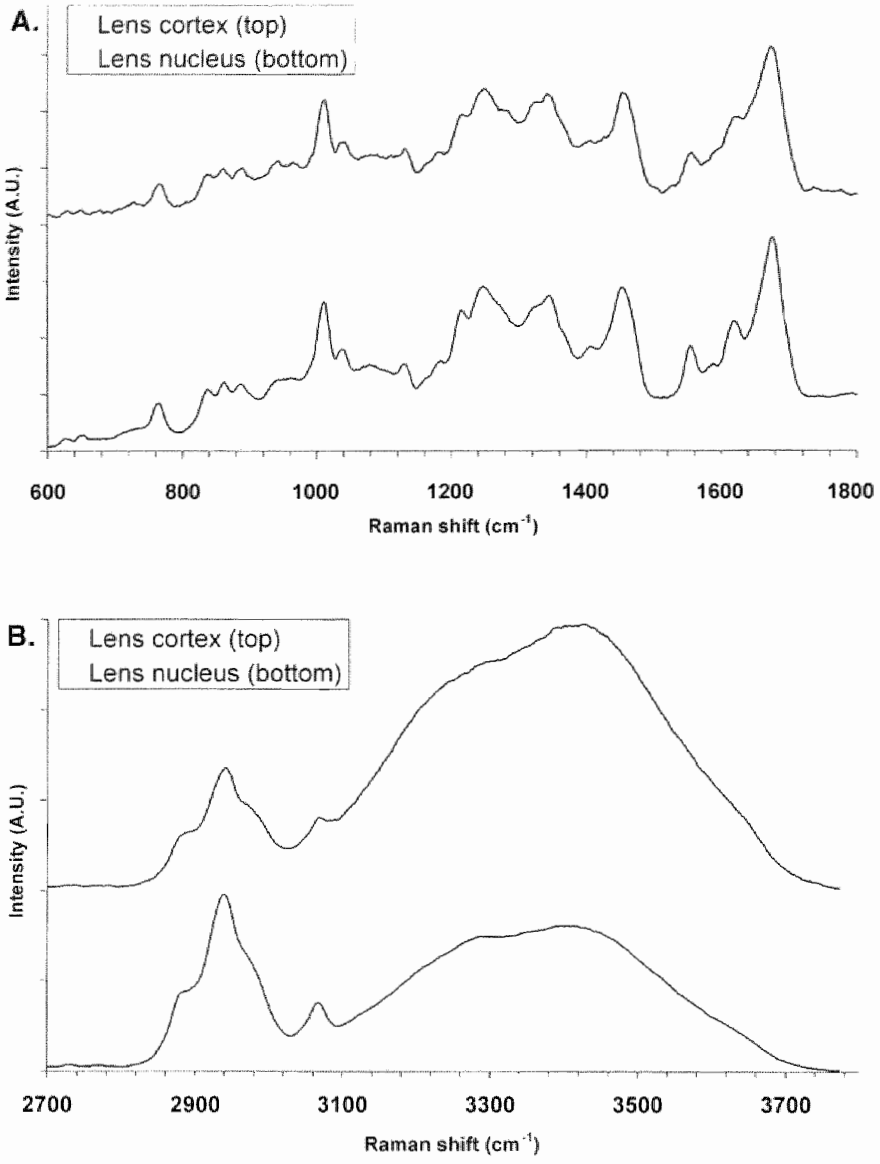

Figure 5. Raman spectra in the lower (A) and higher (B) Raman shift region from 600-1800 cm^{-1} and from 2700-3800 cm^{-1}, respectively, of the cortical and nuclear region of a normal NZW rabbit lens *in situ*. Experimental conditions: CRS with Argon laser (514.5 nm, 25 mW), 25x NA 0.5 long-working distance microscope objective, 50 µm fiber as confocal pin-hole, 1 s exposure times (spectra are digitally smoothed). Top spectra are off-set for clarity.

Table 2. Raman band assignments of *in-situ* NZW rabbit ocular lens.

Raman shift position (cm^{-1})		
Cortex	Nucleus	Raman band assignments Adapted from Ref. 29
622	618	Phenylalanine(Phe)
644	645	Tyrosine (Tyr)
756	758	Tryptophan (Trp)
828	828	Tyr
857	854	Tyr
878	877	Trp
938	927	C-C vibration
960	957	C-C vibration
1003	1003	Phe
1032	1032	Phe
1072	1072	C-N vibration
1127	1125	C-N vibration
1157	1151	C-N vibration
1175	1171	Tyr and Phe
1208	1203	Tyr
1238	1241	Amide III
1320	1320	CH deformation
1340	1340	Trp
1401	1398	$-CO_2^-$
1447	1444	CH_2 deformation
1546	1546	Trp
1581	1584	Trp
1610	1604	Phe
1620	1618	Tyr
1668	1669	Amide I
~2880,~2930,~2960	~2880,~2930,~2960	Aliphatic CH vibration
~3060	~3062	Aromatic CH vibration
~3230,~3390,~3550	~3230,~3390,~3550	OH vibrations

The first proof that conformational changes do prelude opacification was shown in young bird and reptile lenses, since on heat-coagulation a conversion from an α–helical (normal in these species) to the β–pleated sheet conformation was observed.[32] Over the years various species, including the human, have been the subject of investigations on cataract formation, and numerous cataractogenic factors have been studied from normal aging, to UV-induced cataract, heat- or

cold-induced cataract, glucocorticoid-induced cataract, hereditary cataract, and galactose-induced cataract, by characterizing structural changes in the ocular lens with Raman spectroscopy. A significant amount of these studies focused on the conformation of the lens proteins, on the contents of sulfhydryl (SH) and disulfide (SS) in the ocular lens, and consequently on the so-called 2-SH→SS conversion, a possible causative factor in cataractogenesis.[29,33-51] Furthermore, the water content of the lens has been of considerable interest, since lens hydration changes during cataractogenesis.[29,31,40,42,44,47,52-64] In addition, lens membrane lipids and the changes in cholesterol content and distribution have been studied, since they are thought to be involved in the process of cataractogenesis.[49,63,65-71] Notwithstanding different findings among the various species and cataract models used, the overall results of these studies could be summarized as follows:[25]

1. Raman spectroscopy is a powerful diagnostic tool for biochemical characterization of the lens protein structures, protein side chain groups (tyrosine, tryptophan, phenylalanine, sulfhydryl, disulfide), and water;
2. Normal biochemical content of the ocular lens and the protein structural changes that occur upon lens aging and cataract formation are not necessarily the same for each species;
3. Mammalian lens crystallins are all in the β–pleated sheet conformation, as assessed using the information of the Amide I and III Raman vibrational modes;
4. The spatial distribution of sulfhydryl (SH), disulfide (SS), amino-acids (tyrosine and tryptophan), crystallins, and water is not uniform in a normal lens. Both the extent and distribution of these biomolecules change with age and upon cataract formation as a result of posttranslational changes in protein synthesis (i.e. cross-linking, decreased solubility, proteolytic denaturation and degradation, and aggregation);
5. Cataractogenesis is not necessarily preceded by protein conformational changes, but the result of macromolecular disorganization. Furthermore, the SH→SS conversion does not seem to be a predominant factor in cataractogenesis, but rather occurs during stabilization of already formed protein aggregates;
6. In the human, a slight change in SH but not in SS content is detectable upon aging. Possibly, glutathione (GSH) is oxidized by a reaction with protein-disulfide (P-SS) groups to form protein-sulfhydryls (P-SH) and mixed disulfides of protein and glutathione. The mixed disulfides are reduced to P-SH and glutathione-disulfide (GSSG), which is extruded from the lens. Thus, P-SH is kept in a reduced state, while P-SS concentrations remain low. Other reasons for the observed difference between the extent of SH reduction and SS formation could be that during aging α- and

β-crystallins (low in SH) synthesize faster than γ-crystallins (high in SH), and/or the rate of glutathione synthesis changes during aging;
7. Elevated levels of hydrogen peroxide in the aqueous humor of diabetic patients could be the oxidizing agent during this process of cataractogenesis;
8. Changes in tyrosine-hydrogen bonding is caused by protein-water phase separation and is a possible causative factor for cataract formation;
9. Changes in lens biochemistry can be detected prior to visually detectable opacification, and entail changes in hydration and a faster SH→SS conversion as compared to normal aging. This yields the possibility for early diagnosis and intervention.

Although less frequently, Raman spectroscopy (RS) has also been applied for biochemical analyses of the cornea and its constituents[72-76], the aqueous humor[77,78], the vitreous body,[79] and the retina and its visual pigments.[80-88]

In a study by Sebag et al., RS was applied for the biochemical analysis of human vitreous humor in order to investigate the reported increase in nonenzymatic glycation of the vitreous in diabetic retinopathy. With the occurrence of a Raman band at 3057 cm^{-1} (aromatic C-H stretching) and a three-fold increase in a Raman band at 1604 cm^{-1} (C=C vibrations), assigned to π–conjugated and aromatic molecules, the occurrence of advanced nonenzymatic glycation could be confirmed.[79]

Raman spectroscopic studies of the aqueous humor were carried out by our group with the initial objective of determining the feasibility of RS for the non-contact assessment of glucose in the eye.[77] Although the nature of the glucose molecule does not permit unambiguous identification in a mixture of biomolecules, since the Raman signal of glucose is usually non-specific, it was shown that RS is a potentially valuable tool for the non-contact characterization of biomolecules in the aqueous humor.[78]

Only a few studies have focused on using RS for the biochemical characterization of the cornea.[72-75] The typical Raman spectra or a fresh NZW rabbit cornea, a similar cornea after lyophilization (complete dehydration), and a therapeutic collagen shield are depicted in Figure 6, to help illustrate the findings in mentioned RS studies. The Raman band assignments of these spectra are summarized in Table 3. In the lower spectral region (400-1800 cm^{-1}), Raman bands for amino-acids (Tyr, Trp, Phe, Pro, Hypro) are easily distinguishable, together with some group-frequencies (C-C, COO^-, CH_3, CH_2, C-N), and the Amide modes I and III. In the fresh cornea, an Amide I mode ~1648 cm^{-1} and two Amide III modes, of which the one at ~1270 is much stronger than the one at ~1244 cm^{-1}, are visible. The occurrence of two Amide III modes has been explained by Frushour and Koenig as being the result of the polar and non-polar regions of the collagen polypeptide chains.[76] The Amide I mode at 1648 cm^{-1} is suggestive for an α–helical protein conformation, and this confirms

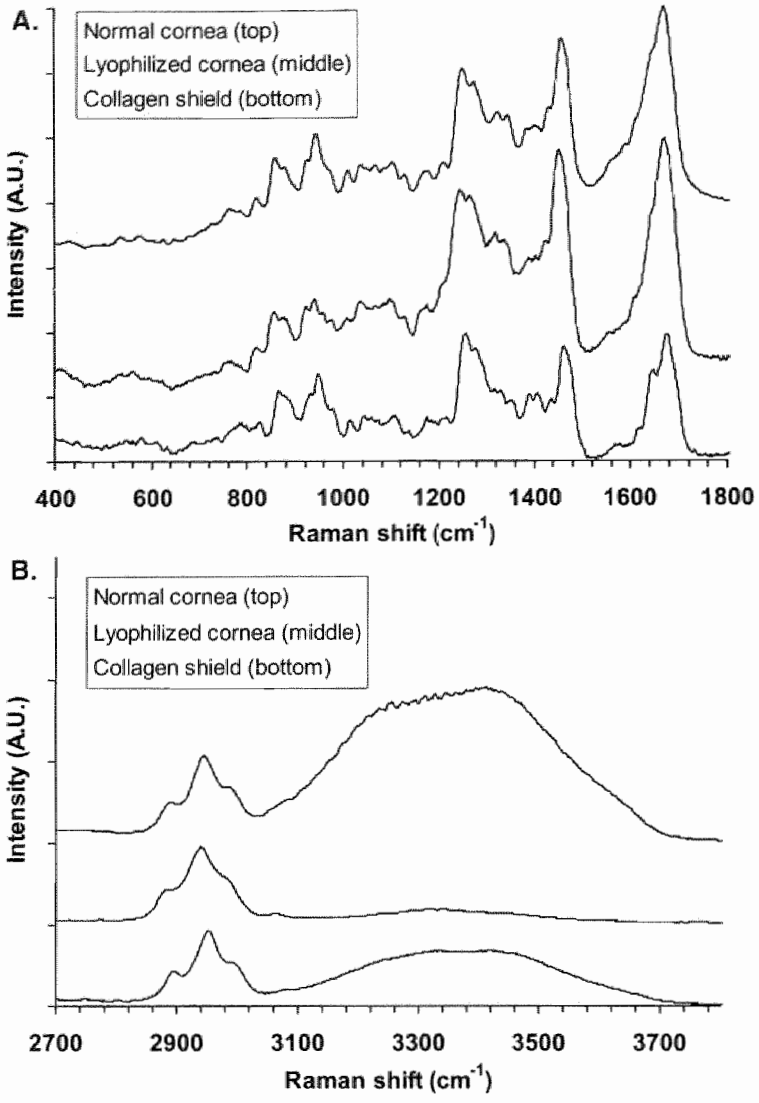

Figure 6. Raman spectra in the lower (A) and higher (B) Raman shift region from 400-1800 cm^{-1} and from 2700-3800 cm^{-1}, respectively, of a normal NZW rabbit cornea measured *in situ*, a lyophilized (completely water-free) NZW rabbit cornea *in vitro*, and a therapeutic collagen shield (Biocor II, Bausch & Lomb, Tapa, FL), made of porcine collagen. Experimental conditions: CRS with Argon laser (514.5 nm, 25 mW), 25x NA 0.5 long-working distance microscope objective, 50 µm fiber as confocal pinhole, 1 s exposure times (spectra are digitally smoothed). Top spectra are off-set for clarity.

Table 3. Raman band assignments in normal and lyophilized NZW rabbit cornea and a collagen shield.

Raman shift position (cm^{-1})			
Normal cornea	Lyophilized cornea	Collagen shield	Raman band assignments
			Adapted from Ref. 74 and 76.
622	-	-	Phenylalanine (Phe)
645	-	-	Tyrosine (Tyr)
824	827	832	C-C vibration of backbone
854	857	863	C-C vibration of Pro ring
875	875	883	C-C vibration of Hypro ring
921	921	924	C-C stretch of Proline (Pro) ring
939	936	944	C-C stretch of protein backbone
968	971	968	C-C stretch
1003	1006	1011	Phe ring mode
1029	1031	1038	Pro
1102	1099	1102	C-N stretch
1203	1203	1215	Hydroxyproline (Hypro)
1244	1245	1253	Amide III
1270	1261	1273	Amide III
1320	1317	1328	CH_3,CH_2 stretching
1343	1334	1349	CH_3, CH_2 stretching
1378	1386	1386	-
1398	1401	1404	-
1427	1421	1433	COO^- stretching
1453	1448	1456	CH_3, CH_2 deformation
1587	-	-	Pro, Hypro
-	1604	-	Phe, Tyr
	-	1613	Tyr
1648	1645	1645	Amide I
2886, 2940, 2984	2890,2941,2978	2898,2951,2991	Aliphatic C-H stretch
3065	3066	3070	Aromatic C-H stretch
	3350	-	N-H
3230, 3390, 3550	-	3300,3399,3542	O-H vibrations

earlier findings that corneal collagen (mainly Type I) is composed of three α-chain fibrils; two identical $\alpha 1$ chains, and one $\alpha 2$ chain. Significant differences in the Raman intensity between a fresh and a lyophilized cornea appear at ~939 cm^{-1} (C-C stretch of protein backbone) and 1244 cm^{-1} (Amide III), while the Amide I mode is broader in the fresh cornea in comparison to the

lyophilized cornea. These differences are suggestive for conformational changes possibly caused by altered fibrillar arrangement due to differences in the water content, similar to events taking place after heat denaturation.[74] The significant differences in relative Raman intensities at 1328, 1349, 1404, and 1645 cm^{-1} between the hydrated collagen shield and the fresh cornea probably are the result of differences in the collagen type, and fibrillar arrangement. Furthermore, Raman spectra of collagen Type I of the sclera has been shown to be lower in intensity for proline and hydroxyproline, suggestive for a larger content of phenylalanine residues in Type I collagen in the cornea.[72]

The corneal water content has also been the object of interest, since maintaining a normal corneal hydration is crucial for the transparency of the cornea.[73,75] The Raman signal of water can be found in the higher spectral region from 3100-3700 cm^{-1}, as depicted in Figure 6B for a normal and a lyophilized cornea and a rehydrated corneal collagen shield (Table 3). It can be seen that the O-H vibrations (at 3230, 3390, and a shoulder at ~3550 cm^{-1}) are rather strong when compared to corneal Raman signals obtained in the 'signature'-region from 400-1800 cm^{-1}. The lack of O-H vibrations in the lyophilized cornea is in agreement with the fact that this cornea is totally devoid of water; the remaining faint structure at ~3350 cm^{-1} is assigned to N-H stretching vibrations of primary amides. Furthermore, all these spectra feature four resolved signals that can be assigned to the aliphatic (2886, 2940, and 2984 cm^{-1}), and aromatic (3065 cm^{-1}) C-H vibrations of proteins (collagen). Like in the lens, the Raman intensity ratio I(3390)/I(2940) is in direct proportion to the relative water content of the cornea, and has been used to assess the total and spatially resolved water content of the cornea.[73,75]

Siew et al. studied total corneal water content using the Raman intensity ratio I(3390)/I(2940) in organ cultured corneas, and sought to correlate this with the metabolic state of the procured corneas. They concluded that RS might provide for a more sensitive non-contact means for quality control of eye-bank corneas, for reasons that a disturbed corneal water content might be indicative of corneal endothelial dysfunction.[73] We extended the application of Raman spectroscopy in the study of corneal hydration by spatially resolving the corneal water content in the rabbit cornea under *in-vivo* circumstances, potentially applicable in those instances where topical changes in corneal hydration are expected to be more important than changes in total corneal hydration, as is the case in for example corneal dystrophies and corneal decompensation after penetrating keratoplasty (this thesis Chapter 5).[75]

Most of the aforementioned Raman spectroscopic studies of ocular tissues have been performed under *in vitro* circumstances because the inherently low Raman signal requires the application of high-level light doses and long probing times. In addition, the signal-to-noise ratio can diminish rapidly with the occur-

rence of fluorescence, which is a likely possibility in biological tissues. Although system designs keep improving and other optical techniques are being used to complement Raman spectroscopy[17,90-96], the applications of Raman spectroscopy in the eye under *in-vivo* circumstances have been limited so far.[89] With this in mind we considered the design of a Raman spectroscopy system that would allow for application of this optical technique for the biochemical characterization of ocular tissues *in-vivo*.

Design considerations for a Raman spectroscopy system for ophthalmic use *in-vivo*

The inherent versatility of Raman spectroscopy systems allows for a system design most optimal for the biological medium of choice. Puppels et al. for example designed a confocal Raman microspectroscopy (CRM) system with the aim to non-invasively assess biochemical properties of cells and chromosomes.[17] Their design considerations were governed by the aim to obtain spectra of a single metaphase chromosome with a volume of ~1 μm^3. Thus, apart from optimizing the throughput of the whole system they incorporated a high numerical aperture microscope objective lens with high magnification (63x Zeiss water immersion objective, NA 1.2) for optimum signal collection from probing volumes $\leq 1\ \mu m^3$, and were able to non-invasively assess single cells and chromosomes, as well as carotenoids in granulocytes and natural killer cells, and applied this novel system for the spatially resolved Raman microspectroscopic studies on water, protein, and cholesterol content of the ocular lens.[17,50,51,56,61,67,68,92,94,97-103]

As stated in the introduction, our aim was to investigate the application of a Raman spectroscopy system for non-contact biochemical assessments of (intra)ocular tissues and fluids *in-vivo*. The ocular tissues consist of multi-layered structures all varying in biochemical content, optical quality, thickness, intraocular location, and light-sensitivity, posing a challenging problem (Table 1 and 4). In order to non-invasively probe all layers of the eye under *in vivo* and thus constantly changing biochemical conditions, the following design parameters for a suitable Raman system had to be considered:

1. use of an irradiation source with low absorbency (high transmittance) in the ocular media of choice;
2. capability to obtain high signal-to-noise ratio Raman spectra of the tear-film, the cornea, the aqueous humor, the lens, and the vitreous humor in a non-contact manner;
3. axial scanning capabilities with adequate spatial resolution;

4. adequate axial resolution in order to spatially resolve thin ocular tissue layers while reducing the detection of fluorescence;
5. the intensity of the chosen irradiation source should be safe;
6. rapid spectral acquisition (~1 s temporal resolution); and
7. elimination of movement artifacts (the incorporation of an eye-tracking device into our Raman spectroscopy system is still under development, and will not be discussed here);

These considerations led to the development of a high-gain laser scanning confocal Raman spectroscopy (CRS) system of which the characteristics and performance are discussed in more detail in Chapter 3 of this thesis.[104] The following will describe in short the most significant components of this system with regards to the aforementioned design parameters.

The choice of laser source was mainly determined by the incorporation into our system of the most sensitive photon-counting device in the visible region (parameter 1) available at the time, a liquid nitrogen cooled CCD (charged coupled device) camera for real-time high signal-to-noise ratio spectral data acquisition (parameter 6). Thus, we opted for either a continuous wave (CW) Argon (514.5 nm) or Helium-Neon laser (632.8 nm). Since the Stokes-lines of interest in a Raman spectrum lie in the region of 0-3800 cm^{-1}, the application of either laser source will result in spectra with a frequency range within the detection limits of the CCD detector. In theory, the high sensitivity of this detector would also permit spectral acquisitions at low laser irradiation intensities (parameter 5). It can be understood that this requirement is as stringent as it is necessary (see Introduction). Notwithstanding the capabilities of this detector, the requirement to use low levels of irradiation and the need for high temporal and spatial resolution (parameters 4 and 6) in conjunction with the inherently inefficient nature of the Raman scattering process, demands optimal signal collection and transport from the sample. This was achieved using a 25x, NA 0.5 long-working distance microscope objective (LDMO), with a backaperture equal to the emitter area of 12.5 mm. The application of this lens not only yielded high light gathering power, but also noncontact probing of all ocular tissues of interest (parameter 2), by virtue of its long working distance of ~13 mm. This entrance lens was applied in a 180° backscatter configuration (analog to an epi-illuminated microscope), and hence utilized for focusing as well as for collecting the Raman scattered light. Furthermore, the optics of this Raman spectroscopy system were setup in a telecentric configuration, meaning that the entrance lens (LDMO) could move along its optical axis without change in distance between the image plane and the focal plane of the exit lens (Figure 7). After placing this lens on an automated translation stage, axial scanning was made possible with 10 μm steps (parameter 3). Incorporating an optical fiber at the exit site of this Raman spectroscopy system, for transport of the Raman scat-

Table 4. Light-tissue interaction in the ocular media*

Light (wavelength)	Cornea	Lens	Retina	Accidental Overexposure	Representative lasers (wavelength)	Ophthalmic use
Mid-UV (180-315 nm)	+++	-	-	Photo-keratitis; "welder's flash"	Excimer ArF (193 nm)	Photoablative therapy (PRK)
Near-UV (UV-A; 315-400 nm)	+	++	-	Cataract	Excimer XeF (351 nm)	-
VIS and NIR (400-1400 nm)	0	0	+++	Retinal toxicity	Argon (488 and 514.5 nm) Krypton (530.8, 568.2, and 647.1 nm) Dye laser (630 nm) Pulsed Nd:YAG (1.06 μm)	Photo-coagulation (diabetic retinopathy) Photodynamic therapy Photodisruption therapy (posterior capsulotomy)
Mid-IR (1.4-3 μm)	+	++	-	"glass-blowers's cataract"	Erbium:YAG (2.94 μm)	Photoablative therapy (PRK)
FIR (3 μm-1 mm)	+++	-	-	Photo-keratitis	CO_2 (10.6 μm)	Photovaporation (blepharoplasty)

*UV = Ultraviolet (180-400 nm); VIS = Visible (400-700 nm); NIR = Near infrared (700-1400 nm);FIR = Far infrared (3 μm-1 mm); PRK: photorefractive keratectomy; 0 = 100% transmission; +, ++, +++ = increasing level of absorbency of light by the tissue; - = light does not reach this tissue in intact eye due to 100% absorption in other tissue(s).

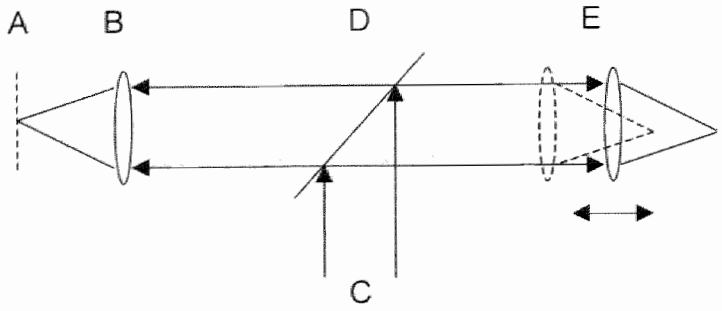

Figure 7. Telecentric principle of the optics of the confocal Raman spectroscopy system. A = focal plane of exit lens (B); C = incident light beam as well as the light collected (D) by the entrance lens (E) is collimated. The entrance lens (E) can be moved along the optical axis, which changes the position of the focal plane of the entrance lens, but not of the exit lens.

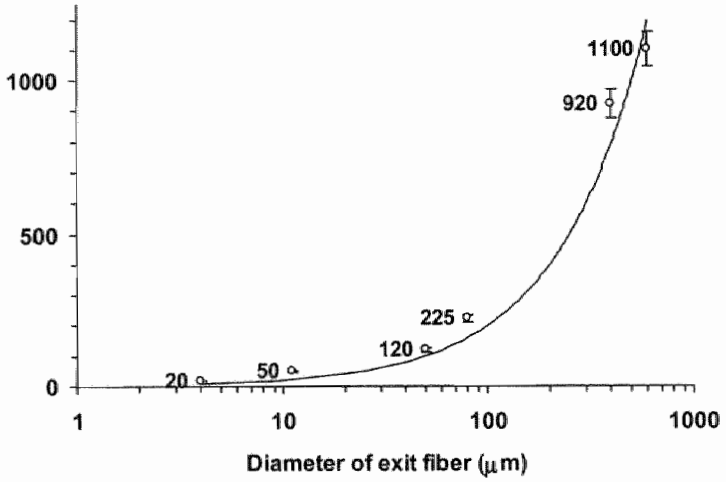

Figure 8. Relationship between fiber diameter (confocal pinhole) and axial resolution (±5%; Labels). Experimental conditions: CRS-system with Ar-laser (514.5 nm; 25 mW incident power), 25x NA 0.5 LDMO, and slit width of the spectrometer set at twice the size of fiber diameter (see Chapter 3).

tered light towards the spectrometer, elegantly solved design parameter 4. Because this fiber is placed in confocal alignment with the entrance lens (LDMO) it acts like a confocal pinhole, effectively eliminating light from out-of-focus places and reducing the detection of fluorescence (see Chapter

1).[17,105,106] This confocal setup allowed for optical sectioning with a maximum axial resolution of ~20 μm when using a 4 μm fiber diameter. Furthermore, the easy exchangeability of this fiber yielded the possibility to optimize the axial resolution to specific needs during the assessment of the ocular tissue of interest. Figure 8 depicts in graphical format the various optical fiber diameters used as function of the axial resolution achieved for each fiber.

The next Chapter will deal in more detail with the optics of the proposed confocal Raman spectroscopy system.

References

1. Raman C.V., and Krishnan K.S. A New Type of Secondary Radiation. *Nature* 1921; 121: 501-505.
2. Carey PR. Biochemical Applications of Raman and Resonance Raman spectroscopies. In Horecker B, Kaplan NO, Marmur J, and Scheraga HA Eds., *Molecular Biology: An International Series of Monographs and Textbooks*. Academic Press Inc., New York (1982).
3. Ozaki Y. Medical Application of Raman Spectroscopy. *Applied Spectroscopy Reviews* 1988; 24(3&4): 259-312.
4. Asher S.A. UV resonance Raman spectroscopy for analytical, physical, and biophysical chemistry. Part 2. *Analytical Chemistry* 1993; 65(4):201A-210A.
5. Asher S.A. UV resonance Raman studies of molecular structure and dynamics: applications in physical and biophysical chemistry. *Annual Review of Physical Chemistry* 1988; 39:537-88.
6. Keller S, Schrader B, Hoffman A, et al. Application of Near-Infrared-Fourier Transform Raman Spectroscopy in Medical Research. *Journal of Raman Spectroscopy* 1994; 25: pp. 663-671.
7. Schrader B, Keller S, Loechte T, et al. NIR FT Raman Spectroscopy in Medical Research. *Journal of Molecular Structure* 1995; 348: pp. 293-296.
8. Feld MS, Manoharan R, Salenius J, et al. Detection and Characterization of Human Tissue Lesions with Near Infrared Raman Spectroscopy. *SPIE* 1995; 2388: pp. 99-104.
9. Mahadevan-Jansen A and Richards-Kortum R. Raman Spectroscopy for the Detection of Cancers and Precancers. *Journal of Biomedical Optics* 1996; 1(1): pp. 31-70.
10. Lewis A. Tunable laser resonance Raman spectroscopic investigations of the transduction process in vertebrate rod cells. *Federation Proceedings* 1976; 35(1):51-3.
11. Lewis A., Spoonhower J., Bogomolni R.A., Lozier R.H., Stoeckenius W. Tunable laser resonance raman spectroscopy of bacteriorhodopsin. *Proceedings of the National Academy of Sciences of the United States of America* 1974; 71(11):4462-6.

12. Bursell S-E and Yu N-T. Fluorescence and Raman Spectroscopy of the Crystalline Lens. In: Masters BR Ed., *Noninvasive Diagnostic Techniques in Ophthalmology*. Springer-Verlag, New York (1990): pp. 319-341.
13. Schwab SD and McCreery RL. Versatile, Efficient Raman Sampling with Fiber Optics. *Anal. Chem.* 1984; 56: 2199-2204.
14. Myrick ML, Angel SM, and Desiderio R. Comparison of Some Fiber Optic Configurations for Measurement of Luminescence and Raman Scattering. *Applied Optics* 1990; 29(9): 1333-1344.
15. Schoen CL, Cooney TF, Sharma SK, and Carey DM. Long Fiber-Optic Remote Raman Probe for Detection and Identification of Weak Scatterers. *Applied Optics* 1992; 31(36): 7707-7715.
16. Baraga JJ, Feld MS, and Rava RP. Rapid Near-Infrared Raman Spectroscopy of Human Tissue with a Spectrograph and CCD Detector. *Applied Spectroscopy* 1992; 46(2): 187-190.
17. Puppels GJ, Colier W, Olminkhof JHF, et al. Description and Performance of a Highly Sensitive Confocal Raman Microspectrometer. In: Puppels GJ. Confocal Raman Spectroscopy: a new look at cells and chromosomes. Thesis. University Twente, The Netherlands. 1991.
18. Tu AT, Ed., *Raman Spectroscopy in Biology*. Wiley & Sons, New York (1982). Lockwood GG, Landon MJ, Chakrabarti MK, and Whitwam JG. The Ohmeda Rascal II. A New Gas Analyzer for Anesthetic Use. *Anaesthesia* 1994; 49(1): 44-53.
19. Parker FS, Ed. *Applications of Infrared, Raman, and Resonance Raman Spectroscopy in Biochemistry*. Plenum Press, New York (1983).
20. Harada I, and Takeuchi H. Raman and Ultraviolet Resonance Raman Spectra of Proteins and Related Compounds. In: Clark RJH and Hester RE, Eds., *Spectroscopy of Biological Systems. Volume 13: Advances in Spectroscopy*. John Wiley & Sons, Chichester (1986), pp113-176.
21. Spiro TG, Ed., *Biological Applications of Raman Spectroscopy. Volume 1: Raman spectra and the Conformations of Biological Macromolecules*. John Wiley & Sons, Chichester (1987).
22. Brame Jr. EG and Grasselli JG, Eds., *Practical Spectroscopy. Volume 1: Infrared and Raman Spectroscopy. Part A-C*. Marcel Dekker, Inc., New York (1977).
23. Winefordner JD and Kolthoff IM, Series Eds., *Chemical Analysis: A Series of Monographs on Analytical Chemistry and its Applications. Volume 114*. Grasselli JG and Bulkin BJ, Eds., *Analytical Raman Spectroscopy*. John Wiley & Sons, New York (1991).
24. Tu A.T. Peptide Backbone Conformation and Microenvironment of Protein Side Chains. In: Clark RJH and Hester RE, Eds., *Spectroscopy of Biological Systems. Volume 13: Advances in Spectroscopy*. John Wiley & Sons, Chichester (1986), pp 47-112.

25. Yu N-T., De Nagel D.C., and Kuck J.F.R. Ocular Lenses. In: Spiro TG, Ed., *Biological Applications of Raman Spectroscopy. Volume 1: Raman spectra and the Conformations of Biological Macromolecules*. John Wiley & Sons, Chichester (1987).
26. Forrester JV, Dick AD, McMenamin P, and Lee WR, Eds., Anatomy of the Eye. In: *The Eye; Basic Sciences in Practice*, Saunders, London (1996), pp. 13-86.
27. Gans, L.A. et al. *Basic and Clinical Science Course. Section 11: Lens and Cataract*. American Academy of Ophthalmology, San Francisco (1995-1996), pp. 45-67.
28. Yu N.T., Jo B.H., Chang R.C., Huber J.D. Single-crystal Raman spectra of native insulin. Structures of insulin fibrils, glucagon fibrils, and intact calf lens. *Archives of Biochemistry & Biophysics*, 1974; 160(2): 614-22.
29. Yu N.T., East E.J. Laser Raman spectroscopic studies of ocular lens and its isolated protein fractions. *Journal of Biological Chemistry*, 1975; 250(6): 2196-202.
30. Schachar R.A., Solin S.A. The microscopic protein structure of the lens with a theory for cataract formation as determined by Raman spectroscopy of intact bovine lenses. *Investigative Ophthalmology*, 1975; 14(5): 380-96.
31. Ondruska O., Hanson D.M. Raman spectra of duck, rat, and flounder lenses and the formation of dry and cold cataracts. *Experimental Eye Research*, 1983; 37(2): 139-43.
32. Yu N.T., East E.J., Chang R.C., Kuck J.F. Raman spectra of bird and reptile lens proteins. *Experimental Eye Research*, 1977; 24(4): 321-34.
33. East E.J., Chang R.C., Yu N.T., Kuck J.F., Jr. Raman spectroscopic measurement of total sulfhydryl in intact lens as affected by aging and ultraviolet irradiation. Deuterium exchange as a probe for accessible sulfhydryl in living tissue. *Journal of Biological Chemistry*, 1978; 253(5): 1436-41.
34. Kuck J.F., Yu N.T., Askren C.C. Total sulfhydryl by raman spectroscopy in the intact lens of several species: variations in the nucleus and along the optical axis during aging. *Experimental Eye Research*, 1982; 34(1): 23-37.
35. Itoh K., Ozaki Y., Mizuno A., Iriyama K. Structural changes in the lens proteins of hereditary cataracts monitored by Raman spectroscopy. *Biochemistry*, 1983; 22(8): 1773-8.
36. Yu N.T., DeNagel D.C., Pruett P.L., Kuck J.F., Jr. Disulfide bond formation in the eye lens. *Proceedings of the National Academy of Sciences of the United States of America*, 1985; 82(23): 7965-8.
37. Ozaki Y., Mizuno A., Itoh K., Iriyama K. Inter- and intramolecular disulfide bond formation and related structural changes in the lens proteins. A Raman spectroscopic study *in vivo* of lens aging. *Journal of Biological Chemistry*, 1987; 262(32): 15545-51.
38. Barron B.C., Yu N.T., Kuck J.F., Jr. Raman spectroscopic evaluation of aging and long-wave UV exposure in the guinea pig lens: a possible model for human aging. *Experimental Eye Research*, 1988; 46(2): 249-58.

39. DeNagel D.C., Bando M., Yu N.T., Kuck J.F., Jr. A Raman study of disulfide and sulfhydryl in the Emory mouse cataract. *Investigative Ophthalmology & Visual Science*, 1988; 29(5): 823-6.
40. Cai M.Z., Kuck J.F., Jr., Yu N.T. Galactose-induced cataract in rat: Raman detection of sulfhydryl decrease and water increase along an equatorial diameter. *Experimental Eye Research*, 1989; 49(4): 531-41.
41. Yu N.T., DeNagel D.C., Slingsby C. Raman spectroscopy of calf lens gamma-II crystallin: direct evidence for the formation of mixed disulfide bonds with 2-mercaptoethanol and glutathione. *Experimental Eye Research*, 1989; 48(3): 399-410.
42. Mizuno A., Ozaki Y. Aging and cataractous process of the lens detected by laser Raman spectroscopy. *Lens & Eye Toxicity Research*, 1991; 8(2-3): 177-87.
43. Pande J., McDermott M.J., Callender R.H., Spector A. The calf gamma crystallins—a Raman spectroscopic study. *Experimental Eye Research*, 1991; 52(2): 193-7.
44. Zigman S., Paxhia T., McDaniel T., Lou M.F., Yu N.T. Effect of chronic near-ultraviolet radiation on the gray squirrel lens *in vivo*. *Investigative Ophthalmology & Visual Science*, 1991; 32(6): 1723-32.
45. Chiou S.H., Chen W. Structural analysis of pigeon lens crystallins by near-infrared Fourier transform Raman spectroscopy. *Biochemistry International*, 1992; 28(3): 401-12.
46. Mizuno A., Shumiya S., Toshima S., Nakano T. Alteration of lens disulfide bonds in newly developed hereditary cataract rat. *Japanese Journal of Ophthalmology*, 1992; 36(4): 417-25.
47. Ozaki Y., Mizuno A. Molecular aging of lens crystallins and the life expectancy of the animal. Age-related protein structural changes studied *in situ* by Raman spectroscopy. *Biochimica et Biophysica Acta*, 1992; 1121(3): 245-51.
48. Tomohiro M., Mizuno A. Alteration of lens sulfhydryl groups induced by oxidative stress: Raman spectroscopic study of hydrogen peroxide-treated rat lens. *Japanese Journal of Ophthalmology*, 1995; 39(2): 130-6.
49. Duindam J.J., Vrensen G.F., Otto C., Greve J. Cholesterol, phospholipid, and protein changes in focal opacities in the human eye lens. *Investigative Ophthalmology & Visual Science*, 1998; 39(1): 94-103.
50. Siebinga I., Vrensen G.F., Otto K., Puppels G.J., et al. Ageing and changes in protein conformation in the human lens: a Raman microspectroscopic study. *Exp Eye Res* 1992; 54(5):759-67.
51. Smeets M.H., Vrensen G.F., Otto K., Puppels G.J., Greve J. Local variations in protein structure in the human eye lens: a Raman microspectroscopic study. *Biochim Biophys Acta* 1993; 1164(3):236-42.

52. Thomas D.M., Schepler K.L. Raman spectra of normal and ultraviolet-induced cataractous rabbit lens. *Investigative Ophthalmology & Visual Science*, 1980; 19(8): 904-12.
53. Iriyama K., Mizuno A., Ozaki Y., Itoh K., Matsuzaki H. An application of laser Raman spectroscopy to the study of a hereditary cataractous lens; on the Raman band for a diagnostic marker of cataractous signatures. *Current Eye Research*, 1982; 2(7): 489-92.
54. Ozaki Y., Mizuno A., Itoh K., Yoshiura M., et al. Raman spectroscopic study of age-related structural changes in the lens proteins of an intact mouse lens. *Biochemistry*, 1983; 22(26): 6254-9.
55. Mizuno A., Kanematsu E.H., Suzuki H., Ihara N. Laser Raman spectroscopic study of hereditary cataractous lenses in ICR/f-strain rat. *Japanese Journal of Ophthalmology*, 1988; 32(3): 281-7.
56. Huizinga A., Bot A.C., de Mul F.F., Vrensen G.F., Greve J. Local variation in absolute water content of human and rabbit eye lenses measured by Raman microspectroscopy. *Experimental Eye Research*, 1989; 48(4): 487-96.
57. Mizuno A., Nishigori H., Iwatsuru M. Glucocorticoid-induced cataract in chick embryo monitored by Raman spectroscopy. *Investigative Ophthalmology & Visual Science*, 1989; 30(1): 132-7.
58. Takise S., Horiguhi S., Fukumura H., Hayashi K., et al. Morphological change and Raman spectrum of rabbit lens irradiated with ultraviolet laser beam. *Osaka City Medical Journal*, 1989; 35(1): 29-37.
59. Mizuno A., Toshima S., Mori Y. Confirmation of lens hydration by Raman spectroscopy. *Experimental Eye Research*, 1990; 50(6): 647-9.
60. Toshima S., Miyazaki H., Mizuno A. Raman study of the lenses of spontaneously-occurring and streptozotocin-induced diabetic rats. *Japanese Journal of Ophthalmology*, 1990; 34(4): 436-41.
61. Siebinga I., Vrensen G.F., De Mul F.F., Greve J. Age-related changes in local water and protein content of human eye lenses measured by Raman microspectroscopy. *Experimental Eye Research*, 1991; 53(2): 233-9.
62. Horikiri K., Nakajima H., Matsuura T., Narama I., et al. Estimation of structural changes in the cataractous rat lens using Raman spectroscopy. *Jikken Dobutsu. Experimental Animals*, 1992; 41(2): 225-30.
63. Borchman D., Lamba O.P., Ozaki Y., Czarnecki M. Raman structural characterization of clear human lens lipid membranes. *Current Eye Research*, 1993; 12(3): 279-84.
64. Dai S., Qi S., Zhang L., Bai C., et al. Laser Raman spectrometry study on experimental galactose-induced cataract. *Yen Ko Hsueh Pao [Eye Science]*, 1995; 11(3): 143-6.

65. Shun-Shin G.A., Vrensen G.F., Brown N.P., Willekens B., et al. Morphologic characteristics and chemical composition of Christmas tree cataract. *Investigative Ophthalmology & Visual Science*, 1993; 34(13): 3489-96.
66. Borchman D., Ozaki Y., Lamba O.P., Byrdwell W.C., et al. Structural characterization of clear human lens lipid membranes by near-infrared Fourier transform Raman spectroscopy. *Current Eye Research*, 1995; 14(6): 511-5.
67. Duindam H.J., Vrensen G.F., Otto C., Puppels G.J., Greve J. New approach to assess the cholesterol distribution in the eye lens: confocal Raman microspectroscopy and filipin cytochemistry. *Journal of Lipid Research*, 1995; 36(5): 1139-46.
68. Vrensen G.F., Duindam H.J. Maturation of fiber membranes in the human eye lens. Ultrastructural and Raman microspectroscopic observations. *Ophthalmic Research*, 1995; 27(Suppl 1): 78-85.
69. Duindam J.J., Vrensen G.F., Otto C., Greve J. Aging affects the conformation of cholesterol in the human eye lens. *Ophthalmic Research*, 1996; 28(Suppl 1): 86-91.
70. Sato H., Borchman D., Ozaki Y., Lamba O.P., et al. Lipid-protein interactions in human and bovine lens membranes by Fourier transform Raman and infrared spectroscopies. *Experimental Eye Research*, 1996; 62(1): 47-53.
71. Paterson C.A., Zeng J., Husseini Z., Borchman D., et al. Calcium ATPase activity and membrane structure in clear and cataractous human lenses. *Current Eye Research*, 1997; 16(4): 333-8.
72. Mizuno A., Tsuji M., Fujii K., Kawauchi K., Ozaki Y. Near-infrared Fourier transform Raman spectroscopic study of cornea and sclera. *Japanese Journal of Ophthalmology* 1994; 38(1):44-8.
73. Siew DCW, Clover GM, Cooney RP, and Wiggins PM. Micro-Raman Spectroscopic Study of Organ Cultured Corneae. *Journal of Raman Spectroscopy* 1995; 26: 3-8.
74. Goheen SC, Lis LJ, and Kauffman JW. Raman Spectroscopy of Intact Feline Corneal Collagen. *Biochimica et Biophysica Acta* 1978; 536(1): 197-204.
75. Bauer NJC, Wicksted JP, Jongsma FHM, March WF, Hendrikse F, and Motamedi M. Noninvasive Assessment of the Hydration Gradient Across the Cornea Using Confocal Raman Spectroscopy. *Invest. Ophthalmol. Vis. Sci.* 1998; 39(4): 831-835.
76. Frushour B.C. and Koenig J.L. Raman Scattering of Collagen, Gelatin, and Elastin. *Biopolymers* 1975; 14: 379-391.
77. Wicksted JP, Erckens RJ, Motamedi M, and March WF. Raman Spectroscopy Studies of Metabolic Concentrations in Aqueous Solutions and Aqueous Humor Specimens. *Applied Spectroscopy* 1995; 49(7): 987-993.
78. Erckens RJ, Motamedi M, Wicksted JP, and March WF. Raman Spectroscopy for Non-Invasive Characterization of Ocular Tissue: Potential for Detection of Biological Molecules. *J. Raman Spectroscopy* 1997; 28: 293-299.
79. Sebag J., Nie S., Reiser K., Charles M.A., Yu N.T. Raman spectroscopy of human vitreous in proliferative diabetic retinopathy. *Investigative Ophthalmology & Visual Science* 1994; 35(7):2976-80.

80. Eyring G., Curry B., Mathies R., Fransen R., et al. Interpretation of the resonance Raman spectrum of bathorhodopsin based on visual pigment analogues. *Biochemistry* 1980; 19(11):2410-8.
81. Eyring G., Mathies R. Resonance Raman studies of bathorhodopsin: evidence for a protonated Schiff base linkage. *Proceedings of the National Academy of Sciences of the United States of America* 1979; 76(1):33-7.
82. Huang L., Deng H., Koutalos Y., Ebrey T., et al. A resonance Raman study of the C=C stretch modes in bovine and octopus visual pigments with isotopically labeled retinal chromophores. *Photochemistry & Photobiology* 1997; 66(6):747-54.
83. Loppnow G.R., Miley M.E., Mathies R.A., Liu R.S., et al. Structure of the retinal chromophore in 7,9-dicis-rhodopsin. *Biochemistry* 1990; 29(38):8985-91.
84. Oseroff A.R., Callender R.H. Resonance Raman spectroscopy of rhodopsin in retinal disk membranes. *Biochemistry* 1974; 13(20):4243-8.
85. Palings I., Pardoen J.A., van den Berg E., Winkel C., et al. Assignment of fingerprint vibrations in the resonance Raman spectra of rhodopsin, isorhodopsin, and bathorhodopsin: implications for chromophore structure and environment. *Biochemistry* 1987; 26(9):2544-56.
86. Pande C., Deng H., Rath P., Callender R.H., Schwemer J. Resonance raman spectroscopy of an ultraviolet-sensitive insect rhodopsin. *Biochemistry* 1987; 26(23):7426-30.
87. Rimai L., Kilponen R.G., Gill D. Resonance-enhanced Raman spectra of visual pigments in intact bovine retinas at low temperatures. *Biochemical & Biophysical Research Communications* 1970; 41(2):492-7.
88. Yoshizawa T., Imamoto Y. Structure and photobleaching process of chicken iodopsin.
89. Yu N.T., Kuck J.F., Jr., Askren C.C. Laser raman spectroscopy of the lens *in situ*, measured in an anesthetized rabbit. *Current Eye Research* 1981; 1(10):615-8.
90. Mizuno A., Ozaki Y., Kamada Y., Miyazaki H., et al. Direct measurement of Raman spectra of intact lens in a whole eyeball. *Current Eye Research*, 1(10):609-13, 1981.
91. Yu N.T., Cai M.Z., Ho D.J., Kuck J.F., Jr. Automated laser-scanning-microbeam fluorescence/Raman image analysis of human lens with multichannel detection: evidence for metabolic production of a green fluorophor. *Proceedings of the National Academy of Sciences of the United States of America*, 85(1):103-6, 1988.
92. Bot A.C., Huizinga A., de Mul F.F., Vrensen G.F., Greve J. Raman microspectroscopy of fixed rabbit and human lenses and lens slices: new potentialities. *Experimental Eye Research*, 49(2):161-9, 1989.
93. Nie S.M., Bergbauer K.L., Kuck J.F., Jr., Yu N.T. Near-infrared Fourier transform Raman spectroscopy in human lens research [letter]. *Experimental Eye Research*, 51(5):619-23, 1990.

94. Schyns M.W., Huizinga A., Vrensen G.F., de Mul F.F., Greve J. Paraformaldehyde fixation and some characteristics of lens proteins as measured by Raman microspectroscopy. *Experimental Eye Research*, 50(3):331-3, 1990.
95. Yaroslavsky I.V., Yaroslavsky A.N., Otto C., Puppels G.J., et al. Combined elastic and Raman light scattering of human eye lenses. *Experimental Eye Research*, 59(4):393-9, 1994.
96. Goldstein S.R., Kidder L.H., Herne T.M., Levin I.W., Lewis E.N. The design and implementation of a high-fidelity Raman imaging microscope. *Journal of Microscopy*, 184(Pt 1):35-45, 1996.
97. Bakker Schut T.C., Puppels G.J., Kraan Y.M., Greve J., et al. Intracellular carotenoid levels measured by Raman microspectroscopy: comparison of lymphocytes from lung cancer patients and healthy individuals. *Int J Cancer* 1997; 74(1):20-5.
98. Puppels G.J., de Mul F.F., Otto C., Greve J., et al. Studying single living cells and chromosomes by confocal Raman microspectroscopy [see comments]. *Nature* 1990; 347(6290):301-3.
99. Puppels G.J., Garritsen H.S., Kummer J.A., Greve J. Carotenoids located in human lymphocyte subpopulations and natural killer cells by Raman microspectroscopy. *Cytometry* 1993; 14(3):251-6.
100. Puppels G.J., Garritsen H.S., Segers-Nolten G.M., de Mul F.F., Greve J. Raman microspectroscopic approach to the study of human granulocytes. *Biophys J* 1991; 60(5):1046-56.
101. Puppels G.J., Olminkhof J.H., Segers-Nolten G.M., Otto C., et al. Laser irradiation and Raman spectroscopy of single living cells and chromosomes: sample degradation occurs with 514. 5 nm but not with 660 nm laser light. *Exp Cell Res* 1991; 195(2):361-7.
102. Puppels G.J., Otto C., Greve J., Robert Nicoud M., et al. Raman microspectroscopic study of low-pH-induced changes in DNA structure of polytene chromosomes. *Biochemistry* 1994; 33(11):3386-95.
103. Salmaso B.L., Puppels G.J., Caspers P.J., Floris R., et al. Resonance Raman microspectroscopic characterization of eosinophil peroxidase in human eosinophilic granulocytes [see comments]. *Biophys J* 1994; 67(1):436-46.
104. Jongsma F.H.M., Erckens R.J., Wicksted J.P., Bauer N.J.C., et al. Confocal Raman Spectroscopy System For Noncontact Scanning Of Ocular Tissues - an *In Vitro* Study. *Optical Engineering* 1997; 36(11):3193-3199.
105. Tabaksblat R., Meier R.J., and Kip B.J. Confocal Raman Microspectroscopy: Theory and Application to Thin polymer Samples. *Applied Spectroscopy* 1992; 46(1): 60-68.
106. Brenan C.J.H and Hunter I.W. Confocal Image Properties of a Confocal Scanning Laser Visible Light FT-Raman Microscope. *Applied Spectroscopy* 1995; 49(7): 971-976.

Appendix

Formulas

1. Light energy: $E=h\nu$ (in J); with h = Planck's constant, and ν = frequency

2. Wavelength: $\lambda=c/\nu$ (in cm); with c = lightspeed ($\sim 3 \cdot 10^{10}$ cm/sec)

3. Photon-energy: $E_p=1.986 \cdot 10^{-16}/\lambda$ (nm) (in J)

4. Raman scattering frequency (in wave-numbers):
   $\nu=\nu_0-\nu_{vib}$ (Stokes lines)
   $\nu=\nu_0+\nu_{vib}$ (anti-Stokes lines)

5. Wave-number: $\omega=1/\lambda$ (in cm^{-1})

6. Population ratio of molecular vibrational states: $N_1/N_0=\exp(-h\nu_{vib}/kT)$; with N_1 and N_0 = number of molecules in the v"=1 and v"=0 vibrational states in the ground electronic state, respectively; ν_{vib} = difference between incident and scattered frequency; h = Planck's constant; k = Boltzmann's constant; T = the absolute temperature (in Kelvin).

7. Raman intensity: $I=CI_0\nu_s^4\alpha^2$ (in photons/s); with C = constant, I_0 = intensity of incident light, ν_s = frequency of scattered light, and α = molecular polarizability

CHAPTER 3

Confocal Raman spectroscopy system for noncontact scanning of ocular tissues: an *in vitro* study

Franciscus HM Jongsma, Roel J Erckens, James P Wicksted,
Noël JC Bauer, Fred Hendrikse, Wayne F March, Massoud Motamedi

Optical Engineering 1997; 36(11): 3193-3199

ABSTRACT

Purpose: A long-working distance fiber-optic based confocal Raman spectroscopy (CRS) system, operating in the backscatter mode, was developed for rapid non-contact characterization of ocular tissue.

Materials and methods: In vitro near real-time axial scanning through ocular tissue was achieved using a CCD camera and a high numerical aperture long-working distance microscope objective in a telecentric configuration. The system provides high spatial resolution (20-150 μm) of transparent ocular tissues up to 11 mm deep into the eye in a non-contact fashion while utilizing low argon laser power and rapid scanning times (25 mJ) yielding a S/N ratio range from 30-75. To test the performance of the system for characterizing ocular tissue, Raman spectra from rabbit eyes were obtained *in vitro*.

Results: Axial scans of the cornea, the aqueous humor and the lens provided discrete and specific Raman spectra from each tissue, in both the lower and the higher wavenumber region. Characteristic Raman signals common to all tissues are the OH-vibrations (1650 and 3100-3700 cm^{-1}) and the vibrations corresponding to amino acids (Phenylalanine at 1003 cm^{-1}, Tryptophan at 760 and 881 cm^{-1}, and Tyrosine at 646 cm^{-1}). The ocular lens can be identified by three distinct peaks (aromatic- and aliphatic CH stretching and OH bending modes) of which the aromatic CH stretching mode (~3057 cm^{-1}) is lens-specific. The cornea can be identified by the presence of two distinct peaks (aliphatic CH stretching and OH bending), and the absence of the aromatic CH stretching mode. The aqueous humor can be identified by the presence of the OH bending mode, and the lack of the both CH stretching modes.

Conclusion: A long-working distance confocal Raman spectroscopy system may offer a novel technique for the non-contact spatially resolved biochemical characterization of various tissue layers of the anterior segment of the eye.

Introduction

The human eye provides an ideal site for the use of non-contact optical techniques for diagnostic purposes because of the transparency of its tissues to visible and near infrared light.[1,2] However, most of the currently used clinical methods in ophthalmology, such as slitlamp examination of the anterior segment, fundoscopic visualization of the retina and specular microscopy of the endothelial layer of the cornea, provide no specific information on the biochemical properties of the ocular tissues.[2] This however may be of great importance since many ocular diseases involve changes in the biochemical content of the eye. For example, diabetics have an elevated level of glucose in their aqueous humor, the early onset of cataract formation involves changes in the water content of the ocular lens, and a decreased optical acuity is present as a result of increased water content and swelling of the corneal stroma in patients with decreased corneal endothelial function. Thus, a technique capable of detecting these changes in an early stage of the disease could have important diagnostic applications in the practice of ophthalmology.[3,4]

In recent years many studies have explored the potential application of Raman spectroscopy for the biochemical characterization of various tissues.[5-8] In particular, Raman spectroscopy has been applied to investigate various structures of the eye *in vitro*, demonstrating that specific Raman signals can be obtained for the cornea,[9,10] the ocular lens,[11-14] and the vitreous humor.[15] However, these studies have shown that the inherently weak Raman signals generally require the application of high level light doses and long scanning times in order to obtain an acceptable signal-to-noise ratio (SNR). Furthermore, the heterogeneous nature of the tissue structures can significantly contribute to the emission of sizable broad fluorescence which tends to mask most of the Raman signature. The low SNR in both situations is the main reason that *in vivo* ophthalmic applications of Raman spectroscopy have been limited.[11]

Two recent developments could significantly improve the potential biomedical applications of Raman spectroscopy. First, confocal Raman systems have been developed in order to limit the size of the probing volume, thus minimizing the influence of autofluorescence and background noise, and effectively improving the signal-to-noise ratio.[16,17] Puppels et al. recently reported on a confocal Raman microspectrometry setup, specifically optimized for the *in vitro* study of single cells and chromosomes, yielding high signal-to-noise ratio spectra while resolving volumes as small as 1 μm^3.[18] The second development is the application of highly sensitive CCD detectors, which has significantly contributed to the deployment of Raman spectroscopy as a powerful diagnostic tool for characterization of biological materials.

Our main objective has been to develop a Raman spectroscopy system for ophthalmic application, capable of characterizing the biochemical content of the anterior segment of the eye (cornea, aqueous humor and lens). This required the development of a flexible high-gain system capable of assessing all three tissues in a non-contact fashion while using low light dose. Furthermore, the axial depth resolution was considered to be more important in the laminated structure of the ocular tissues than the radial resolution. These considerations led to the development of a novel high-gain, long-working distance fiber-optic based confocal Raman spectroscopy (CRS) system. The system works in a backscattered mode and incorporates a high NA long working distance microscope objective lens in a telecentric configuration. The system provides high spatial resolution (20-150 μm) of transparent ocular tissues up to 11 mm deep into the eye in a non-contact fashion. The fiber-optic probe acts as the pinhole for confocal measurements and for flexible coupling with the spectrometer. The degree of confocality (and consequently the depth resolution) can be adapted to the tissue. A single grating spectrometer with a liquid nitrogen cooled CCD camera is applied for the collection of high signal-to-noise ratio spectra over a large Raman shift range. This manuscript will describe the details of this newly developed confocal Raman spectroscopy system and evaluates its performance in characterizing fresh rabbit eyes *in vitro*.

Materials & Methods

A schematic of the optical components of the confocal Raman spectroscopy (CRS) system is given in Figure 1. The light source is an argon-ion laser (Coherent Radiation model CR-4, Coherent Laser Group, Palo Alto, CA) emitting a linearly polarized beam at 514.5 nm. A combination of a polarization rotator (model 310-21, Spectra Physics, Mountain View, CA) and a beam expander, consisting of a microscope objective (NA=0.66/43x, Bausch and Lomb, Rochester, NY) and a 80 mm achromatic lens (model 06 3200, Spindler & Hoyer Inc., Milford, MA), is used to provide a collimated p-polarized laser beam with a diameter of 12.5 mm, matching the back aperture of the entrance lens ("aus Jena", Planachromat LD, f=10 mm, NA=0.5/25x, Karl Zeiss, Jena, Germany).

To probe ocular tissue with high spatial resolution, it is important to select a microscope objective with adequate compensation with respect to the optics of the target. Most microscope objectives are corrected for the thickness of a cover glass (170 μm), and optical performance diminishes drastically in samples with greater thicknesses (for example the cornea). To ensure effective operation of the CRS system, we have chosen an objective lens as entrance lens ("aus Jena"

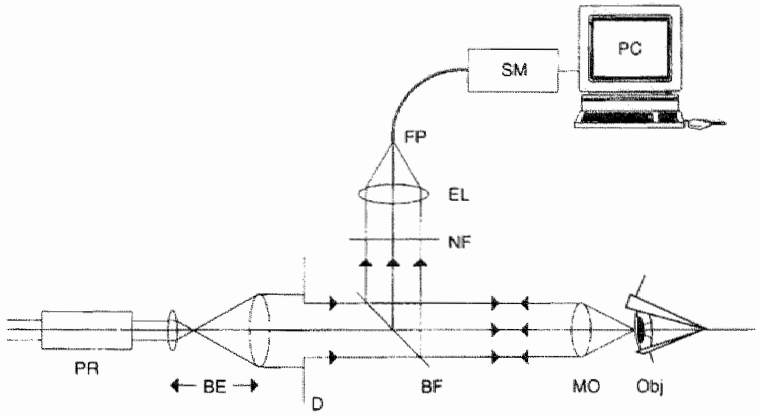

Figure 1. Confocal Raman spectroscopy (CRS) system consisting of a polarization rotator (PR), beam expander (BE), diaphragm (D), band pass filter/Raman scattered light reflector (BF), long working distance microscope objective (MO), notch filter (NF), exit lens (EL), fiber probe (FP), spectrometer (SM), and computer (PC). *See text for details.*

Planchromat) that allows for correcting astigmatism that can be introduced by the optics of the target tissue (for example when probing the ocular lens through the cornea). The entrance lens used in our system is corrected for a 2 mm window glass.[19] If there are no optical barriers between the lens and the sample, a 2 mm thick correction window must be fitted onto the lens to obtain the maximum optical performance. In the integration depth measurements, with the excitation beam focused into the saline through the cuvette, the cuvette wall (1 mm) acts partly as the compensating window. In this case and also while probing the various ocular tissues of the *in-situ* rabbit eye, the correcting optical component was removed from the entrance lens.

Due to the anatomy of the eye, both non-contact detection of the Raman signal and working in a backscattered mode is desired. This is achieved when using the long working distance (~13 mm) entrance lens, of which the secondary conjugate plane is located at infinity. This lens is employed both for focusing the laser light into the sample as well as for collecting the scattered Raman light. Since this lens is part of a telecentric configuration, we are able to obtain a free mechanical distance.[20] This configuration allows us to move the entrance lens axially in order to focus the light within the sample without influencing the position and the size of the spot in the focal plane of the exit lens. Thus, the entrance lens is placed on a translation stage (model 433 with SM-50 actuator, Newport Research Co., Mountain Valley, CA) suitable for micro

positioning (motion = 1 μm, range 51 mm) and can be step wise moved along the optical axis of the Raman probe and sequentially focused in the sample of interest. A holographic beamsplitter (model 514.5NB1, Omega Optical Corporated, Brattleboro, VE) designed to work at a 45° angle with respect to the laser beam serves as a bandpass filter for the incident p-polarized laser beam and also for the backscattered light, allowing most of the scattered Rayleigh light to pass while reflecting the scattered Raman shifted light sideways. The Raman shifted light is then directed through a notch filter (HNF-514-1.0, Kaiser Optical Systems Inc., Ann Arbor, MI) to minimize the effects of elastically scattered light. A camera lens (25 mm, F:0.95, Navitar, Rochester, NY) is used as the exit lens and couples the Raman scattered light into a collection fiber (50 μm core, NA=0.22, CeramOptec, East Longmeadow, MA), which acts as the confocal pinhole and allows for flexible coupling into the spectrometer (Model 500M, Spex Industries, Edison, NJ). The exit lens is diaphragmed to match both the etendue of the telecentric system and the NA (0.22) of the 50 μm collecting fiber. The collecting optics on the spectrometer receives light from the fiber and focuses it with a 0.125 NA onto the 200 μm entrance slit of the spectrometer. The spectrometer has a focal length of 0.5 meter and an aperture of F:4. A holographic type grating blazed at 500 nm with 1200 grooves/mm, a resolution of 0.02 nm and a size of 110 x 110 mm^2, is used to disperse the light. The spectrometer is equipped with a liquid nitrogen cooled backthinned Charge Coupled Detector array (Spectrum One LN_2, Spex Industries, Edison, NJ) consisting of 1024 x 256 pixels with a spectral response of 400-1000 nm. The gain of the CCD was set at 8 electrons / count. Signal processing and presentation are performed by a computer employing DM3000S software (DM3000s ver2.50, Spex Industries, Edison, NJ) interfaced with the Raman spectrometer.

In order to establish the spectral response of the entire system we have used a 100 W Quartz Tungsten halogen lamp (QTH #6333, Oriel, Stratford, CT) at a setting of 12 V and a distance of 50 cm from the entrance lens. The lamp is positioned in its housing which contains lenses that are adjusted to get a collimated beam. The irradiance of the QTH-lamp at 50 cm over the spectral range from 200 to 900 nm was derived using curves, in power units, provided by the company. Spectra with our CRS system are obtained over a broad spectral range from 450 to 750 nm. The spectral response of our entire system is given by: S(I) = Out(I) / In(I) , with Out(I) being the spectral output of our system as it measures the intensity of the light, and In(I) the real spectral irradiance of the QTH-lamp. This response is normalized for a throughput of 13.6% at 632.8 nm, as measured with a Helium-Neon laser (NEC Co., Minato-Ku, Tokyo, Japan) in front of our entrance lens, to obtain the throughput vs. wavelength for unpolarized light.

The performance of the entire confocal system with respect to axial resolution is evaluated in a phantom medium. The phantom medium consists of a fused quartz cuvette filled with saline (0.9% NaCl Irrigation USP, Baxter, Deerfield, IL). In order to demonstrate the advantages of confocal probing, the influence of the fiber diameter on the integration depth is established, by comparing two fibers with a diameter of 50 and 400 μm diameter (400 μm core, NA=0.22, CeramOptec, East Longmeadow, MA), respectively. In both situations 25 mW of argon light was used and all spectra were the result of a single acquisition (1 second). The focal plane of the entrance lens was positioned outside the cuvette, and with step increments of 10 μm the focus was moved towards and into the sample. After background correction, the relative Raman intensity of the OH bending mode at 3430 cm^{-1} was plotted as function of the probing depth.

The ability of the confocal setup to detect Raman spectra of various ocular tissues is examined *in vitro* in four normal eyes of three NZW rabbits (Ray Nichols Rabbitry, TX), less than 10 minutes following euthanasia with 100 mg/kg sodium pentobarbital (Nembutal, Abbot Labs., Chicago, IL). We used the configuration with the 50 μm fiber (integration depth of 120 μm in air), an incident laser power of 25 mW, and an acquisition time of 1 second to obtain the entire spectrum. No spectral averaging was performed, unless mentioned otherwise. Axial scans with step increments of 50 μm were made to obtain spatially-resolved Raman spectra of the cornea, the aqueous humor and the ocular lens. The spectral response of all three tissues is analyzed qualitatively over two Raman shift ranges; the lower region ranges from 300-1833 cm^{-1}, and the higher region ranges from 2580-3750 cm^{-1}. The Raman spectra were baseline corrected by subtracting the offset of the CCD-camera from the raw spectral data. The SNR for the spectral response of each tissue is calculated by dividing its maximum Raman intensity by its noise level at a region without Raman activity (usually ~2750 cm^{-1}).

Results and Discussion

The imperfection in the collimation of the laser beam, objective lens and the holographic beamsplitter, could introduce a considerable distortion in the probing beam size. In order to estimate the actual size of the beamwaist produced using a collimated argon laser beam and microscope objective (25x/NA=0.5), we inserted three pinholes with diameters of 6, 12, and 25 μm in the focal plane of the entrance lens. The measurement of the transmitted laser power through each pinhole showed that 71% of the available laser power was present in the central 6 μm, 21% was present in the ring between the 6 and 12

μm diameters, 7 % in the ring between the 12 and 25 μm diameters, and the remaining 1% outside the 25 μm diameter of the beam. Therefore, the diameter of the beamwaist was estimated to be ~6 μm. Thus, when using 25 mW of laser power the incident irradiance is ~$9 \cdot 10^4$ W/cm^2.

The measured spectral response of the system is shown in Figure 2. The spectrum of the QTH lamp, the measured spectral distribution of this lamp with our CRS system, and the spectral response of the CRS system for unpolarized light are shown in Figure 2A, B, and C, respectively. The spectral response of our entire system depicted in Figure 2C, is highly influenced by the quantum efficiency of the CCD array, in the wavelength range of 400-1000 nm. The large drop around 515 nm is caused by the notch filter, which blocks any Rayleigh scattered light. The small dips around 650 and 680 nm are believed to be caused by the holographic beamsplitter. Since our regions of interest lie in the range of 520-630 nm, where no significant Raman signals can be detected beyond this region, these dips are of minor importance here.

Next, the performance of the CRS system using different size collection fibers (50 μm and 400 μm) was assessed. Saline was used as a phantom because of its relatively strong Raman scattering signature and its biological compatibility. In Figure 3 the normalized Raman peak intensity of the 3430 cm^{-1} Raman mode of saline is plotted against the translation of the entrance lens along the optical axis for the 50 μm fiber. Using this setup, a knife edge response curve for both the small (50 μm) and large (400 μm) collection fiber was obtained, and the depth resolution for both instances could be established. Conventionally, the depth resolution in microscopy has been defined as the full-width-at-half-maximum (FWHM) of a knife edge response curve.[21,22] As described earlier by Tabaksblat et al. this approach is justified in fluorescence microscopy in general but in Raman spectroscopy this approach does not suffice.[23] In a spatial map of, for instance, a fluorescent sample, the spatial differences remain more or less visible even when they are (locally) greatly distorted by the light from out-of-focus planes. However, in Raman spectroscopic sampling where quantitative information is required, the data become unreliable with such a considerable distortion. Therefore we have arbitrarily defined the depth resolution of our system as the change in normalized Raman intensity from 10% to 90% of the maximum signal, comprising the straight part of the knife edge response curve as seen in Figure 3. Thus we determined the depth resolution of the 50 μm fiber to be 120 μm (Figure 3) and 920 μm when using the 400 μm fiber (see also Chapter 2, Figure 8).

Some remarks about the integration depth of this confocal Raman spectroscopy system have to be made. Puppels et al. already noted that, in confocal Raman spectroscopy, the depth resolution for point like objects is controlled by a defocusing effect, in which the Raman signal decreases if the dimensions of the

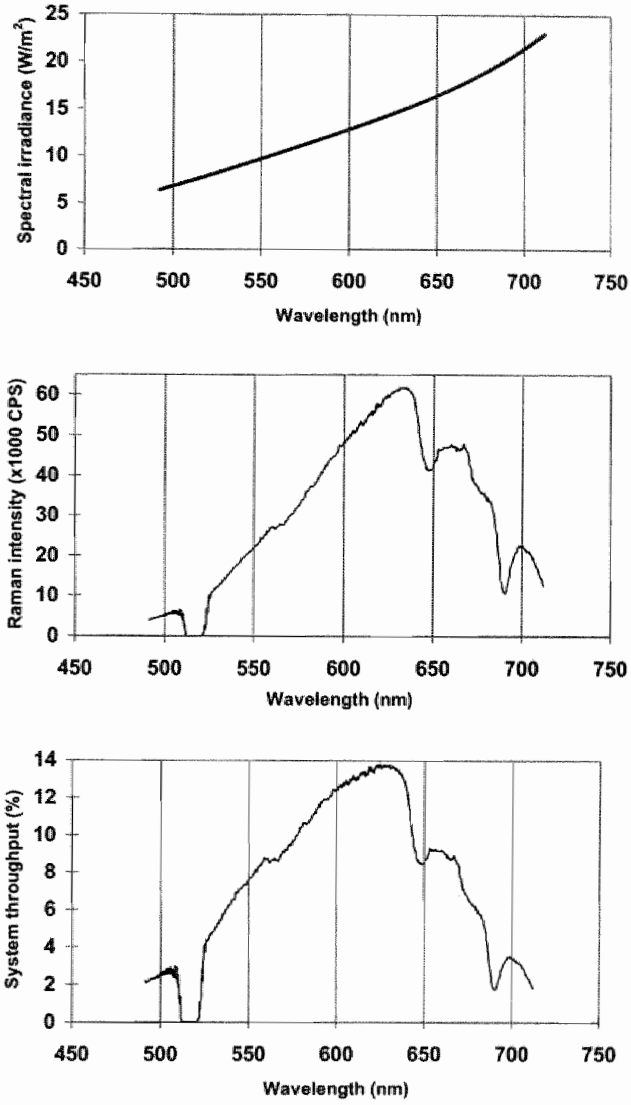

Figure 2. Spectral response of the CRS system for unpolarized light over a range of 500 to 700 nm, normalized for an efficiency of 13.6 % at 632.8 nm. **A**. Spectral irradiance of Quartz Tungsten Halogen (QTH) lamp, **B**. the spectral distribution of the QTH-lamp as measured with the CRS system, **C**. the resulting spectral response of the CRS system (wavelength vs. relative throughput)

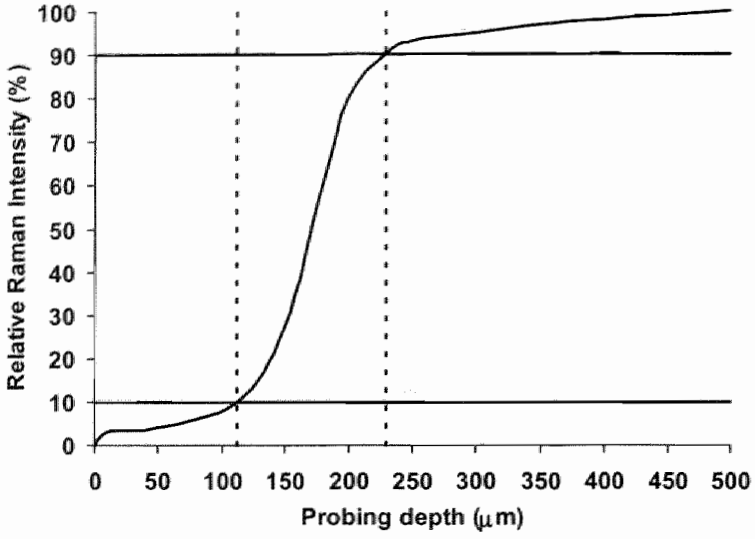

Figure 3. Relative Raman intensity of the OH bending mode of water as function of the distance of the microscope objective in relation to the sample. This resolution in depth "edge response curve" of the CRS setup yields an integration depth of 120 μm with the 50 μm optical fiber. The same setup with the 400 μm optical fiber yielded an integration depth of 920 μm (data not shown). Phantom sample was a quartz cuvette filled with 0.9% saline solution. Step increments through sample were 10 μm.

object are smaller than that of the light cone of the laser focus in the optical axis. This resolution however, is considerably higher than the depth resolution for planar objects (as used in this study), which mainly depends on the spatial filtering of the confocal pinhole.[18] Optimizing the size of this pinhole implies a balance in blocking light from out of focus places (depth of field control) and preserving the Raman signal from the sample under investigation. Puppels et al. explain, that when a planar object is moved along the optical axis through the laser focus, the light intensity on the object decreases as is the case for the point object, but since light intensity times irradiated area remains constant, the Raman intensity from the object will not change.[18] In fact, a decrease of the Raman intensity occurs as the emitter area increases with respect to the lens diameter. This implies that the longer the working distance of the entrance lens is, the less the extent of this decrease will be. Finally, it should also be noted that due to the adaptation of the numerical aperture from the exit fiber to the spectrometer, the minimum width of the entrance slit of the spectrometer must be twice the effective diameter of the exit fiber. Consequently, it depends on the

required spectral resolution if the full gain in light gathering power can be used when using larger fiber diameters. A lot of useful light was lost using the 400 μm fiber at an entrance slitwidth of 200 μm. However, for the biochemical characterization of the ocular tissues, the 50 μm optical fiber was used since it yields a relatively small integration volume and a high SNR (SNR in the cornea is 70 for a laser power of 25 mW and an acquisition time of 1 second). Since the combination of entrance lens (f=10 mm) and exit lens (f=25 mm) provides a sample spot size of 20 μm when using the 50 μm fiber (depth resolution of 120 μm), this volume is considerably larger than the 1 μm^3 sample volume obtained by Puppels et al., using a 63x water immersion objective.[18] However, our objective is not to study single living cells or chromosomes, but to determine the spatially-resolved assessment of various laminated ocular tissues within the eye in a non-contact fashion.

To test the performance of our system in assessing various ocular tissues within the eye, rabbit eyes were characterized *in vitro* (not enucleated after euthanasia of the animal). Axial scans of the cornea, the aqueous humor and the lens provide discrete and specific Raman spectra from each tissue, in both the lower and the higher wavenumber regions, as can be seen in Figures 4A and 4B. In the lower wavenumber range (Figure 4A), we find the so-called 'signature-region'. As far as the aqueous humor is concerned, no distinct features can be seen in the lower spectral range, apart from the region around 1640 cm^{-1} (fundamental bending mode of OH). In the cornea and the lens, we can clearly resolve several peaks. Here we identify only the most clearly resolved features of both tissues. The Amide-modes of proteins can be seen (Amide III ~1225-1275 cm^{-1}, Amide I ~1640-1675 cm^{-1}), and are usually used to study protein conformation, i.e. the α-helix or β-sheet conformation of proteins.[24] Furthermore, several other peaks can be identified for example those corresponding to various amino acids (Phenylalanine at 1003 cm^{-1}, Tryptophan at 760 and 881 cm^{-1}, Tyrosine at ~646 cm^{-1}) and the CH_2/CH_3-bending band at ~1375-1500 cm^{-1}.[25] The peak at ~935 cm^{-1}, which is clearly resolved in the cornea but could not be resolved in the lens, is assigned to C-C stretching vibrations. In the higher wavenumber region from 2580 to 3750 cm^{-1} (Figure 4B), the strong signal of the OH bending mode at ~3100-3700 cm^{-1} and the C-H stretching mode at ~2850-3030 cm^{-1} are clearly distinguishable in both the cornea and the lens, and are mainly caused by the high amount of water and structural proteins in both tissues, respectively. The OH response consists of three resolved peaks.[10] The CH signal depends on the kind of proteins or lipids found in the cornea and the lens. In the cornea mostly collagen, glycosaminoglycans and proteoglycans whereas in the lens the contribution of the lipids and crystallins can be found. In both tissues, the peak at ~2886 cm^{-1} is most likely caused by the antisymmetric stretching mode of CH_2. In both the lens and the cornea a

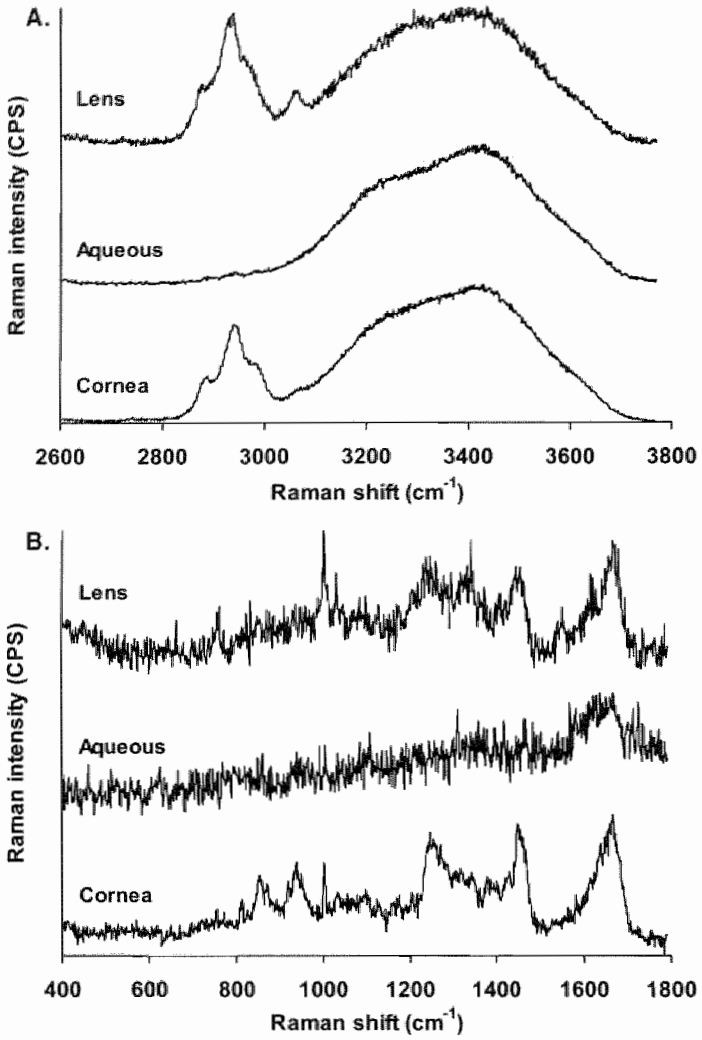

Figure 4. Post mortem Raman spectrum of an *in-situ* eye of a rabbit showing typical Raman spectra for the cornea, aqueous humor, and the lens in both the lower and higher Raman shift region (*see text for details*). Depicted is the Raman intensity as function of the Raman shifted wavelength (cm^{-1}). **A** = higher wavenumber region, **B** = lower wavenumber region. Noteworthy is the decrease in SNR when going from the cornea through the aqueous humor to the ocular lens. SNR for the cornea, aqueous humor and lens spectra is 75, 50, 30, respectively. All spectra are obtained with the 50 μm optical fiber as the confocal pinhole, using 25 mW of sample laser power and acquisition times of 1 second per spectrum (no averaging).

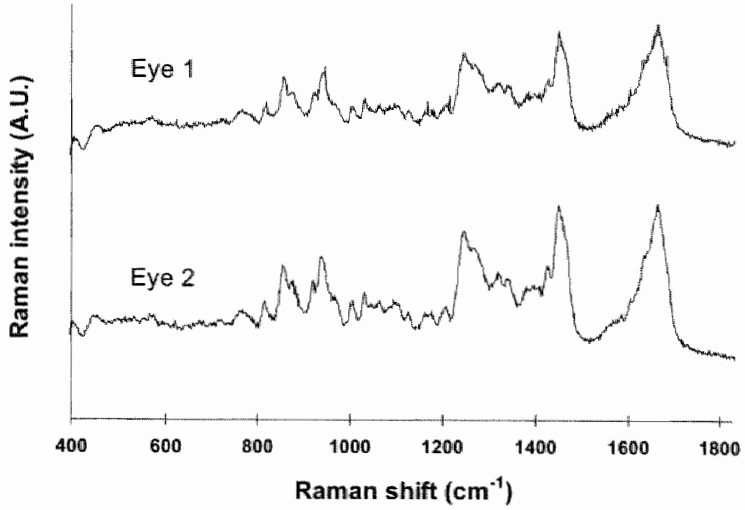

Figure 5. Raman spectra in the lower Raman shifted region (400-1830 cm^{-1}) from two eyes (left and right) of the same rabbit. Parameters: 25 mW sample laser power, 1 second per spectrum (no averaging), 50 μm optical fiber (spectra are digitally smoothed).

combination of the anti-symmetric CH_2 stretch (~2930 cm^{-1}), the symmetric stretching mode of CH_3 (2935 cm^{-1}) together with the out of plane asymmetric CH_3 stretching mode (~2960 cm^{-1}) can be seen. The signal at ~3057 cm^{-1} is the so-called aromatic C-H stretching mode and, as can be seen in Figure 4B, its presence is rather confined to the lens. Thus, a distinction between both the cornea and the lens tissues can be made based on this finding. The aqueous humor mainly shows the spectral response of the OH bending mode since it almost solely consists of water, and its Raman shift position closely resembles that of pure water at ~3400 cm^{-1}. In order to investigate the reproducibility of the tissue signals, four different eyes in three different animals were compared with each other. Figure 5 shows the result in two of these samples. The spectra were obtained from about the same position within the cornea. It can be seen that the spectra show comparable profiles as far as peak positions are concerned.

The Raman intensity of each specific peak depends on the concentration of the molecule(s) that cause it. Therefore, a closer analysis is always necessary to obtain either relative or absolute values for the biochemical content of a certain sample. This was investigated with regard to the phenylalanine peak intensity. The Raman intensity ratio I_{1003}/I_{1640} represents the relative content of phenylalanine, with I_{1003} being the absolute Raman intensity for phenylalanine and I_{1640} being the absolute Raman intensity for the fundamental bending mode

for water. For similar places in the cornea of the four different eyes this ratio was: 0.120, 0.112, 0.125, 0.113, with a mean of 0.118 and a standard deviation of 0.006, proving high reproducibility between tissues from different subjects.

Conclusions

The CRS system as presented here has several unique modalities combining the features of confocal microscopy with Raman spectroscopy. These modalities include: (1) a high NA long working-distance entrance/collection lens with correction for 2 mm window glass in a telecentric configuration, yielding high gain scanning properties for optical sectioning through transparent media in a non-contact fashion; (2) a rapid CCD detector array, for fast spectral acquisition of a broad Raman shift range; (3) controllable integration depth by being able to change the degree of confocality by adjusting the collection fiber diameter.

In summary, the novel confocal Raman spectroscopy system allows for the non-contact spatially-resolved biochemical characterization of the anterior ocular segment. However, future ophthalmic applications of this system requires determining the optimum dose of light for safe diagnosis as well as the integration of an eye tracking system which will correct for movement artifacts.

Acknowledgements

The experiments for this study were performed in the Biomedical Laser and Spectroscopy Program at UTMB, Texas and funded in part by a grant from the Department of Energy and a Research to Prevent Blindness Development Grant.

References

1. P. Gwynne, "A new window on biomedicine with spectroscopy," *Biophotonics* 1, 52-59 (1994).
2. B. R. Masters, *Non-invasive Diagnostic Techniques in Ophthalmology*, Masters B.R. Ed., Springer-Verlag, New York, NY (1990).
3. J. Eppstein and S. E. Bursell, "Non-invasive detection of diabetes mellitus," in *Proceedings of the Physiological Monitoring and Early Detection Diagnostic Methods Symposium*, SPIE 1641, (1992).

4. J.A. van Best and P.H. van Gessel, "Autofluorescence and light scatter in the human lens as measured by a fluorophotometer," *Experimental Eye Research* 49, 511-3 (1989).
5. C.J. Frank, R.L. McCreery and D.C. Redd, "Raman spectroscopy of normal and diseased human breast tissues," *Analytical Chemistry* 67, 777-83 (1995).
6. A. Mizuno, T. Hayashi, K.Tashibu, S. Maraishi, K. Kawauchi and Y. Ozaki, "Near-infrared FT-Raman spectra of the rat brain tissues," *Neuroscience Letters* 141, 47-52 (1992).
7. R.H. Clarke, J.M. Isner, T. Gauthier, K. Nakagawa, F. Cerio, E. Hanlon, E. Gaffney, E. Rouse, and S. DeJesus, "Spectroscopic characterization of cardiovascular tissue," *Lasers in Surgery & Medicine* 8, 45-59 (1988).
8. M. Pezolet, M. Pigeon-Gosselin, R. Savoie and J.P. Caille, "Laser Raman investigation of intact single muscle fibers. On the state of water in muscle tissue,"*Biochimica et Biophysica Acta* 544, 394-406 (1978).
9. S. C. Goheen, L.J. Lis, and J.W. Kauffman,"Raman spectroscopy of intact feline corneal collagen," *Biochimica et Biophysica Acta* 536, 197-204 (1978).
10. D.S.W. Siew, G.M. Clover, R.P. Cooney, P.M. Wiggins, "Micro-Raman spectroscopic study of organ cultured corneae," *J. Raman Spec. 26*, 3-8 (1995).
11. N-T. Yu, J.F.R. Kuck,Jr. and C.C. Askren,"Laser Raman spectroscopy of the lens *in situ*, measured in an anesthetized rabbit," *Current Eye Research* 1, 615-618 (1982).
12. N-T. Yu, M.Bando, J.F.R. Kuck,"Fluorescence/Raman intensity ratio for monitoring the pathologic state of human lens," *Investigative Ophthalmology & Visual Science* 26, 97-101 (1985).
13. A.C.C. Bot, A. Huizinga, F.H.M. de Mul, G.F.J.M. Vrensen, J. Greve. "Raman microspectroscopy of fixed rabbit and human lenses and lens slices: new potentialities," *Experimental Eye Research* 49, 161-169 (1989).
14. S. Dai, S. Qi, L. Zhang, C. Bai, T. Ni, X. Deng, "Laser Raman spectrometry study on experimental galactose-induced cataract. Yen Ko Hsueh Pao [Eye Science] 11(3), 143-6 (1995).
15. J. Sebag, S. Nie, K. Reiser, M.A. Charles, and N-T Yu, "Raman spectroscopy of human vitreous in proliferative diabetic retinopathy," *Investigative Ophthalmology & Visual Science* 35, 2976-80 (1994).
16. J. Pawley, *Fundamental Limits in Confocal Microscopy. Handbook of biological confocal microscopy*, J.B. Pawley, Ed., pp. 15-26, Plenum Press, New York and London (1990).
17. G.J. Brakenhoff, P. Blom, and P. Barends, "Confocal scanning light microscopy with high aperture immersion lenses," *J. of Microsc.* 117, 219-32 (1979).
18. G.J. Puppels, W. Collier, J.H.F. Olminkhof, C. Otto, F.M.M. de Mul, and J. Greve,"Description and performance of a highly sensitive confocal Raman microspectrometer," *J. Raman Spec.* 22, 217-25 (1991).

19. H. Beyer, H. Riesenberg, *Handbuch der Mikroskopie*, VEB Verlag Technik, Berlin 1988).
20. D. W. Slaaf, R. Alweijnse, and H. Wayland,"Use of telescopic imaging in intravital microscopy: a simple solution for conventional microscopes," *International Journal of Microcirculation: Clinical and Experimental* 1, 121-134 (1982).
21. H. T. M. van der Voort, G. J. Brakenhoff, and G. C. A. M. Janssen, "Determination of the 3-dimensional optical properties of a confocal scanning lasermicroscope," *Optik* 70, 48-53 (1988).
22. R. W. Wijnaendts van Resandt, H. J. B. Marsman, R. Kaplan, J. Davoust, E. H. K. Stelzer, and R. Stricker,"Optical fluorescence in three dimensions: microtomoscopy," *J. Microsc.* 138, 29-34 (1985).
23. R. Tabaksblat, R. J. Meier, and B. J. Kip, "Confocal Raman Microspectroscopy: theory and application to thin polymer samples," *Appl. Spec.* 46, 60-8 (1992).
24. I. Siebinga, G.F.J.M Vrensen, K. Otto, G.J. Puppels, F.F.M. de Mul, J. Greve. "Ageing and changes in protein conformation in the human lens: a Raman microspectroscopic study," *Exp. Eye Res.* 54, 759-67 (1992).
25. A. Mizuno and Y. Ozaki, "Aging and cataractous process of the lens detected by laser Raman spectroscopy," *Lens & Eye Tox. Res.* 8(2-3), 177-187 (1997).

CHAPTER 4

Applications of confocal Raman spectroscopy for biochemical characterization of ocular tissues and fluids

Noël JC Bauer, Massoud Motamedi, James P Wicksted,
Gerwin Jan Puppels, Wayne F March, Fred Hendrikse

Submitted

ABSTRACT

The first and, until recently, only report on the *in vivo* application of Raman spectroscopy (RS) in the eye was published in 1981 by Yu et al. It showed promising results on obtaining high signal-to-noise ratio Raman spectra of the intraocular lens of an anesthetized rabbit. The lack of spatial resolution and the need for high, potentially hazardous, laser light energies have limited the *in vivo* application of RS in the eye. Hence we initiated investigations into the application of Raman spectroscopy for biochemical characterization of ocular tissues and fluids under *in vivo* circumstances.

The proposed optical system consisted of a high gain and sensitive confocal Raman spectroscopy (CRS) system with a long working distance enabling non-contact optical sectioning of the pre-corneal tearfilm, the cornea, the aqueous humor, the ocular lens, and the vitreous humor *in vivo*. This paper summarizes our investigation into the potential uses of a this optical system for diagnostic purposes in the field of ophthalmology.

Apart from the biochemical characterization and identification of normal rabbit ocular tissues *in vivo*, the main topics in this paper deal with the *in vivo* application of CRS for the assessment of transport rates of a topical ocular drug from the pre-corneal tearfilm into the cornea, the assessment of the extent and distribution of corneal hydration in the rabbit eye under normal conditions, directly after epithelial debridement, and during corneal procurement, and the assessment of corneal hydration in legally blind patients. Furthermore, the potential use of CRS for non-contact biochemical characterization of the aqueous humor for diagnosing and monitoring systemic metabolic alterations such as diabetes mellitus and phenylketonuria was investigated *in vitro*. In addition, the potential application of CRS for non-contact intraocular temperature measurements is described. Lastly, future clinical application of CRS in the seeing human eye is considered with the eye on system safety and practicality.

The CRS system portrays various advantageous characteristics such as an inherently high specificity, non-contact probing, rapid biochemical characterization of complete tissues, the confocal property, enabling optical sectioning and effectively increasing the signal-to-noise ratio, and the ability to apply this optical system *in vivo*. Hence it is concluded that CRS is suitable for biochemical characterization of ocular tissues and fluids in a non-contact manner under *in vivo* circumstances.

Introduction

Raman spectroscopy (RS) is an optical vibrational spectroscopic technique. It provides detailed information about the molecular composition of a sample and about molecular structure and interactions between molecules. It enables non-contact investigation of very small samples or sample volumes, e.g. multi-component analysis of complex molecular mixtures. The optical design of the sampling compartment of a Raman instrument can easily be optimized to the specific application. For biological or biomedical applications Raman spectroscopy holds a significant advantage over infrared spectroscopy, which provides information of the same nature. Water strongly absorbs in the infrared. This makes it very hard to obtain infrared spectra of the molecules of interest in solution or in the presence of water. The Raman signal of water on the other hand does not appreciably interfere with the other Raman signals of the molecules of interest.

Applications of RS in biology and medicine have been the field of interest of many investigators.[1] Our investigations deal with the application of RS in the anterior portion of the eye, including the tearfilm, the cornea, and the aqueous humor. The eye as a whole consists of different lamellar tissue structures, each with a different biochemical content, optical properties, thickness, intraocular location, and light-sensitivity, which poses a challenging problem. Thus, our initial aim was to apply a novel confocal Raman spectroscopy (CRS) system for non-contact biochemical characterization of ocular tissues.[2] We have applied this technique under *in vivo* circumstances to assess the spatial distribution of corneal hydration and the drug transport through the eye.[3,4] Furthermore we were the first to apply this technique in legally blind subjects to detect changes in corneal hydration after topical application of a dehydrating agent.[5] In addition, we have shown that CRS could play a significant role for the non-contact detection of biomolecules in the aqueous humor.[6] These and various other potential applications of Raman spectroscopy in the anterior region of the eye are the subject of this paper.

Methods

The characteristics and performance of the confocal Raman spectroscopy system that we used (Figure 1) are discussed in more detail elsewhere.[2] The monochromatic light is provided by either an argon (514.5 nm) or a helium-neon (632.8 nm) laser. Since the Stokes-lines of interest in a Raman spectrum lie in the region from 0 to 3800 cm^{-1}, the application of either laser source will result in spectra with a frequency range within the detection limits of

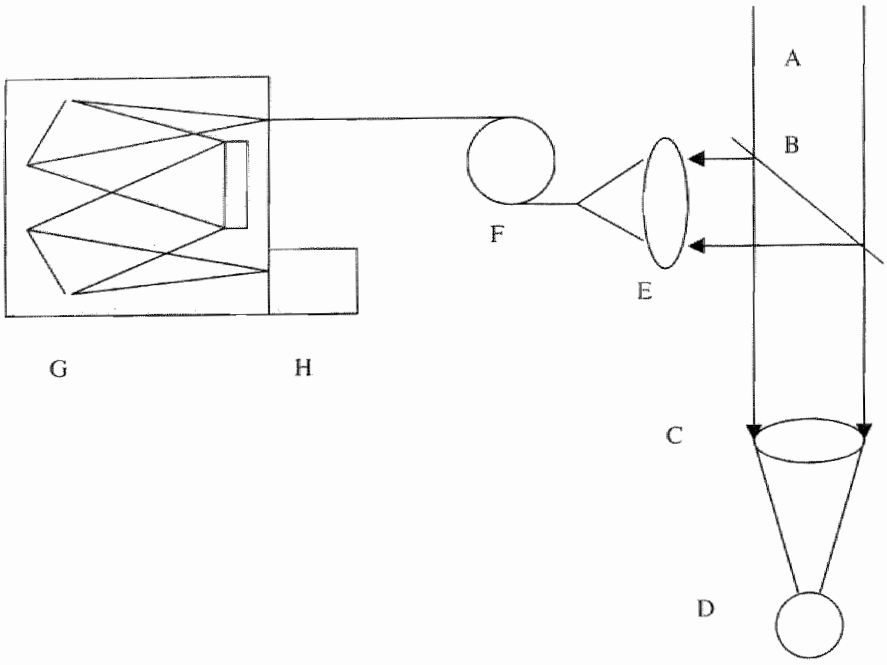

Figure 1. Schematic of the confocal Raman spectroscopy system. A = collimated laser beam; B = beamsplitter; C = long working-distance microscope objective lens; D = sample (i.e. the eye); E = exit lens; F = optical fiber; G = spectrometer; H = CCD-camera.

the photon-counting device, a liquid nitrogen cooled charge coupled device (CCD; detection limits 400-1000 nm with a maximum quantum yield of 80% at ~700 nm). A long working distance microscope objective (LDMO, 25x, NA0.5, working distance 13 mm) is employed in a 180° backscatter configuration, and is used both for focusing the laser light onto the sample as well as for collecting the backscattered light. Furthermore, this lens is part of a telecentric setup allowing for axial displacement of this microscope lens without changing the focal distance at the exit lens, yielding axial scanning capabilities. The LDMO permits non-contact sampling of all ocular tissues of the anterior segment from tearfilm to the anterior vitreous humor just behind the ocular lens. An optical fiber at the exit site of the optical system is used for transporting the Raman scattered light to the spectrometer, but also acts like a confocal pinhole. The confocal configuration increases the signal-to-noise ratio (SNR) by decreasing the detection of light from out of focus places. By choosing the appropriate fiber diameter (diameters ranging from 4 to 80 μm, or larger) probing volumes can be obtained that are either much larger or much smaller

than the thickness of the tissue we prefer to probe, with a range of 20 to 225 μm, or larger. Depending on the experiments, we used laser light exposures of 3 mJ (6 mW for 0.5 s) to 3 J (50 mW for 60 s). The animal studies mentioned in this manuscript were performed in accordance with the ARVO Resolution on the Use of Animals in Research, while the reported human study was performed after approval of our Institutional Review Board and after signed informed consent.

Results

Raman spectra of normal ocular tissues *in vivo*

Using CRS we were able to obtain high SNR Raman spectra from all ocular media of the normal rabbit eye under *in vivo* circumstances, from pre-corneal tearfilm to the vitreous humor. The Raman features of these spectra are very specific for the tissues they originate from (Figure 2), thus RS can be applied to differentiate between the various ocular tissues. Even within the same tissue, biochemical differences can be observed, noticeable in both the lower as well as the higher Raman spectral region. In the higher Raman shift region for example, we can observe that the Raman intensity of the OH-vibrational modes (~3100-3700 cm^{-1}) in relation to the CH-vibrational modes (~2800-3050 cm^{-1}), is significantly higher in the posterior than the anterior region of the cornea. This corresponds well with the spatial distribution of corneal hydration as assessed using various other biochemical assays.[7] For the ocular lens, the hydration is higher in the cortex than in the nucleus as indicated by the lower Raman intensity ratio OH/CH in the central region of the lens, also in accord with the current literature.

The next few paragraphs will describe the potential applications of CRS in the tearfilm, the cornea, and the aqueous humor, respectively.

The tearfilm

Topical application of ocular drugs forms an important part of ocular therapy. It should be clear that the efficacy of topical ocular drugs or drug delivery systems is of utmost importance for a successful treatment. Factors that determine this efficacy, apart from the actual working mechanism on receptor level at the target tissue, include the rate of absorption, distribution, and elimination of the drug, called the pharmacokinetic behavior of the drug. In other words, how much of the drug gets to the target tissue at what speed and how long is its working action. This can be quantified by determining the drug

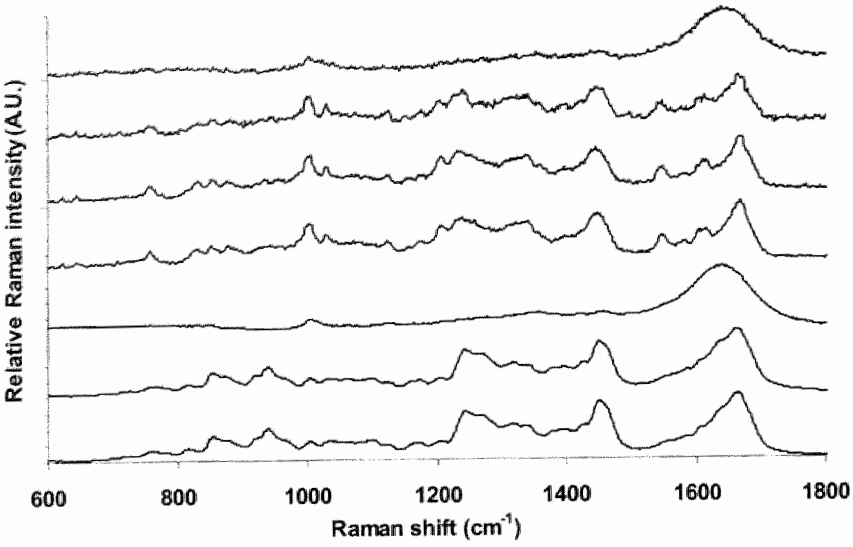

Figure 2A. Typical Raman spectra of a normal rabbit eye under *in vivo* conditions in the lower Raman shift region. From bottom to top: anterior cornea, posterior cornea, aqueous humor, anterior lens cortex, lens nucleus, posterior lens cortex, vitreous humor.

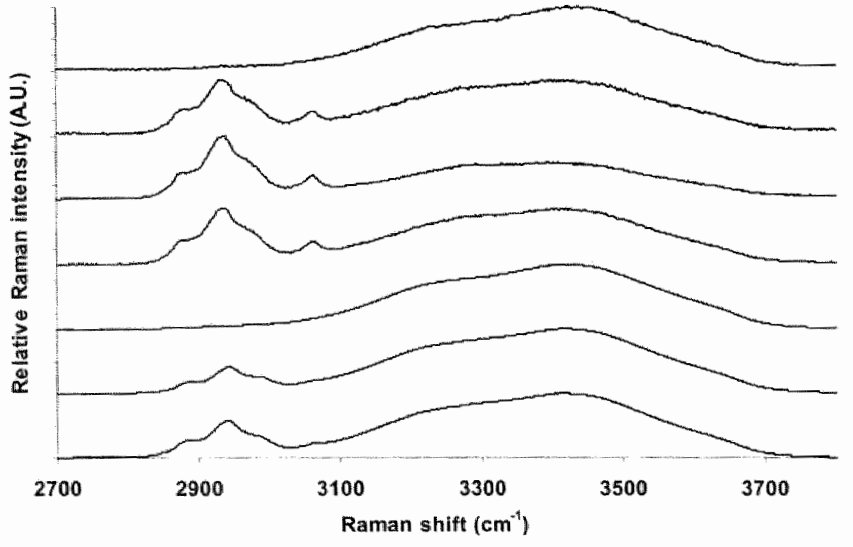

Figure 2B. Typical Raman spectra of a normal rabbit eye under *in vivo* conditions in the higher Raman shift region. From bottom to top: anterior cornea, posterior cornea, aqueous humor, anterior lens cortex, lens nucleus, posterior lens cortex, vitreous humor.

concentration as a function of time in the tissues of interest. For topical ocular drugs that have a target tissue situated inside the eye, such as anti-inflammatory or anti-glaucoma drugs, it is important to know how well this drug crosses the various barriers that lie between the site of application and the site of action. Nowadays, pharmacokinetic measurements are mainly performed using invasive methods by quantifying drug concentrations in cornea or aqueous humor specimens *ex vivo* utilizing sensitive assays such as high performance liquid chromatography (HPLC).[8] Apart from the potential introduction of artifacts it is clear that these invasive methods are rather destructive to the eye. The consequent need to use animal models has disadvantages because of the obvious differences in anatomy and physiology in relation to the human, and the non-continuous sampling, since one animal is used for one measurement. Non-contact means of determining the drug concentration in ocular tissues are limited to the quantification of drug concentrations by means of fluorescence detection. Although this method is sensitive and is safe to be applied in humans, fluorometry is rather unspecific. An ideal method for pharmacokinetic measurements should thus be non-invasive, sensitive, drug-specific, and enable quick and continuous assessment of drug concentrations over time in one and the same tissue. We have investigated if RS could be utilized to quantify drug concentrations in the eye using its inherent specificity and non-contact character. The first step in our investigations entailed the assessment of drug-concentrations as a function of time in the anterior most part of the living rabbit eye. Using a fiber diameter of 50 μm, an integration depth could be achieved of 120 μm, exclusively probing the tear-film and corneal epithelial layer, the most important obstructive barrier to almost all topical ocular drugs. Figure 3 depicts the Raman spectra in the lower Raman shift region that we would find in a typical pharmacokinetic experiment in the living rabbit eye, after topical application of a clinically used anti-glaucoma medication with a specific Raman signal at 1420 cm^{-1}. First of all it can be seen that the specificity of RS can be applied to discriminate between drug and tissue signals, since no Raman peak is found at 1420 cm^{-1} in the normal cornea before drug application. In addition, an important observation is that all measurements are performed in one and the same eye, thus fewer animals are needed in relation to conventional pharmacokinetic studies. Furthermore, it can clearly be seen that the Raman peak intensity at 1420 cm^{-1} decreases as a function of time due to drug absorption into the cornea and non-absorptive losses from the tearfilm. By quantifying this peak intensity as a measure for the relative drug concentration at sufficiently spaced time intervals, we were able to construct reproducible pharmacokinetic drug-concentration vs. time curves.[4] Using these pharmacokinetic curves, rate constants for the drug transport from the tearfilm to the anterior cornea could be determined for this drug. Given these results we believe that confocal Raman

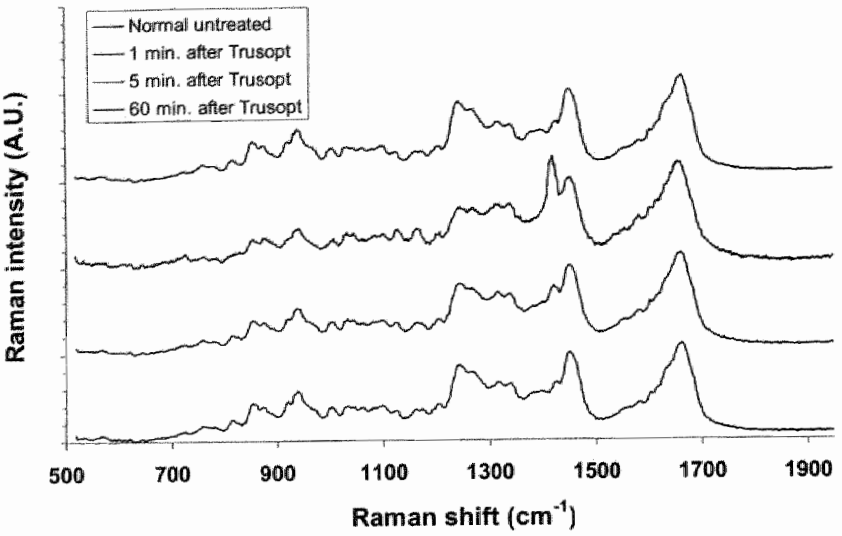

Figure 3. Raman spectral features of the anterior region of the cornea during pharmacokinetic measurements. From top to bottom: prior to drug deposition (normal), 1, 5 and 60 min. after drug deposition.

spectroscopy could be a valuable tool for pharmacokinetic measurements, and with adequate improvements in the system, in particular the safety, could potentially be used in the human situation (Chapter 7 of this thesis).

The cornea

The cornea forms the anterior border of the eye and consists almost entirely of water (>75%) and structural proteins, mostly collagen. The cornea is transparent because it is devoid of blood vessels, contains only a small number of cells, but mostly because of the spacing between the collagen fibrils which in turn is closely related to the hydration of the cornea. Corneal hydration is actively regulated by a single layer of cells at the posterior site of the cornea, the endothelial layer, which acts by pumping water out of the cornea which, by virtue of its swelling pressure, has the tendency to imbibe water. Dysfunction of the endothelial layer can lead to an increase in corneal hydration and corneal swelling which effectively increases the spacing between the collagen lamellae, consequently leading to increased light scattering and some degree of vision loss. Since current methods to assess corneal hydration can only detect gross changes or do not possess the capabilities to perform spatially resolved measurements *in vivo*, we decided to investigate the possibility of non-contact RS to perform

these kinds of measurements (Chapter 5 of this thesis). Huizinga et al. have shown that the Raman intensity ratio of the OH-mode (at ~3390 cm^{-1}) vs. the CH-mode (at ~2935 cm^{-1}) is in direct proportion to the hydration of the ocular lens.[9] We employed a similar ratio in order to quantify corneal hydration under *in vivo* circumstances. Figure 4A shows the Raman spectra in the higher Raman shift region of a rabbit cornea at different degrees of hydration; completely dehydrated after lyophilization (H=0 mg water / mg dry wt.), normally hydrated (H=3.05) and hyper-hydrated (H=8.3). The confocal configuration of our system permitted adjustment of the integration depth to 1/10th of the corneal thickness, yielding the possibility to spatially resolve corneal hydration along the optical axis of the cornea. We employed CRS for these kinds of measurements *in vivo* under normal circumstances, and also documented the changes in corneal hydration over time during normal exposure of the living eye to the surrounding environment.[3] Typical results of spatially resolved corneal hydration measurements are shown in Figure 4B. Clearly noticeable is the distinct difference in stromal hydration between the anterior and the posterior region of the cornea, in agreement with our current knowledge on the non-homogeneous distribution of water in the cornea. This kind of assessment might be clinically useful to diagnose local variations in water content as a result of therapeutic interventions such as photorefractive keratectomy or topical application of ocular drugs, or as a result of local or systemic alterations in corneal physiology indicative of impending pathology, as is the case in various forms of corneal dystrophies. Furthermore, time-resolved assessment of the distribution of water in the cornea might possibly be used to further our understanding in corneal deturgescence under various hyper- or hypo-osmotic perturbances. Spatially resolved hydration measurements can also be performed in the radial direction (Figure 4C). These results too agree favorably with the literature because corneal hydration has been found to be higher at the periphery than in the central part of the cornea.[10] The clinical relevancy of these results has still to be determined.

Several studies have stressed that corneal hydration could play an important role with regards to the therapeutic outcome and the observed side effects of laser refractive surgery of the cornea.[11,12,13] During the normal procedures of this kind of treatment, corneal hydration can change as a result of the application of a topical anesthetic, the removal of the epithelial layer, called corneal debridement, and the laser-tissue interaction itself. Thus, an attractive hypothesis is that a more accurate prediction of the therapeutic outcome is preceded by a better understanding of the laser–tissue interaction, especially through the assessment of changes in corneal hydration during this treatment. At present, corneal hydration is estimated through assessing corneal thickness (pachymetry) at merely one point in time: after topical application of the anesthetic and before

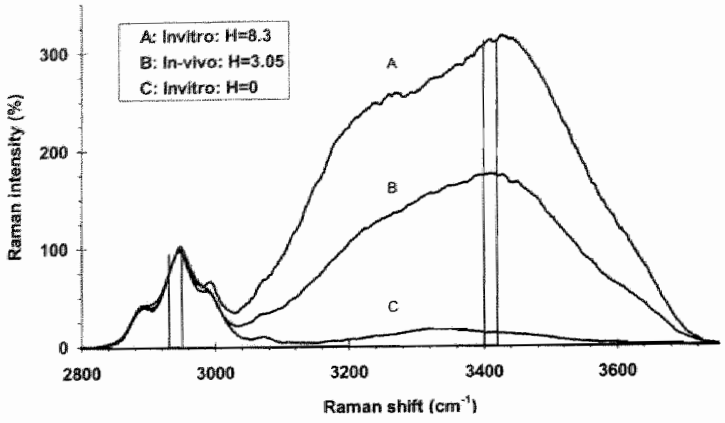

Figure 4A. Raman spectra in the high spectral region of the medial corneal stroma as assessed using standard methods. (A) hyper-hydrated, (B) normal, and (C) lyophilized cornea. Spectra are normalized to the Raman peak of the CH-vibrational mode at ~2950 cm^{-1}.

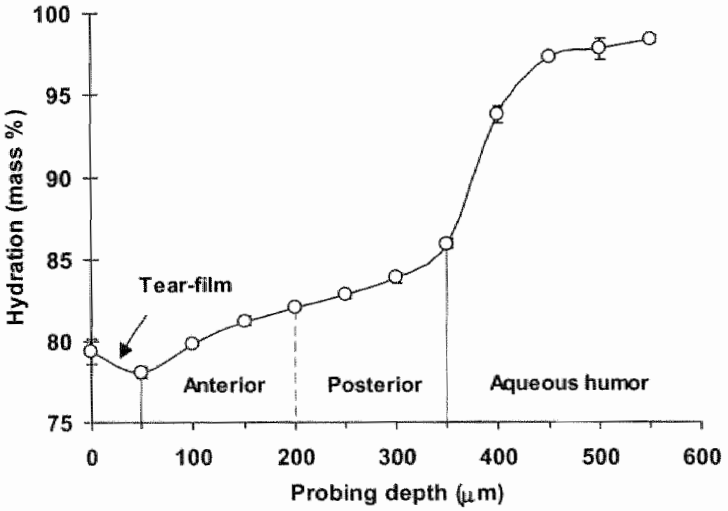

Figure 4B. Spatially resolved hydration assessments using CRS along the optical axis of the rabbit eye under *in vivo* conditions (average of 3 assessments).

corneal debridement. Furthermore, the routinely used ultrasound pachymetry can only determine the full thickness of the cornea, but is unable to assess local variations in corneal hydration, specifically of the corneal region to be treated. Thus, we decided to use CRS to document the acute changes in hydration of

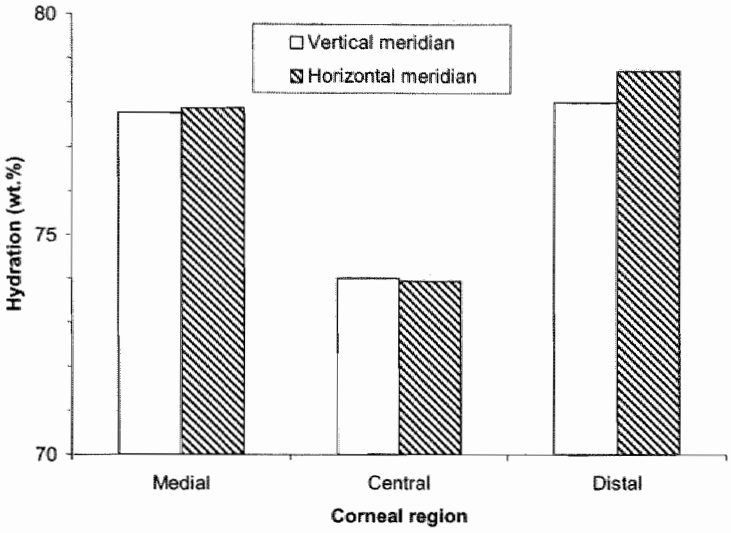

Figure 4C. Spatially resolved corneal hydration assessments using CRS at similar regions of the superficial corneal stroma along the vertical and horizontal meridian in the rabbit eye under *in vivo* conditions.

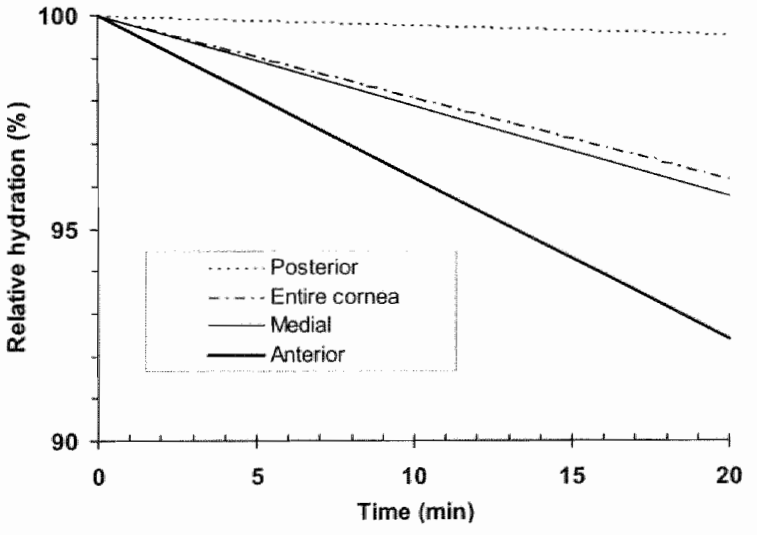

Figure 4D. Assessment of the changes in corneal hydration as assessed using CRS of various corneal regions of the *in vivo* rabbit eye (n=7) as a function of time after epithelial debridement.

the anterior part of the cornea after epithelial debridement in the rabbit under *in vivo* circumstances. Figure 4D shows the changes in stromal hydration of various regions within the rabbit cornea (n=7 eyes) under *in vivo* circumstances, as well as of the full thickness stroma hydration as a function of time after de-epithelialization. Significant changes in corneal hydration were noticed during the whole time-interval after de-epithelialization in the anterior and medial stromal region, but not at the posterior site (0.38, 0.21, and 0.02 % dehydration per minute, respectively). The relevance of these time-dependent changes has yet to be determined, certainly because the inter-sample variation was found to be significantly higher than these dehydration rates. This led to the preliminary conclusion, that it might be valuable to assess corneal hydration from a subject to subject basis, in order to have a better control over the ablation process during photo-refractive surgery of the cornea. By reducing the variability caused by cornea hydration, the predictability of the refractive outcome might eventually be increased.

The assessment of the function of the endothelial layer is of utmost importance in order to determine the well-being of a cornea, especially prior to transplantation, and can be estimated through assessing corneal hydration (see above). A study by Siew et al. recently reported on the potential use of RS for the assessment of corneal hydration in organ cultured corneas, possibly applicable for the quality control of transplant corneas.[14] A more sensitive and specific means of determining corneal viability could mean that the number of suitable corneas that would normally be discarded using other methods could possibly be reduced. Siew et al. observed significant changes in full thickness corneal hydration that could be related to type of storage medium and concluded that RS might make a valuable contribution to the quality control of eye bank corneas. We went one step further since we found it of significant interest to investigate the *spatial distribution* of corneal hydration as a function of *storage time*, with the hypothesis that endothelial dysfunction might manifest itself through significant changes in hydration at the posterior region of the cornea. Our initial experiments entailed the assessment of the spatially-resolved corneal hydration as described earlier (Ref. 3) of rabbit corneas under *in situ* circumstances, and after enucleation and storage of the same eye in a moist chamber at 4°C for different periods of time. Typical results are shown in Figure 4E in graphical format for one cornea. The most striking feature of this Figure is the increase in hydration at the posterior site of the cornea from ~120 to 190 minutes after euthanasia, possibly due to the anti-metabolic effect of the euthanasia agent, effectively 'slowing' the endothelial cells down and causing local swelling of the cornea. After an initial dehydration of the anterior corneal region in the first ~20 minutes after enucleation corneal hydration reaches an equilibrium. Storage of the whole eyes causes the whole cornea to swell gradually,

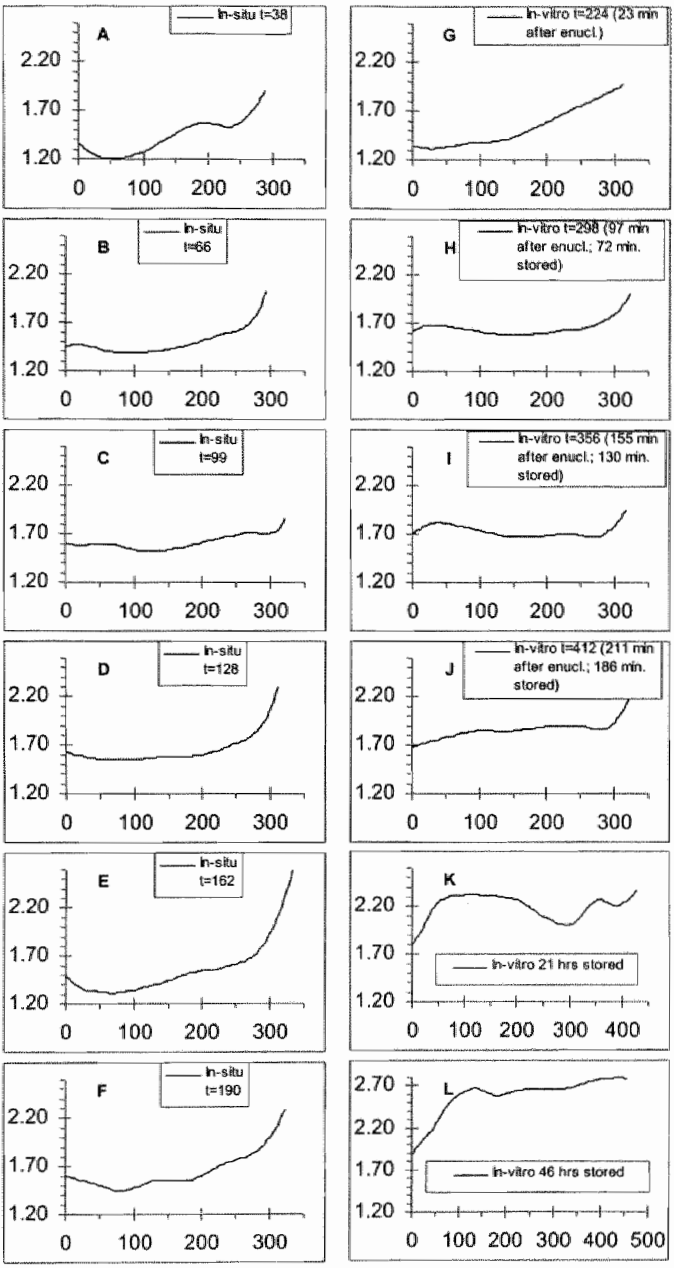

Figure 4E. The extent (y-axis) and distribution (x-axis) of corneal hydration as assessed using CRS in an experiment resembling corneal procurement (*see also Figure 4F*). Graph *A* through *F* are obtained with the eye still *in-situ* (time *t* after euthanasia of the rabbit). Graph *G* is obtained just after enucleation of the eye and just prior to cold storage. Graph *H* through *L* are obtained as a function of time after cold storage of the whole bulb at 4°C.

which is depicted in numerical format in Figure 4F. Here the absolute water content of the anterior and posterior corneal stroma is plotted as a function of storage time. It can be seen that within three hours of storage, the difference between anterior and posterior stromal hydration has become insignificant, and both regions hydrate at an equal rate thereafter. The function of the endothelial cell layer, i.e. corneal hydration *control*, was not monitored in our or Siew's study. This requires the assessment of corneal hydration over a continuous period of time at physiological temperatures in order to quantify corneal deswelling as a measure of the pump function of the endothelial layer. This however can also be performed utilizing RS (see for example Figure 4B in Ref. 3) and remains one of the interesting focuses of our studies.

With the experience gained from our animal experiments and preceding future clinical studies, we extended our investigations to the human situation. In two legally blind human subjects the hydration of the cornea was assessed using CRS, before and after topical application of a mild corneal dehydrating agent. Movement artifacts were unavoidable in the conscious humans, and prevented spatially resolved measurements. Thus, the focus of the laser beam was maintained at the same superficial region of the cornea during the time of probing. Significant changes in corneal hydration could be observed in one subject but not the other because of the frequent blinking (Chapter 6 of this thesis).

Pterygia

A pterygium is a treatable ailment of the eye with an incompletely understood pathology, and entails the occurrence of abnormal fibrovascular tissue that can invade the cornea potentially obstructing vision. Most of the time this growth is benign but in rare occasions can turn malignant. More importantly, after surgical removal of the pterygia a large percentage of patients experience recurrences. Thus, we investigated the possibility of using Raman spectroscopy as a diagnostic tool for the biochemical assessment of (superficial) ocular pathologies, such as pterygia. In Figure 5 typical (A through E) and atypical (F) Raman spectra are shown from human pterygium samples, and from a fresh cornea, and ocular lens of the rabbit for comparison reasons. In general is can be seen that the Raman spectrum of a human pterygium resembles the one from a cornea with similar Amide I (at ~1665 cm^{-1}) and III (~1245 cm^{-1}) modes as expected for connective tissues. Pterygia-specific Raman spectral features appear around ~860, ~880, and ~1005 cm^{-1} (respectively the C-C vibration of the proline and hydroproline ring and the phenyl-ring mode). Furthermore, the very broad feature at ~1100 cm^{-1} is not observed in the fresh cornea, but could be assigned to the contributions of the formalin, the agent used to fixate the pterygia. The atypical spectral features of graph F can be found at ~1362, ~1555, and ~1610

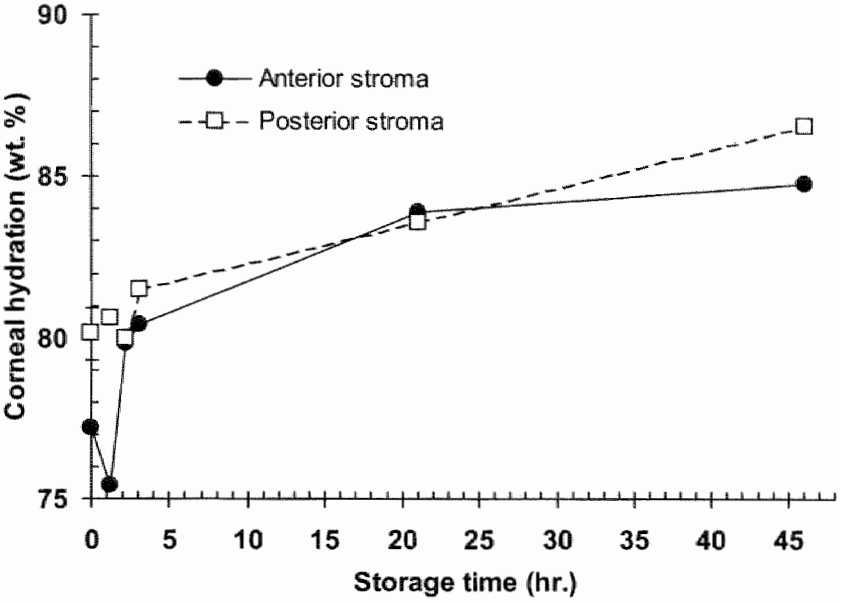

Figure 4F. Assessment of the hydration of the anterior and posterior corneal region as a function of time after cold storage of a whole rabbit eye *(see also Figure 4E).*

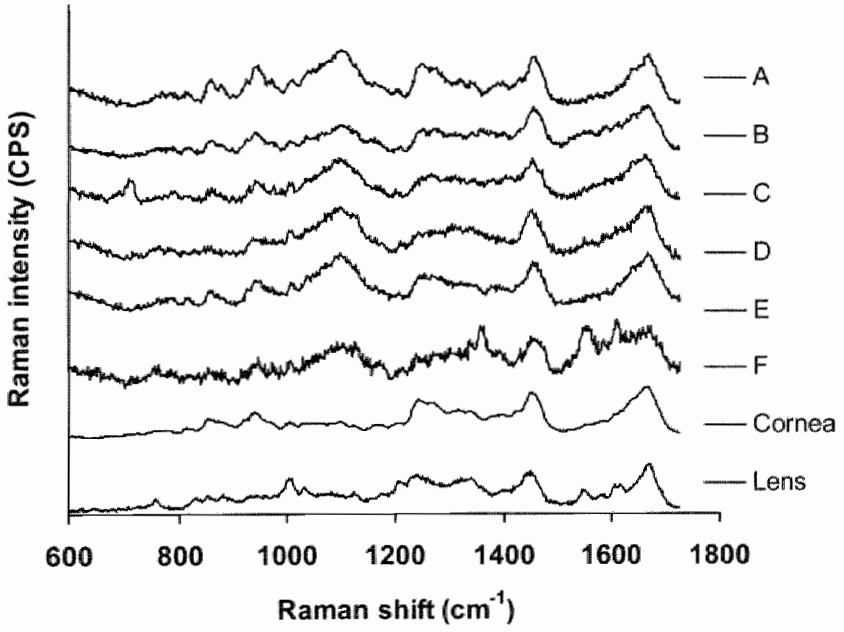

Figure 5. Typical (A through E) and atypical (F) Raman spectra of human pterygium samples and from a human cornea and rabbit lens (for comparison reasons).

cm^{-1} and are possibly due to contribution to the Raman signal of the haemoglobin of blood still present in the sample. This pilot study suggests that non-contact probing of these translucent pterygia samples is possible *in vitro* and yield *specific* Raman signals. With regards to the frequent recurrences of pterygia after surgical removal, a potential clinical application of RS might be to sample the surgery site for possible remnants in order to ensure complete removal of the pterygium.

The aqueous humor

A very attractive clinical application for RS in ophthalmology is the possibility to detect biomolecules in the aqueous humor that might be indicative of systemic alterations in metabolism.[6,15] Certain important biomolecules might possibly be detected in real-time in which case real-time therapeutic interventions would be possible to regulate the underlying metabolic disturbances. Although we are still far from this ideal picture of a closed-loop system, we did obtain valuable results during feasibility studies utilizing CRS.

Diabetes mellitus is a metabolic disease in which an absolute or relative shortage of insulin leads to an increased level of glucose in the blood, which in the long run is responsible for the morbidity of the disease. Numerous patients need to monitor their blood glucose in order to self-administer the right amount of insulin. Normally a monitoring device is used that requires a drop of blood, which can be most inconvenient because of its invasive character. Thus, various research teams are in search of non-invasive means of determining the blood-glucose levels. Since the concentration of glucose in the aqueous humor is related to its concentration in blood, we investigated the possibility to use Raman spectroscopy for the non-contact monitoring of glucose in the eye.[15] *In vitro* experiments showed a linear relationship between the glucose concentration and the Raman intensity of the CH-peak at ~2935 cm^{-1} in aqueous sugar solutions (Figure 6A). The proposed method seems sensitive enough since glucose concentrations below the physiological level of ~50-100 mg/dL could be assessed. We are currently investigating the feasibility of CRS for the non-contact sampling of glucose in the aqueous humor of anesthetized rabbits. However, the interpretation of the results are not straightforward since the changes in Raman spectral features as observed in the *in vitro* experiments are not specific for glucose alone when applied *in vivo*. Other biomolecules possess chemical structures which are highly similar to glucose, such as lactate and urea. Additionally, other situations can change the level of CH-bonds in the aqueous humor such as an increased level of proteins as a result of breaking of the blood-aqueous barrier in intra-ocular inflammation. Thus, further investigations are necessary in order to determine specific changes in Raman spectral

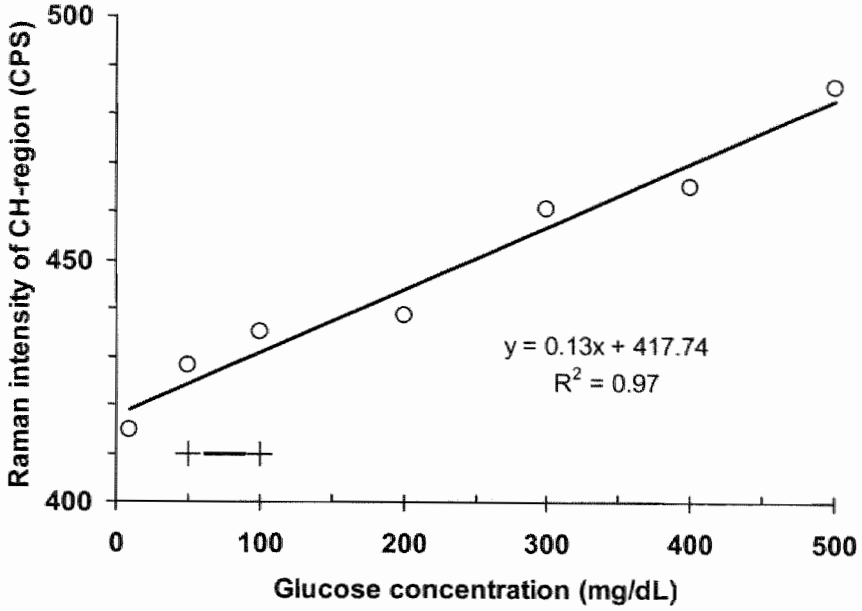

Figure 6A. Raman spectroscopic assessment of the glucose concentration in aqueous solutions (physiological value is ~50-100 mg/dL).

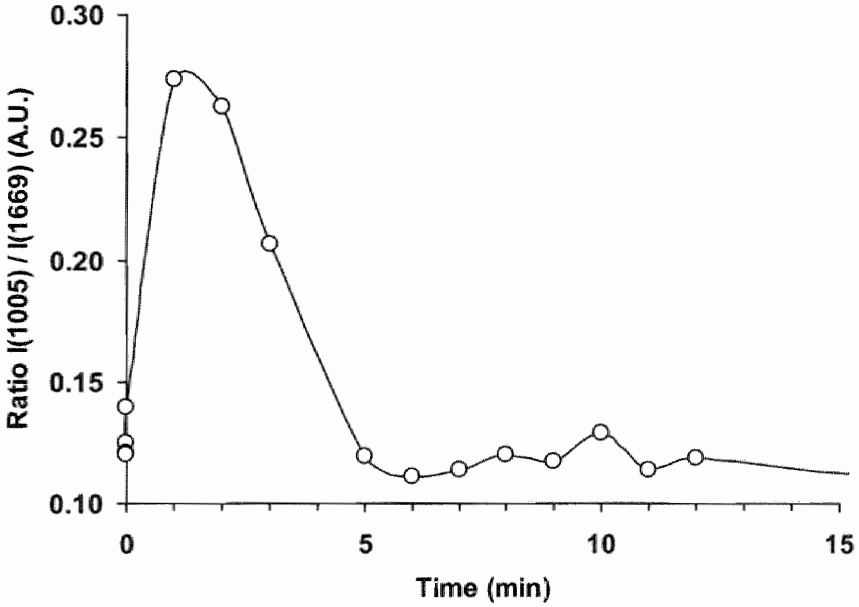

Figure 6B. Assessment of a phenylalanine Raman peak at 1005 cm^{-1} in the aqueous humor of the rabbit eye under *in vivo* conditions as a function of time after an intravenous bolus injection of phenylalanine.

features enabling the unambiguous assessment of the glucose concentration in the aqueous humor. One of the possible improvements could be the use of advanced spectral analysis algorithms, utilizing the partial least squares or principle components analysis routine which can be used to detect changes in a complete spectrum rather than one or two Raman spectral lines.[16]

Another biomolecule that might possibly be monitored is phenylalanine (PHE) which is elevated in untreated or insufficiently regulated phenylketonuria (PKU), an inborn error-of-metabolism. Newborns are screened for this underlying enzyme-deficiency through a bloodsample which is taken in the first few days after birth. In case PKU is diagnosed the patient has to remain on a phenylalanine-deficient diet for the rest of their lives. Much like glucose-monitoring, the level of PHE needs to be monitored on a regular basis in order to adjust the patients diet if necessary. Here RS could be of use, since it could perform these measurements in a non-contact fashion, and because phenylalanine has a very specific Raman signal at ~1003 cm^{-1}. Initial attempts at detecting phenylalanine were performed in the aqueous humor of the eyes of an anesthetized rabbit. After an intravenous bolus-injection of phenylalanine (425 mg in 20 mL saline) Raman spectra in the lower wavenumber region (500-1800 cm^{-1}) were obtained from the aqueous humor at regular time-intervals. The Raman intensity of the peak at ~1003 cm^{-1} was determined and plotted as a function of time after injection. These results are shown in Figure 6B. As can be seen, the relative intensity of the phenyl-ring vibration increases rapidly due to the increase in phenylalanine in the aqueous humor, from the first minute after injection and returns to normal within 5 minutes. This suggests that RS could indeed be used for monitoring changes in the concentration of phenylalanine and possibly other specific Raman active biomolecules.

Other potential applications of CRS in the aqueous humor entail pharmacokinetic studies and the detection of cells and proteins as a result of intra-ocular inflammation, currently being investigated in our laboratory.

Non-tissue-specific applications

Since Raman spectra are by definition temperature dependent, it is possible under certain circumstances to use RS for assessing the sample temperature. The most widely used method utilizes the relation between sample temperature and the Raman intensity ratio of the Stokes- vs. the anti-Stokes lines of the same Raman peak.[17] In theory this method can be used for non-contact thermometric assessments of samples irrespective of their nature over a wide range of temperatures. However, the extremely low Raman yield of the anti-Stokes lines in a Raman spectrum at physiological temperatures generally requires a prolonged exposure to laser light at high intensities, which is not desirable in

tissues such as the eye because of the potential damaging effect of the visible light. Moreover the required light intensities might locally heat the sample interfering with the accuracy of the temperature measurement. Another established method for assessing the temperature of a sample merely utilizes the Stokes-region of a Raman spectrum and entails the assessment of the temperature-dependent changes in the Raman spectral features of water. This method has been applied to non-invasively assess sub-surface ocean water temperatures and biological tissues.[18,19] The latter could be of significant interest in biology and medicine, since most living materials are embedded in water. Also in ophthalmology the application of RS for remote temperature measurements might be of clinical significance. Various therapeutic interventions in the eye, such as phaco-emulsification of the ocular lens, induced hyperthermia for increasing the therapeutic effect of ocular chemotherapy, and laser surgery of the cornea, result in more or less pronounced temperature increases which ideally would need to be monitored because of the potential hazardous effect to the ocular tissues. Furthermore, with the use of a suitable remote thermometric method it might be possible to quantify the temperature-reducing effect of ocular anti-inflammatory drugs and to validate temperature models of the eye. We used RS for non-contact temperature measurements of water at temperatures ranging from 13 to 48°C and of the aqueous humor of the rabbit eye under *in vivo* and *in vitro* conditions at temperatures ranging from 14 to 34°C, applying the Raman integrated intensity ratio OH2/OH1 = I(3430-3729)/I(2878-3430) in the spectrum of water (Chapter 8 of this thesis). This OH2/OH1 ratio proved very suitable for non-contact thermometric assessments in the aqueous humor, which is mostly comprised of water (Figure 7). However, this ratio was not directly applicable for thermometric assessments in the cornea or the ocular lens because of the non-homogeneous distribution of water and proteins and consequently the non-homogenous distribution of 'bound' and 'free' water in these tissues. Furthermore, the N-H vibrational modes of proteins at ~3300 cm^{-1} could have interfered thus resulting in an aberrant relationship between tissue temperature and Raman intensity ratio. In conclusion we can remark, that temperature information is included in both the Raman spectra of aqueous solutions as well as ocular tissues. The increasing concentrations of non-aqueous substances in tissues influences the linear relationship between the Raman intensity ratio OH2/OH1 and tissue temperature. This has two important implications: 1) when using RS for thermometric assessments care should be taken to extract the right information from the Raman spectra of tissues, and 2) the tissue temperature should remain constant when performing comparison Raman spectroscopy in the same tissue, in order to avoid changes in Raman spectral features due to changing temperatures. The latter is of particular significance when probing tissues that exhibit temperature gradients, such as is obviously the case in the eye.

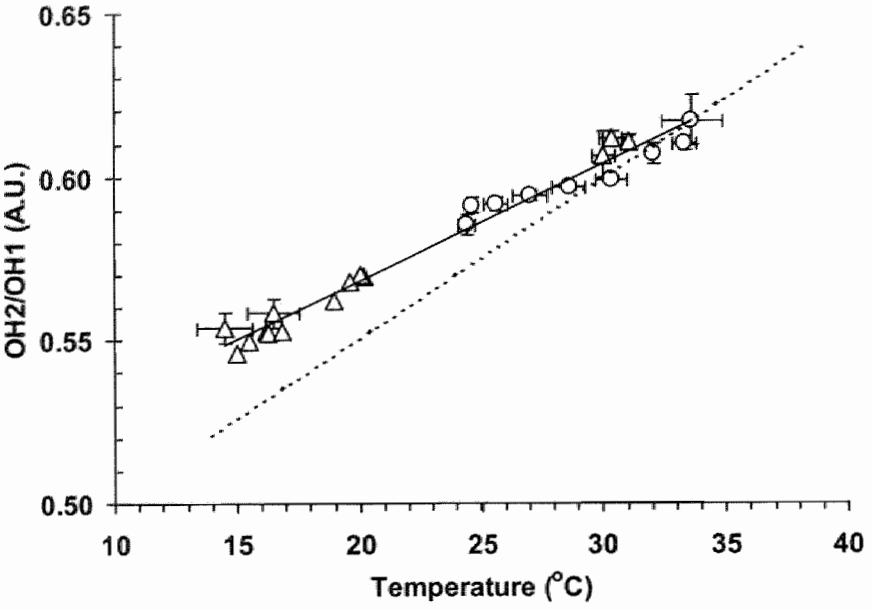

Figure 7. Relationship between Raman intensity ratio OH2/OH1 (n=162) and the water temperature of the rabbit aqueous humor *in situ* (solid line) and HPLC-grade water in a cuvette.

Considerations for the use of CRS in the human situation

Apart from the clinical relevancy of the proposed applications, future utilization of CRS for diagnostic purposes in ophthalmology is largely dependent on the design of a safe system. It should be obvious that when applying such a diagnostic system the benefits should significantly outweigh the risks of damage, injury or discomfort. The main drawback of the currently used CRS system is the use of visible light sources which are potentially harmful to the retina of the eye. In order to circumvent this problem we have various options:

1. use of wavelengths outside the visible range (ultraviolet, 180-400 nm or near infra-red, 700-1400 nm),
2. increasing the detection efficiency enabling the use of low intensities of visible light, or
3. prevent the light from reaching the retina altogether.

Option 1) has the disadvantages of a possible increase in the occurrence of tissue-fluorescence and increased tissue absorption in the cornea in the case of

using UV, while the use of NIR necessitates a significant increase in light exposure, since the Raman intensity is a function of the frequency of the scattered light to the fourth power. Option 2) has some room for improvement but not to the extent of being able to decrease the light exposure by two or three orders of magnitude, because the currently used detection camera already has a high quantum efficiency of 80% at 700 nm. Option 3) seems to be the safest and most feasible option for the near future. When the incident laser light is reshaped to obtain an annular shape and is focused on the cornea the beam diverges behind the cornea to become an ever increasing ring of light. With the right size of annulus and a sufficiently small pupil size, all the incident light will be absorbed by the iris and not go past the pupil to hit the retina. However, movement of the subject might still pose the possibility for light of the annular beam to pass the pupil. Future application of the confocal Raman spectroscopy system in a safe fashion will prove whether this technique is suitable in the human situation.

Conclusions

This manuscript described the potential applications of confocal Raman spectroscopy in ophthalmology. The advantageous characteristics of this biochemical assessment technique, such as non-contact probing yielding the possibility to assess living tissues, rapid detection, variable spatial resolution, scanning properties enabling the assessment of various ocular tissues (tearfilm, cornea, aqueous, lens, vitreous, outside of the eye: pterygium), and the ability to assess water and physical properties such as temperature, make confocal Raman spectroscopy an attractive tool for biochemical investigations of the eye, whether under physiological or pathological situations. With adequate improvements in safety, the potential clinical uses could be explored in human subjects.

References

1. Spiro TG, Ed., *Biological Applications of Raman Spectroscopy. Volume 1: Raman spectra and the Conformations of Biological Macromolecules*. John Wiley & Sons, Chichester (1987).
2. Jongsma, F. H. M., Erckens, R. J., Wicksted, J. P., Bauer, N. J. C., Hendrikse, F., Motamedi, M. and March, W. F. A confocal Raman system for scanning through ocular tissues: An *in vitro* study. *Optical Engineering* 1997; 36(11): 3193-3199.
3. Bauer NJC, Wicksted JP, Jongsma FHM, March WF, Hendrikse F, and Motamedi M. Noninvasive Assessment of the Hydration Gradient across the Cornea Using Confocal Raman Spectroscopy. *Invest Ophthalmol Vis Sci* 1998; 39(4): 831-835.

4. Bauer NJC, Motamedi M, Wicksted JP, et al. Non-Invasive Assessment of Ocular Pharmacokinetics using Confocal Raman Spectroscopy. *J Oc Pharm Ther* 1999; 15(2): 123-134.
5. Bauer NJC, Hendrikse F, and March WF. *In vivo* Confocal Raman Spectroscopy of the Human Cornea. *Cornea* 1999;18:483-488.
6. Erckens RJ, Motamedi M, March WF, Wicksted JP. Raman spectroscopy for noninvasive characterization of ocular tissue: potential for detection of biological molecules. *Journal of Raman Spectroscopy*. 1997; 28:293-298.
7. Castoro JA, Bettelheim AA, Bettelheim FA. Water gradients across bovine cornea. *Invest. Ophthalmol. Vis. Sci.* 1988; 29:963-968.
8. Sugrue M.F. The Preclinical Pharmacology of Dorzolamide Hydrochloride, a Topical Carbonic Anhydrase Inhibitor [review]. *J. Oc. Pharm. Ther.* 1996; 12(3):363-376.
9. Huizinga A, Bot ACC, de Mul FFM, Vrensen GFJM, Greve J. Local variation in absolute water content of human and rabbit eye measured by Raman microspectroscopy. *Exp. Eye Res.* 1989; 48:487-496.
10. Chan T, Payor S, Holden BA. Corneal thickness profiles in rabbits using an ultrasonic pachometer. *Invest. Ophthalmol. Vis. Sci.* 1983; 24:1408-1410.
11. Doherty PJ, Wellish KL, and Maloney RK. Excimer Laser Ablation Rate and Corneal Hydration. *Am J Ophthalmol* 1994; 118: 169-176.
12. Levin S, Carson CA, Garrett SK, and Taylor HR. Prevalence of central islands after excimer laser refractive surgery. *J Cataract Refract Surg* 1995; 21: 21-26.
13. Seiler T, and McDonnell PJ. Excimer Laser Photorefractive Keratectomy. *Survey of Ophthalmol* 1995; 40(2): 89-118.
14. Siew DCW, Clover GM, Cooney RP, Wiggins PM. Micro-Raman spectroscopic study of organ cultured corneae. *Journal of Raman Spectroscopy* 1995; 26:3-8.
15. Wicksted JP, Erckens RJ, Motamedi M, and March WF. Raman Spectroscopy Studies of Metabolic Concentrations in Aqueous Solutions and Aqueous Humor Specimens. *Appl Spectrosc* 1995; 49(7): 987-993.
16. Goetz MJ, Cote GL, Erckens R, March W, and Motamedi M. Application of a Multivariate Technique to Raman Spectra for Quantification of Body Chemicals. *IEEE Transactions on Biomedical Engineering* 1995; 42(7): 728-731.
17. Malyj M and Griffiths J.E. Stokes/Anti-Stokes Raman Vibrational Temperatures: Reference Materials, Standard Lamps, and Spectrophotometric Calibrations. *Applied Spectroscopy* 1983; 37(4): 315-333.
18. Leonard DA, Caputo B and Hoge FE. Remote sensing of subsurface water temperature by Raman scattering. *Applied Optics* 1979;18(11): 1732-1745.
19. Baranska H and Labudzinska. *Applied Spectroscopy* 41: 1068 (1987).

CHAPTER 5

Noncontact assessment of the hydration gradient across the cornea using confocal Raman spectroscopy

Noël JC Bauer, James P Wicksted, Franciscus HM Jongsma, Wayne F March, Fred Hendrikse, Massoud Motamedi

Invest. Ophthalmol. Vis. Sci. 1998; 39(4): 831-835

A B S T R A C T

Aim: The feasibility of Raman spectroscopy for the noncontact assessment of the axial corneal hydration is investigated.
Methods: A scanning confocal Raman spectroscopy system, with an axial resolution of 50 μm, was utilized to assess the water (OH-bond) to protein (CH-bond) ratio as measure for the concentration of water in collagen-based phantom media, and rabbit corneas.
Results: Over a wide range of corneal hydration (H = 0.0 - 8.3 mg water/mg dry wt.) Raman spectra with high signal-to-noise ratios were obtained under both *in vitro* as well as *in vivo* conditions. The Raman intensity ratio OH/CH showed strong correlation with the hydration of the phantom medium (R^2>0.99) and rabbit corneas (R^2>0.95). A high degree of reproducibility was seen in measurements performed at a specific depth within the cornea (SD=1.2-2.7%). Quantitatively, the spatially resolved corneal water content as assessed with our method, showed an increasing gradient from the anterior to the posterior region, with a difference of ~0.9 mg water/mg dry wt. Significant qualitative differences in the axial hydration gradient were observed between the *in vitro* and *in vivo* situation, caused by the presence of an intact tearfilm *in vivo*. Characterization of the axial corneal hydration using Raman spectroscopy provided a reliable estimation of total corneal hydration, as compared with conventional measurements using pachymetry and lyophilization.
Conclusion: The proposed noncontact confocal Raman spectroscopic technique has the potential to assess the axial corneal water gradient with a high degree of sensitivity and reproducibility.

Introduction

Several techniques have been suggested in the past to investigate the corneal hydration and its non-uniform spatial distribution. These include refractive index measurements,[1] optical sectioning,[2] mechanical sectioning after *in vivo* freezing[3], and differential scanning calorimetry.[4] A direct noncontact technique capable of quantifying the spatial distribution of water in the cornea could potentially contribute to the diagnostics of the cornea.

Raman spectroscopy (RS) is an optical technique that allows for the identification of molecular vibrations using monochromatic light from a laser. The technique has been utilized extensively to characterize the ocular lens and its transformation from normal to the cataractous state.[5] More recently it has been applied to determine the total water content in human organ cultured corneas.[6] Furthermore, applications of RS for the noncontact quantitative assessment of biomolecules in aqueous humor specimens and aqueous solutions have been proposed.[7]

The ratio of Raman intensities of the OH-bond (~3100-3700 cm^{-1}) and the CH-bond (~2850-3030 cm^{-1}), can be used to determine the absolute water content of tissue[5-6]. In the present study, we investigate the ability of this novel noncontact technique for the accurate assessment of the spatial distribution of water in phantom media with known properties and the rabbit cornea, both under *in vitro* and *in vivo* conditions.

Materials & Methods

Instrumentation

Recently, we reported on the development of a scanning confocal Raman spectroscopy (SCRS) system with long-working distance for the noncontact biochemical characterization of ocular tissue.[8] The key components of the system are, 1) a single grating spectrometer (SPEX500M, Spex Industries, Edison, NJ), with CCD-camera for rapid signal detection, 2) an argon laser (514.5 nm), and 3) a long-working distance microscope objective lens (25x/NA=0.5, f=10 mm, Jena, Karl Zeiss, Germany) that acts both as the focusing device for the incident light as well as the collecting lens for the Raman backscattered light. This lens permits noncontact probing of a considerable axial distance in the eye. An optical fiber coupled to the spectrometer collects the Raman backscattered light, and acts like a confocal pinhole. Changing the diameter of the fiber will change the probing volume, mainly by changing the integration depth (≥20 μm).

In order to assess the spatial distribution of water in the cornea, a high signal-to-noise ratio (SNR) and an integration depth significantly smaller than the corneal thickness were required. Optimum probing parameters were found using a laser power of 25 mW and a 3 second integration time, in conjunction with an 11 μm fiber, yielding an integration depth of 50 μm. Each spectrum reported here was the result of the average of three acquisitions.

Hydration assessments in phantom media

To demonstrate the ability of our method to quantify the hydration of a sample, commercially available collagen shields (BioCor II 24 HR, Bausch & Lomb, Tampa, FL), clinically used to improve corneal wound healing, were used as a phantom medium. These shields are described by the manufacturer as clear, thin, pliable films fabricated from porcine collagen, with an average thickness of 0.013-0.071 mm. After rehydration in HPLC-grade water for 3 minutes, these shields have an average thickness of ~0.200 mm and a hydration of ~1.92±0.01 mg water/mg dry wt. The Raman intensity ratio OH/CH of these shields was plotted against sample hydration 'H' (in mg water / mg dry wt.), and their relationship investigated for linearity. Furthermore, to examine the ability of RS to probe deep layers, Raman spectra were obtained at different probing depths (100-700 μm) within a thick phantom medium (1 mm) made up of albumin (96% pure, Sigma, St. Louis, MO) with a hydration of H=10.

In vitro and *in vivo* studies

A total of 16 eyes of young NZW rabbits (~1.8 kg) were enucleated immediately after euthanasia. The eyes were either stored in a moist chamber at 4°C (n=4), used fresh (n=7) or left exposed (n=5) to the ambient environment (23°C, 70% humidity), yielding different degrees of corneal hydration. In 5 fresh eyes and 1 eye left to dehydrate in air, we used ultrasound pachymetry (Pach-Pen™ XL, 20 MHz transducer, Bio-Rad, Glendale, CA) as the standard to compare our methods with, and determined the central corneal thickness (CCT). Each CCT assessment was the average of 5 measurements. The hydration was calculated using CCT vs. hydration relationships as postulated by Hedbys and Mishima.[9] In the other 10 eyes (2 fresh, 4 rehydrated, and 4 dehydrated) we used lyophilization *in vacuo* (100 mTorr, -60°C, 24 hr.) as the standard. Before and after lyophilization, the corneas were probed with our technique and weighed on an analytical balance (0.1 mg readability), and corneal hydration was calculated as (wet wt. - dry wt.) / dry wt.

Under an approved animal protocol that complied with the ARVO Resolution on the Use of Animals in Research, the *in vivo* studies were performed on

the 4 eyes of two female NZW rabbits (3.6 kg). The animals were restrained in a holder, anesthetized using intramuscular ketamine hydrochloride (25 mg/kg) and xylazine (5 mg/kg), while the involuntary eye movements were minimized by immobilizing the eye by a custom made applanation device.

At the start of each scan, the laser beam was positioned in front of the central cornea and was aligned such that the optical axis of the system and the cornea matched. The entire cornea was scanned by moving the microscope objective lens toward the eye with step-increments equal to that of the integration depth (50 μm). Each scan was repeated three times to investigate reproducibility. Since each scan took 1-2 minutes to perform, changes in sample hydration may occur leading to the observed differences among various scans. To establish the reproducibility of our measurements, each cornea was probed repeatedly (n=10) at the same depth, in both the *in vitro* and *in vivo* situation. The standard deviation (SD) of the mean Raman intensity ratio OH/CH for each single point assessment was utilized as a measure for the reproducibility.

Spectral data analysis

An algorithm was used (Matlab™, Mathworks Inc.) to correct for background noise observed in the Raman spectra, using the spectral information in the high range (3100-3700 cm^{-1}). Then the mean and standard deviation (SD) for the OH and CH peaks obtained in the repeated measurements were calculated.

Complete scanning of the cornea requires a series of measurements of Raman spectra. The CH-signal is mostly confined to the cornea and was used as a biological marker for the determination of the corneal boundaries. The actual distribution of the CH-signal as measured by our probe, which was moved from air (no CH) through the cornea and into the aqueous humor (no CH), was curvefitted (cubic spline interpolation). The corneal boundaries were arbitrarily chosen as the probing depths corresponding to the 10^{th} and 90^{th} percentile of the area under the curve (AUC). These boundaries were also used to evaluate the spatially resolved corneal hydration as well as total corneal hydration.

Since rabbit corneal thickness has been shown to be uniform,[10] and corneal hydration is a linear function of corneal thickness,[9] we tested if it was feasible to determine total corneal hydration from the axial scans after assessment of the corneal boundaries. The Raman intensities of OH and CH were integrated between these boundaries, and total corneal hydration as assessed with our method (H_R) was then given by the ratio between these integrated intensities; AUC(OH)/AUC(CH). The results were plotted vs. total corneal hydration H as assessed both by lyophilization and ultrasound pachymetry, and analyzed for linearity in order to validate this method.

The axial distribution of water within the cornea, can be determined by plotting the Raman intensity ratio OH/CH vs. the depth of probing. The spatially-resolved corneal hydration was evaluated qualitatively and quantitatively, under *in vitro* and *in vivo* conditions, as well as during dehydration in air over time.

Results

No significant change in Raman intensity ratio OH/CH ratio was observed at different depths (100-700 μm) within an albumin sample with uniform water distribution (OH/CH=5.25±0.03, n=11). This implies that the Raman intensity ratio OH/CH is independent of the probing depth, which justifies attributing differences in this ratio at different depths within an inhomogeneous medium like the cornea to differences in hydration.

Figure 1 shows typical spectra of the normal rabbit cornea, and also illustrates the ability of our methods to assess the relative changes in OH-intensity over a broad range of corneal hydration (H=0-8.3 mg water/mg dry wt.) without significant loss of signal-to-noise ratio (SNR=20-30). It can also be seen that the Raman spectral response of a cornea in a freshly enucleated eye (graph B) exhibits the same characteristics as a normal cornea in the *in vivo* situa-

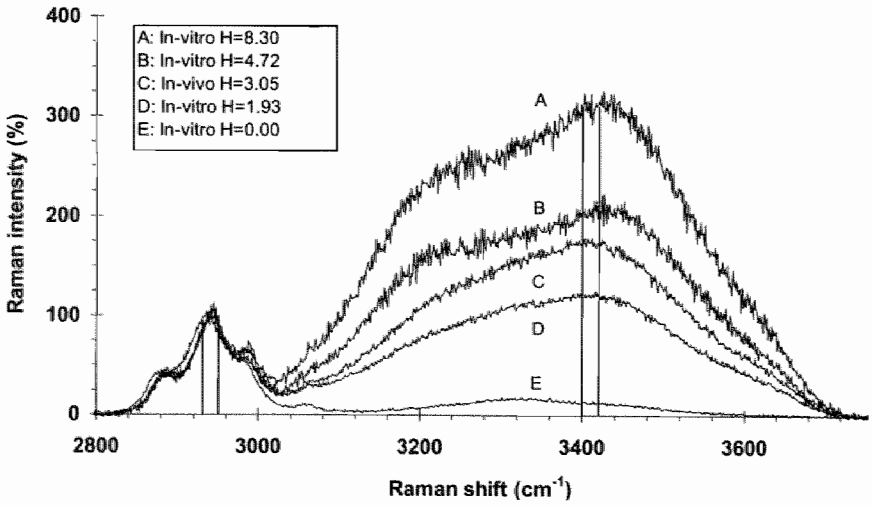

Figure 1. *In-vivo* and *in vitro* assessment of Raman spectra from the anterior region of corneas at various degrees of hydration. The regions of the spectra that are used to obtain the absolute OH- and CH-signal intensity are outlined.

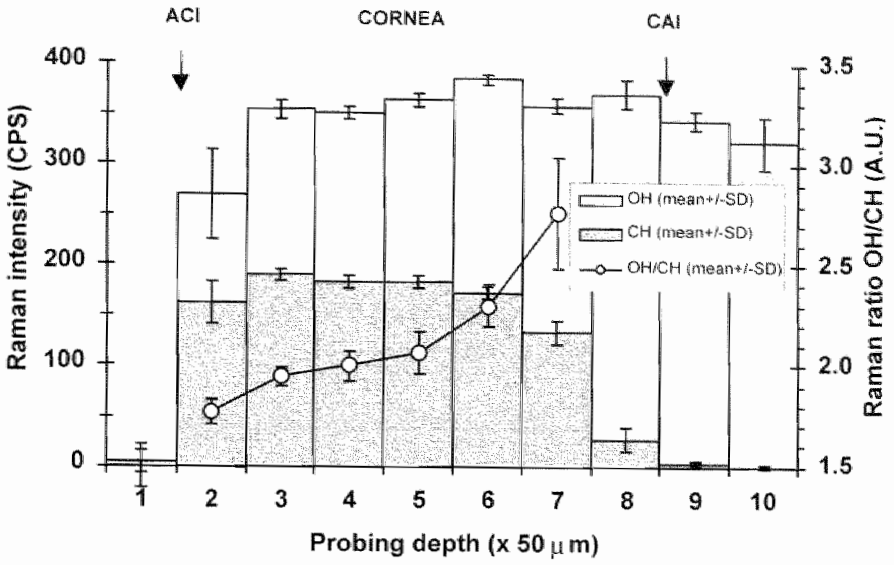

Figure 2. The axial distribution of the Raman intensities of OH and CH (bar graphs; left ordinate) and the Raman intensity ratio OH/CH (line graph; right ordinate) as function of the probing depth in a cornea of a freshly enucleated rabbit eye (H=3.80±0.20). The tear-film/cornea interface (ACI) and the cornea/aqueous humor interface (CAI) can be identified by the changes in the extent of the CH-response (arrows).

tion (graph C). Since we observed a 40-50% change in absolute Raman signal per 1.0 mg water / mg dry wt. change in hydration, and because a change of 5% in the absolute signal is easily resolved at a SNR of 30, we determined that the sensitivity of our methods both *in vitro* and *in vivo* was ~0.1 mg H_2O/mg dry wt.

A strong correlation is found for the linear relationship [a=b (mean±SD)x +c(mean±SD)] between corneal hydration as assessed with our method (H_R) and the two conventional methods, i.e. lyophilization (H_L) and ultrasound pachymetry (H_P). For the phantom medium simulating corneal structure (BioCor collagen shields) this relationship is described by: H_R=0.45 (±0.08)H_L+0.23(±0.01) where R^2=0.900 (n=17). For the rabbit corneas this relationship is given by either H_R=0.49(±0.03)H_P+0.47(±0.44) where R^2=0.976 (n=14) or H_R=0.46(±0.04)H_L+0.14(±0.01) where R^2=0.951 (n=24), depending on which conventional method was used. We calibrated the Raman intensity ratio OH/CH using latter results. Thus we were able to quantify the axial distribution of corneal hydration. Furthermore, a correlation was observed for the relationship between the corneal thickness as assessed with our

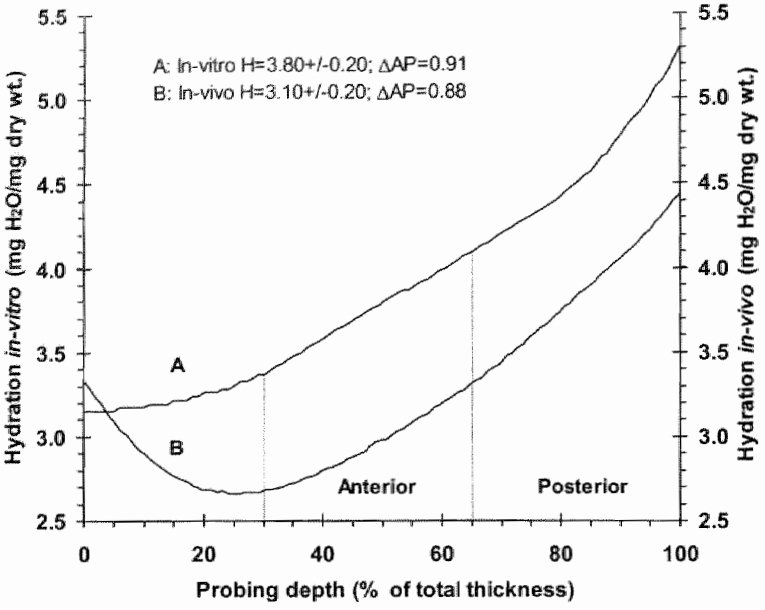

Figure 3. Comparison of *in vitro* (graph A) and *in vivo* (Graph B) axial distribution of rabbit corneal hydration as assessed with Raman spectroscopy vs. normalized probing depth.

method (CCT_R) and pachymetry (CCT_P); $CCT_R=0.81(\pm0.02)CCT_P$ where $R^2=0.760$ (n=14). The SD of 10 single point assessments of the Raman intensity ratio OH/CH as a measure for the reproducibility was 1.2% *in vitro* and 2.7% *in vivo*.

An example of how intensities of Raman peaks can be used to assess the distribution of corneal hydration is shown in Figure 2. Here the Raman intensities of OH and CH are plotted against probing depth for a fresh *in vitro* cornea. The spatial distribution of the OH/CH ratio illustrates the increase in hydration when probing from the anterior to the posterior region of the cornea. It can be seen that the assessment of the spectral response per probing depth is highly reproducible, since the SD of the mean value for the Raman peaks (n=3) for each probing depth is rather small, even when probing deeper into the cornea (steps 7 and 8). As demonstrated in this figure it is possible to outline the extent of the cornea, by identifying the abrupt increase in both CH- and OH-signal at the anterior border (step 2) and the abrupt decrease of the CH-signal (step 8) at the posterior border.

Using our noncontact approach the axial distribution of water in the rabbit cornea under *in vivo* and *in vitro* conditions is exhibited in Figure 3. For the *in*

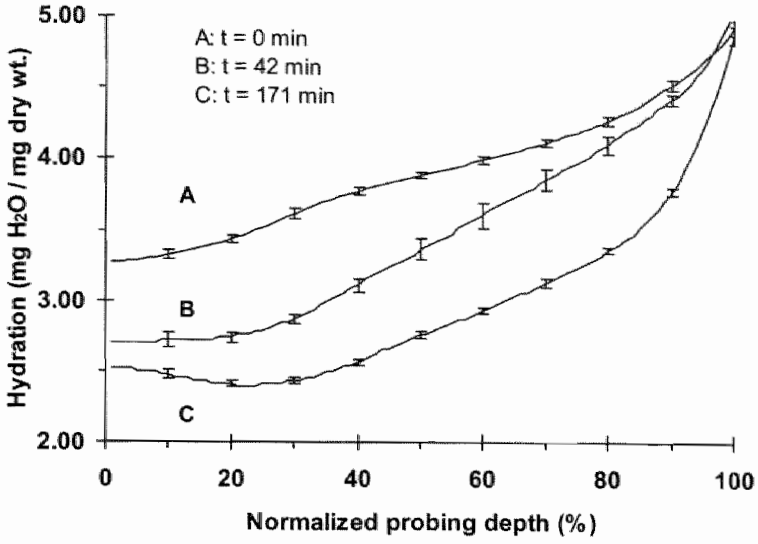

Figure 4A. Typical changes observed in the axial distribution of water in an intact rabbit cornea left exposed to the ambient environment (23°C, 70% relative humidity).

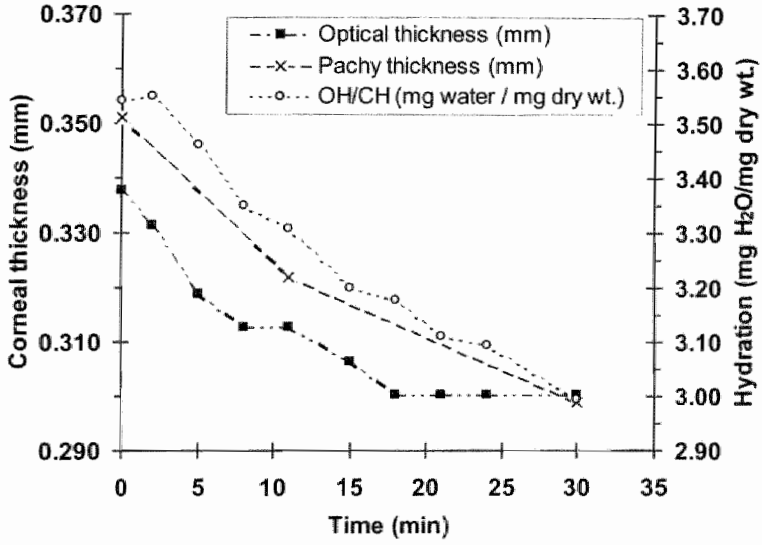

Figure 4B. Central corneal thickness (CCT) and the state of corneal hydration as measured by ultrasound pachymetry and by our optical method as function of dehydration time.

vivo measurements a 'dip' in the anterior region of the cornea was observed. Using a mechanical sectioning technique, Turss et al. found a difference of 0.81 in the hydration of the anterior region of the rabbit cornea as compared to the posterior region.[3] Our technique yielded values of 0.88 and 0.91 for *in vivo* and *in vitro* corneas respectively (Fig. 3). Although these results agree favorably with the literature, the values are obviously highly dependent on the stromal regions compared. Smaller regions at the periphery of both the anterior (A) and posterior (P) stroma for instance would yield a greater AP-difference in hydration in the corneas of Figure 3.

Figure 4A shows the typical changes that occur in the axial hydration gradient of the rabbit cornea as function of time that the cornea is exposed to the ambient environment. Significant changes in hydration appear in the anterior part of the stroma within the first 42 minutes, and throughout the posterior part of the cornea thereafter. The SD per probing volume at t=0 and t=171 are rather small, indicating that the changes in hydration during assessment of the axial scans are small. These results illustrate the feasibility of assessing the spatially resolved hydration of a cornea over time, and thus the ability to identify the location within the cornea responsible for a decrease in hydration. Figure 4B shows the changes in CCT and H assessed by both pachymetry and our optical method as a function of time in a rabbit cornea exposed to air. It can be seen that all three parameters decrease over time in a similar manner. Both total corneal hydration and CCT as assessed with our methods can again be shown to be linearly related to pachymetric measurements.

Discussion

In this investigation, we have shown the applicability of scanning confocal Raman spectroscopy to assess the axial hydration gradient of the cornea both under *in vitro* as well as *in vivo* conditions. The proposed optical sectioning technique offers some key advantages, including the ability to obtain direct information about corneal hydration and its distribution, with a high axial resolution in a noncontact manner. The inherent specificity of Raman spectra, together with adequate sensitivity (SNR) over a wide range of corneal hydration (H=0.0 to H=8.3), may provide a promising technique for qualitative and quantitative analysis of the axial distribution of water in the cornea.

The sensitivity of our approach was found to be ~0.1 mg H_2O/mg dry wt. (=~3% in a normo-hydrated cornea) (Fig. 1). Clinically, a corneal swelling of 5-10% subjectively increases the haze around lights noticeably, but only when corneal hydration increases by 100% to H=7, will a dramatic decrease in visual acuity occur.[11] Thus, the observed sensitivity of our methods is believed to be

sufficient, not only to detect the time- and spatially-resolved changes in hydration within a cornea, but also to detect even the smallest clinically significant aberration in corneal hydration.

Total corneal hydration as assessed with both pachymetry and lyophilization showed a high correlation ($R^2>0.95$, $p<0.05$) with the values for hydration as measured by the Raman technique, and both methods gave similar slopes for the regression curves, indicating consistency between the two conventional techniques used in this study.

The axial scan measurements demonstrated the spatial distribution of the Raman signals for OH and CH as function of probing various layers of the cornea (Fig. 2). In air Raman peaks corresponding to the OH and CH bonds are negligible and are contributed to noise. Since in a normal eye the aqueous humor is regarded as a homogenous medium mainly consisting of water and a very low protein content, the Raman peaks corresponding to the OH and CH bonds when probing past the cornea were expected to exhibit high and low amplitudes, respectively. Indeed, a high Raman peak corresponding to the OH bond and a Raman peak slightly higher than the noise level for the CH bond were observed in the aqueous humor. However, both the OH and CH Raman signals dropped gradually when probing deeper into the eye. This can be explained by changes in coupling efficiency of our optics and losses due to scattering. These changes also occurred in a homogeneous phantom sample made up of albumin (H=10) but did not change its Raman intensity ratio OH/CH. From 100 - 700 μm into the sample, the OH/CH ratio was 5.25±0.03, and no significant correlation was found between probing depth and OH/CH ratio ($R^2=0.05$, $p<0.05$, $n=11$).

Qualitatively, the axial corneal hydration gradient can be assessed with our methods with a high degree of reproducibility. Although the actual hydration gradient has not been measured and compared by any other means, like mechanical sectioning,[3] the trend and extent of the anterior-posterior corneal hydration gradient as found in the *in vivo* corneas, was in close agreement with our current knowledge regarding the non-isotropic properties of corneal hydration.[3] A small difference in the hydration of the anterior part of the cornea is found between the *in vitro* and the *in vivo* corneas. The level of hydration control and the extent of the pre-corneal tear film are believed to be the cause of the observed 'dip' in hydration of the anterior part of the *in vivo* cornea (Fig. 3B). The tear-film/epithelium layer is more hydrated than the most anterior region of the stroma. It is likely that the depth resolution of 50 μm permitted identification of the tear-film (~40 μm) plus epithelial layer (~50 μm). If desired, the axial resolution of our system can be further increased by utilizing a smaller integration depth (i.e. using a smaller fiber) and probing with smaller step-increments.

Small changes can be observed in the axial hydration gradient within the same sample as a result of changing total corneal hydration (Fig. 4A). This was shown *in vitro*, by following the axial hydration gradient across the same cornea over time during dehydration in air. Furthermore, total corneal hydration and corneal thickness as measured by our optical method vs. ultrasound pachymetry in a dehydrating cornea over time, showed congruent curves. This suggests that all three parameters can determine for total corneal hydration, with the sensitivity and spatial resolution of the proposed method as an advantage over the standard techniques.

Since the eye of a rabbit under anesthesia still experiences movement, the rabbit eyes were immobilized in this study, in order to demonstrate the feasibility of our techniques to assess the axial hydration gradient of the cornea in the *in vivo* situation. The results of both the *in vitro* and immobilized *in vivo* corneas are highly comparable with regards to the reproducibility of both the single-point assessments as well as the assessments of corneal hydration as function of probing depth. However, future improvements have to be made by integrating an eye-tracking device into the current setup, in order to assess the hydration gradient of the cornea *in vivo* without any interventions.

A drawback which has to be overcome concerns the safety of this system, since it utilizes a potentially high dose of green light. We explicitly stress, that for future clinical application using scanning confocal Raman spectroscopy as a diagnostic tool, a system configuration will have to be chosen in such a fashion that both retinal and corneal laser safety thresholds are considered. Currently, the proposed method has the potential to be utilized as a highly specific and sensitive biochemical tool for the noncontact diagnostics of the spatially resolved hydration of the cornea, in a variety of experimental settings. For example, the hydration of the anterior part of the cornea seems to play an important role in the successful outcome of photorefractive keratectomy (PRK). During PRK, the hydration of the cornea is altered by the application of a topical anesthetic, the epithelial debridement, and the laser treatment itself. Knowledge of the hydration status of the cornea prior and during PRK could possibly lead to a better understanding of the laser-tissue interaction.

In summary, the proposed biochemical optical sectioning technique using Raman spectroscopy has proven applicable in the *in vivo* animal setting, and could be of value in various experimental studies involving cornea hydration. With adequate improvements in the system, a safe technique could be developed that would allow for the non-invasive diagnostics of human corneas *in vivo*.

Acknowledgments

We thank Mr. Brent Bell and Mr. Marcel Goetz for their technical assistance, and Drs. Judy Brown and Miriam Brysk for their help with lyophilizing the corneas.

References

1. Maurice DM. The structure and transparency of the cornea. *J. Physiol.* 1957; 136:263-286.
2. Wilson G, O'Leary DJ, Vaughan W. Differential swelling in compartments of the corneal stroma. *Invest. Ophthalmol. Vis. Sci.* 1984; 25:1105-1108.
3. Turss R, Friend J, Reim M, Dohlman CH. Glucose concentration and hydration of the corneal stroma. *Ophthalmic Res.* 1971; 2:253-260.
4. Castoro JA, Bettelheim AA, Bettelheim FA. Water gradients across bovine cornea. *Invest. Ophthalmol. Vis. Sci.* 1988; 29:963-968.
5. Huizinga A, Bot ACC, de Mul FFM, Vrensen GFJM, Greve J. Local variation in absolute water content of human and rabbit eye lenses measured by Raman microspectroscopy. *Exp. Eye Res.* 1989; 48:487-496.
6. Siew DCW, Clover GM, Cooney RP, Wiggins PM. Micro-Raman spectroscopic study of organ cultured corneae. *Journal of Raman Spectroscopy* 1995; 26:3-8.
7. Erckens RJ, Motamedi M, March WF, Wicksted JP. Raman spectroscopy for noninvasive characterization of ocular tissue: potential for detection of biological molecules. *Journal of Raman Spectroscopy.* 1997; 28:293-298.
8. Jongsma, F. H. M., Erckens, R. J., Wicksted, J. P., Bauer, N. J. C., Hendrikse, F., Motamedi, M. and March, W. F. (1997). Confocal Raman system for noncontact scanning of ocular tissues: an *in vitro* study. *Optical Engineering* 1997; 36(11): 3193-3199.
9. Hedbys BO, Mishima S. The thickness-hydration relationship of the cornea. *Exp. Eye Res.* 1966; 5:221-228.
10. Chan T, Payor S, Holden BA. Corneal thickness profiles in rabbits using an ultrasonic pachometer. *Invest. Ophthalmol. Vis. Sci.* 1983; 24:1408-1410.
11. Maurice DM. The Cornea and sclera. In: Davson H. ed. *The Eye,* 3rd edition . Orlando: Academic Press. Inc. ; 1984, Vol 1b: 50.

CHAPTER 6

In vivo confocal Raman spectroscopy of the human cornea

Noël JC Bauer, Fred Hendrikse, Wayne F March

Cornea 1999; 18: 483-488

ABSTRACT

Aim: To investigate the feasibility of a confocal Raman spectroscopic technique for the noncontact assessment of corneal hydration *in vivo* in two legally blind subjects.

Methods: A laser beam (632.8 nm; 15 mJ) was maintained on the cornea using a microscope objective lens (25x magnification, NA=0.5, f=10 mm) both for focusing the incident light as well as collecting the Raman backscattered light, in a 180° backscatter configuration. An optical fiber, acting as the confocal pinhole for elimination of light from out-of-focus places, was coupled to a spectrometer that dispersed the collected light onto a sensitive array-detector for rapid spectral data acquisition over a range from 2890-3590 cm^{-1}. Raman spectra were recorded from the anterior 100-150 µm of the cornea over a period of time before and after topical application of a mild dehydrating solution. The ratio between the amplitudes of the signals at 3400 cm^{-1} (OH-vibrational mode of water) and 2940 cm^{-1} (CH-vibrational mode of proteins) was used as a measure for corneal hydration.

Results: High signal-to-noise ratio (SNR 25) Raman spectra were obtained from the human corneas using 15 mJ of laser light energy. Qualitative changes in the hydration of the anterior most part of the corneas could be observed as a result of the dehydrating agent.

Conclusion: With adequate improvements in system safety, confocal Raman spectroscopy could potentially be applied clinically as a noncontact tool for the assessment of corneal hydration *in vivo*.

Introduction

Raman Spectroscopy (RS) is a powerful optical technique for the biochemical characterization of tissues and other biological media.[1] First introduced by Yu et al. in 1974, applications of RS in ophthalmology have mainly been limited to the elucidation of biochemical and conformational changes of the lens proteins.[2] A small number of investigations have focused on Raman spectroscopic characterization of the cornea,[3-7] the aqueous humor,[8,9] the vitreous,[10] and the retinal pigment.[11] Most of these studies were performed *in vitro* because the inherently weak Raman scattering usually demands the use of high level light energies and long exposure times, thus limiting safe and practical *in vivo* applications of RS in the eye.[12]

We recently developed a high gain confocal Raman spectroscopy (CRS) system optimized for ophthalmic use *in vivo*[13] and shown its potential for the detection of biomolecules in ocular tissues,[9] and for pharmacokinetic assessments of topical ocular drugs.[14] Furthermore, we have shown that non-contact CRS can be applied *in vivo* for the rapid and sensitive assessment of the extent and distribution in hydration of the same cornea over time.[6] This could potentially be of clinical relevance for the early diagnosis of disturbances in corneal deturgescence as a result of corneal dystrophies,[15] the wearing of contact lenses,[16] diabetes mellitus,[17] topically applied ocular drugs,[14,18] the laser-cornea interaction during photorefractive surgery,[19,20] and corneal procurement prior to transplantation.[4]

In this study we sought to determine the feasibility of CRS to obtain high-signal-to noise ratio Raman spectra of the human cornea *in vivo* at low level light energies and specifically directed our investigations to the Raman spectroscopic assessment of corneal hydration and changes herein as the result of topical application of a mild dehydrating agent.

Methods & Materials

Subjects

Under an Institutional Review Board approved protocol two physically and mentally healthy subjects, A (65 yr.) and B (69 yr.), were enrolled from our ophthalmology outpatients clinic. The subjects were known to be legally blind in one eye due to dense nuclear cataract while having a vision in the contralateral eye >1/60 in order to see the fixation light. The subjects were not known for any corneal abnormalities or surgeries and did not wear contact lenses. Both subjects gave signed consent and were followed-up for four weeks

while being encouraged to report any ocular abnormalities as a result of the procedure.

Confocal Raman Spectroscopy (CRS)

When monochromatic light interacts with matter almost all of it is scattered elastically, meaning without energy transfer between light and matter. The Raman phenomenon occurs when light is scattered inelastically due to the exchange of energy between photons and molecules, on the molecular vibrational level. The change in photon energy (=frequency) is equal to the change in molecular vibrational energy, which is inherently specific for the molecular bond involved. Raman spectroscopy spatially resolves the frequency changes of the scattered light, yielding a spectrum depicting the Raman intensity (= amount of photons) vs. the Raman shift (= photon frequency change; in cm^{-1}) over a certain frequency range. Using this optical technique each Raman band in a spectrum can be assigned to a known molecular vibrational mode, and spectral analysis provides qualitative and quantitative information on molecular content and conformation.[1] Raman spectroscopy has various advantageous properties, including the inherent specificity, the non-contact character, the ability to rapidly acquire information on the biochemical content and structure of whole biomolecules with a single spectrum, the applicability in gas, solid, or liquid samples, and the ability to assess aqueous solutions. Disadvantages usually include the need for high level light doses, since the Raman scatter yield is inherently low, while the potential occurrence of fluorescence could mask the useful Raman signal.

The development and performance of the high-gain confocal Raman spectroscopy (CRS) system has been described in detail elsewhere.[13] We essentially used the same system for this study, with the exception of the laser light source and is displayed in schematic in Figure 1. In essence, the tight focus of a low power Helium-Neon laser (NEC Co., Minato-Ku, Tokyo, Japan; 632.8 nm; 15 mW) was optically aligned with and maintained at the anterior 100-150 μm of the cornea for a short period of time, using a long working distance microscope objective (LDMO) lens (magnification 25x, NA0.5, focal length = 10 mm) both for focusing the incident light as well as collecting the Raman backscattered light, in a 180° backscatter configuration analog to an epi-illuminated microscope. An optical fiber, acting like a confocal pinhole for elimination of light from out-of-focus places, was coupled to a spectrometer that dispersed the Raman shifted light onto a highly sensitive CCD-camera for rapid spectral acquisitions. A computer digitally stored the data from the CCD and displayed the Raman spectrum on a monitor. With the spectrometer centered at 3250 cm^{-1} a Raman spectrum is obtained with a range of 2890-3580 cm^{-1}. This

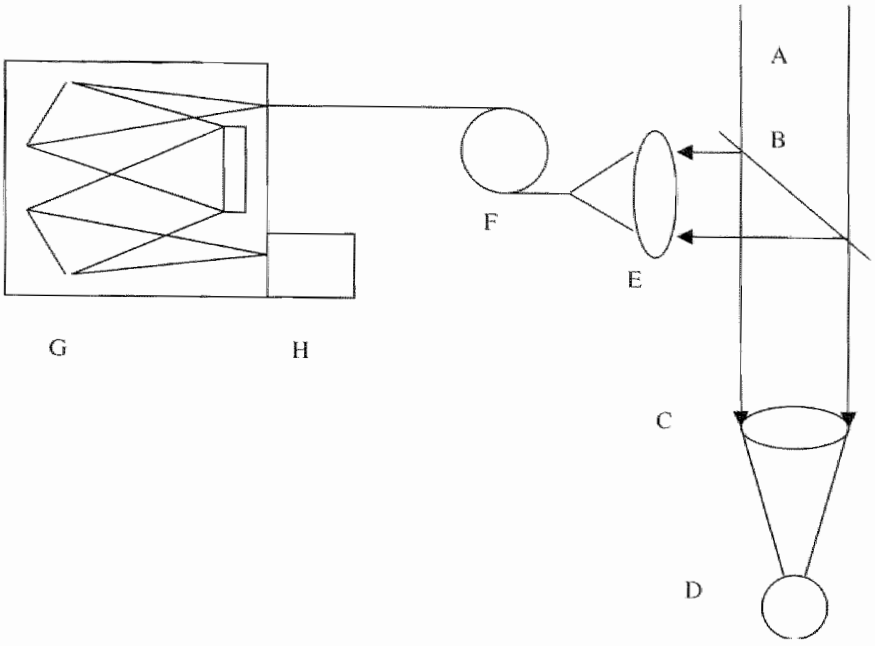

Figure 1. Schematic of the confocal Raman spectroscopy system. A = collimated laser beam (632.8 nm; 15 mW); B = beamsplitter; C = long working-distance microscope objective lens; D = sample (i.e. the eye); E = exit lens; F = optical fiber; G = spectrometer; H = CCD-camera.

entails our region of interest, since the Raman signals corresponding to the aliphatic (~2940 cm^{-1}) and aromatic (~3065 cm^{-1}) C-H vibrational modes of proteins and the OH-vibrational modes (~3240-3540 cm^{-1}) of water can be assessed simultaneously in a single spectrum. The Raman intensity ratio OH/CH=I(3400)/I(2940) is directly related to corneal hydration in mg H_2O/mg dry wt.[4,6], and was used to assess changes in the relative water content of the anterior region of the cornea as a result of the topical application of a dehydrating drug. All individual spectra were obtained using a laser power of 15 mW as measured in front of the LDMO lens at exposure times from 1 to 5 seconds per spectrum.

In vivo assessment of human corneal hydration

Five minutes before the procedure, the subjects received one drop of Alcaine (proparacaine hydrochloride 1%, sterile ophthalmic solution, Alcon Inc., CA) in case of accidental touching of the cornea and a mioticum (Timpilo,

ophthalmic solution, Merck & Co., CA) to limit the effects of fluorescence backscatter from the cataractous lens. The subjects were positioned in a modified adjustable headrest from a slitlamp and the head was restrained to reduce movement artifacts. Optical fixation was performed by instructing the patient to look towards a fixation light. After the focus of the attenuated laser beam was positioned at the surface of the cornea, the attenuation filter was removed and probing started. The subjects were instructed to keep their eyes open during acquisition of the spectral data, but were allowed to blink in-between acquisitions. Three sets of Raman spectra of the anterior 100-150 μm of the cornea were recorded at five minute intervals; six baseline spectra of the normal cornea, and six spectra of the same corneal region after the first and a second topical application of a single drop of Muro128 (NaCl 5%, Ophthalmic Solution, Bausch&Lomb, Tampa, FL), clinically used to reduce corneal hydration prior to surgery. The six spectra in each set were obtained at exposure times of 1, 2, and 5 s. (n=2 per exposure time).

Data analysis

All data were analyzed as previously described.[6] In short, after background correction of each spectrum the amplitudes of the OH- and CH-vibrational modes were assessed using the Raman bands at ~3400 cm^{-1} (OH) and 2940 cm^{-1} (CH), respectively. As previously reported the Raman intensity ratio OH/CH is linearly correlated with corneal hydration, as validated with either lyophilization or pachymetry in both rabbit as well as human corneas.[4,6] However, our previously assessed calibration data were not valid here because of significant differences in the optical setup and the spectral response, since in this study a Helium-Neon laser (632.8 nm) was used in stead of an Argon laser (514.5 nm). Furthermore, no calibration was performed in the present study since only the superficial part and not the total thickness of the cornea was assessed with our optical method unlike when using pachymetry. However, relative changes in the Raman intensity ratio OH/CH could be assessed as a measure for the change in corneal hydration of the superficial layer of the cornea, by comparing all spectra to the ones prior to application of Muro128. Statistical analysis was performed using the Student's t-test ($p<0.05$) for comparison of the mean Raman intensity ratio OH/CH before and after application of the dehydrating agent.

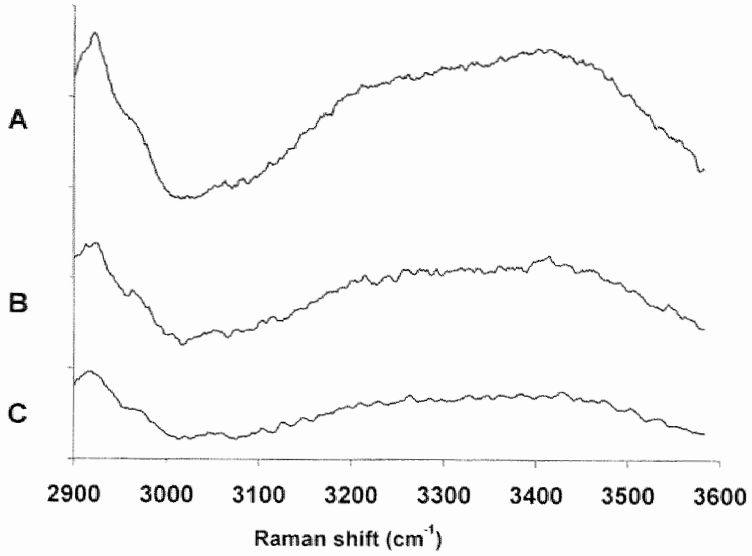

Figure 2. Representative Raman spectra (from 2900-3600 cm^{-1}) of the human cornea *in vivo*, depicting the Raman modes of collagen (CH-vibrations at 2940 and 3065 cm^{-1}) and water (OH-vibrations from 3100-3540 cm^{-1}). Experimental conditions: CRS system utilizing a low power Helium-Neon laser (632.8 nm; 15 mW). A, B, and C are obtained with exposure times of 5, 2, and 1 s., and yield a signal-to-noise ratio of 60, 35, and 25, respectively.

Results

The CRS technique yielded rapid acquisition of high signal-to-noise ratio (SNR) Raman spectra of the human cornea *in vivo* using low power laser irradiation. Figure 2 depicts the typical Raman spectra of a normal human cornea in the higher Raman shift range from 2900-3600 cm^{-1}. Even at exposure time of 1 s. the signal-to-noise ratio was sufficient (~25) to clearly distinguish the Raman modes for the CH- and OH-vibrations. The spectral acquisitions were reasonably reproducible, with an average standard deviation (SD) for the Raman intensity ratio I(3400)/I(2940) per set of six Raman spectra in both subjects of 8.8%(±2.7). Potentially accountable for the extent of the SD were the eye movement artifacts, although the focus was maintained at approximately the same site within the cornea, and the fact that the corneas slightly dehydrated over time as a result of maintaining the eyes open.

The application of Muro128 decreased the hydration of the anterior part of the cornea, as can be seen from Figure 3, depicting Raman spectra of subjects A

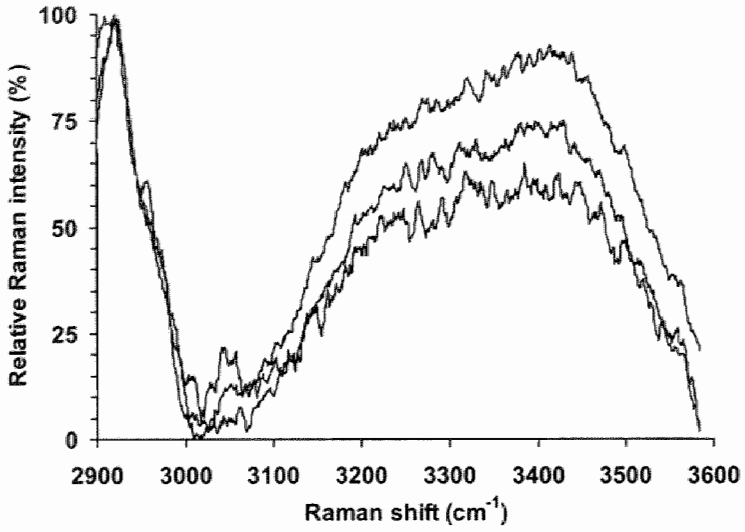

Figure 3. *In vivo* Raman spectra of the cornea of subject A normalized to the amplitude of the CH-vibrations at 2940 cm^{-1} illustrating the decrease in Raman spectral amplitude of the OH-vibrations of water at 3400 cm^{-1} due to the dehydrating effect on the cornea of Muro128.

from the same corneal region before and 5 minutes after both the first and the second application of Muro128, respectively. The largest decrease in the Raman intensity ratio OH/CH in subject A was ~35% from normal after the second topical application of Muro128 (Figure 3). On average however, this decrease in corneal hydration was less pronounced. This is illustrated in Figure 4 depicting the mean (±standard error) of the Raman intensity ratio OH/CH for each set of 6 Raman spectral assessments in both subjects, normalized to the hydration before topical application of Muro128. The dehydrating effect of Muro128 was larger in subject A than in subject B, with a maximum change of the Raman intensity ratio OH/CH of ~12% and ~4%, respectively. However, no significant changes in hydration were observed for subject B, while in subject A significant changes in corneal hydration were assessed only after the second application of Muro128. The fact that the subjects were allowed to blink in-between spectral assessments might have decreased the expected effect of the topical dehydrating agent. This too might be a reason for the observed difference between the two subjects, since subject A was more compliant to keeping the eyes open than subject B.

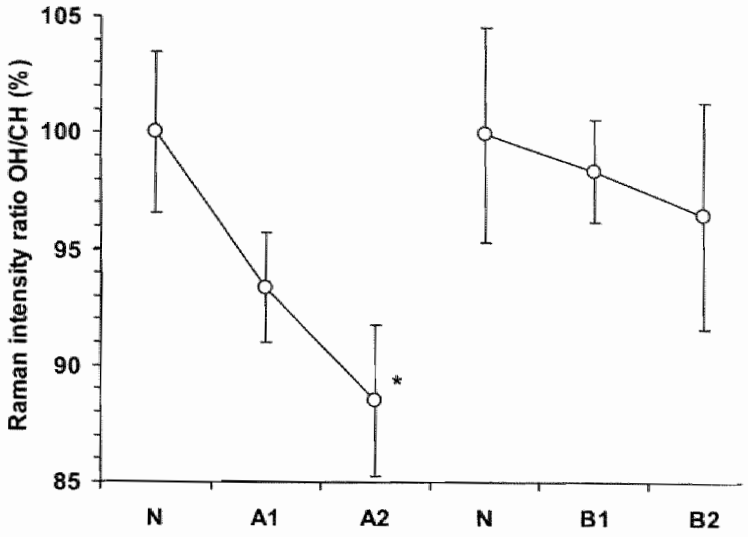

Figure 4. Relative changes in the Raman intensity ratio OH/CH as a measure for the corneal hydration in the human cornea *in vivo*. N=normal. A1, A2, B1, and B2, are the first and the second application of Muro128 in subject A and B respectively. *is statistically significant difference from N ($p<0.05$).

The subjects did not experience any discomfort from the procedure, neither during the exposure to the laser light nor during the four weeks thereafter as assessed with a general ophthalmological examination. In addition, it seems reasonable to believe that the laser-cornea interaction had no effect on the integrity of the cornea since no pain was perceived in the corneas with normal sensitivity after the anesthetic had lost its effect.

Discussion

These are the first successful *in vivo* Raman spectra obtained from the corneas of human subjects. Raman spectra in the region of 2900-3600 cm^{-1} were recorded from the anterior 100-150 μm of the cornea by maintaining the focus of the laser-beam at the same distance from the eye through optical feedback. These spectra were reproducible and yielded the CH-vibrational modes of proteins as well as the OH-vibrational modes of water in a single acquisition using a minimum of 15 mJ of laser light. The Raman intensity ratio I(3400)/I(2940) was used for the qualitative assessment of corneal hydration

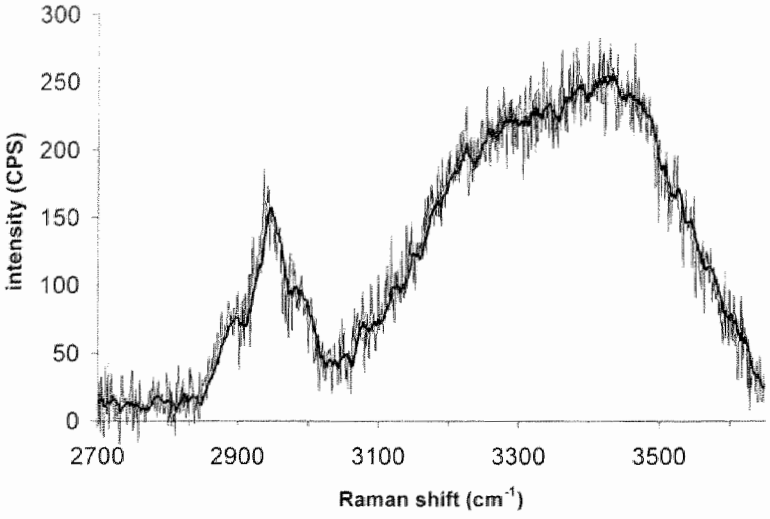

Figure 5. A low intensity (3 mJ) Raman spectrum of a human cornea *in vitro* in the high spectral Raman shift region (2700-3650 cm^{-1}) using the Argon laser (514.5 nm; 0.6 mW; 5 s exposure time). Calculated light exposure on the retina would be safe according to Ref. 21. Signal-to-noise ratio ~25.

from the anterior region of the cornea over a variable period of time before and after topical application of a mild dehydrating drug.

The same optical setup was utilized as for our previous *in vivo* animal study except for the use of a Helium-Neon (HeNe) in stead of an Argon (Ar) laser because of its relative safer wavelength.[6] In the previous report we established the validity of the relationship between the Raman intensity ratio OH/CH and corneal hydration, and performed calibration measurements using both ultrasound pachymetry and a lyophilization technique, thus showing the potential of confocal Raman spectroscopy for the non-contact assessment of the extent and distribution of corneal hydration in anesthetized rabbits.[6] Although the relationship between Raman spectral features and corneal hydration is still valid at present using the HeNe-laser, no calibration (such as using pachymetry) could be performed since the hydration of only the superficial part of the cornea was assessed, because movement artifacts compromised spatially resolved measurements of the total thickness of the cornea. The occurrence of movement artifacts could possibly be of more significance in seeing eyes because of the increased discomfort due to the intense light. Currently, we are exploring the possibility of incorporating an eye-tracking device into our setup, for elimination of movement artifacts during assessments *in vivo*. Furthermore, a significant

decrease in exposure time (<50 ms) would decrease the occurrence of movement artifacts.

The discrepancy between system sensitivity and retinal safety is the main drawback of the confocal Raman spectroscopy system for ophthalmic use still to overcome in order to enable the safe clinical application of this optical technique for the noncontact assessment of corneal hydration *in vivo*. Ideally this system would yield real-time (<50 ms/spectrum) data acquisition at minimal light exposures. In the present study, 15 mW of HeNe-laser light was used and a 1 second exposure time in order to get high signal-to-noise ratio (SNR) spectra of the cornea. According to the ANSI standards for laser safety the ocular maximum permissible exposure (MPE) for a HeNe laser at 632.8 nm is $1.8t^{3/4}$ mJ/cm^2, for exposure times (t) between 18 μs and 450 s.[21] This is equal to a maximum light exposure of ~1-2 mJ/s/cm^2 for exposures between 1 and 10 s. Since the high numerical aperture LDMO yields a retinal irradiation area of ~2.7 cm^2 when focusing in the cornea, as calculated using a ray-tracing program, a HeNe-laser irradiation of 15 mW for 1 s. is ~4x the MPE. Thus, the projected light levels used were not safe for the retina, and legally blind patients had to be used (*see also Chapter 1 of this Thesis*).

Increasing the sensitivity of the proposed method will yield high SNR spectra at light exposures that are safe for the retina. This can be achieved for example by increasing the axial length of the probing volume from 120 μm (as used here) to 500 μm by utilizing a larger confocal pinhole, i.e. fiber diameter, resulting in a higher Raman yield but lower spatial resolution. Furthermore, higher NA objectives will also have a higher Raman yield but at the cost of a shorter working distance. Another method of increasing the system sensitivity is by using a shorter wavelength laser. The Raman intensity (I) is in direct proportion to both the frequency of the incident light to the fourth power ($I \sim \nu^4$), yielding 2.5x higher signals using an Ar-laser at 514.5 nm as opposed to a HeNe-laser, as well as the sensitivity of the CCD camera, which is >2x higher in the same Raman frequency shift region using the Ar-laser as compared to the HeNe-laser.[13] Since the MPE for the more intense Ar-laser (514.5 nm) is the same as for the HeNe-laser (632.8 nm) for exposures between 18 μs and 10 s,[21] and the Raman yield is >5x higher with the Ar-laser, Raman spectra with similar signal-to-noise ratios can be obtained requiring only 1/5th (=3 mJ) of the total light energy as opposed to using a HeNe-laser, and would be below the MPE for exposure times >1 s. This was tested in a human cornea *in vitro* with the optical setup as used in our previous report[6] but using only 0.6 mW of Ar-laser light and a single 5 s. exposure time, yielding a SNR of ~25 and a projected retinal exposure of ~1/5x the MPE (Figure 5). More promising however are techniques currently being devised in our lab that preclude light exposure to the retina altogether while focusing at the cornea. In this manner, light levels that

would potentially be hazardous to the retina but not the cornea could be applied yielding high SNR spectra from small probing volumes at short acquisition times, allowing for real-time spatially resolved assessments of corneal hydration in a safe and noncontact manner.

The confocal Raman spectroscopic (CRS) technique as presented here has various advantageous properties, as outlined in detail in one of our previous reports.[13] The high gain of this optical system design is the result of the 180° backscatter configuration utilizing a high numerical aperture objective lens, and a highly sensitive CCD camera. The confocal arrangement prevents the detection of stray light and enables the probing of small optical volumes, yielding adequate spatial resolution in thicker tissues, such as the cornea. The diameter of the optical fiber can be changed to alter the integration depth from 20-900 μm. The objective lens is part of a telecentric setup, and can therefore be moved along its optical axis without changing the location of its focal plane, while the long working distance of ~13 mm allows for noncontact probing of ocular tissues at depths ranging from the superficial tearfilm to the anterior vitreous without moving the sample and without causing probing artifacts.[6] Lastly, the CRS technique provides direct information on the biochemical content of ocular tissues, i.e. corneal hydration, unlike for example ultrasound pachymetry, which derives corneal hydration through corneal thickness measurements.

Thus, we believe that with adequate improvements in system safety, confocal Raman spectroscopy could potentially be applied as a noncontact tool for the assessment of corneal hydration *in vivo* with clinical relevance for the early diagnosis of the extent and localization of disturbances in corneal deturgescence.

Acknowledgements

This work was sponsored in part by a Research to Prevent Blindness Unrestricted Grant. We thank Dr. Massoud Motamedi in the Dept. of Biomedical Engineering of the University of Texas Medical Branch in Galveston and Dr. James P. Wicksted in the Dept. of Physics of the Oklahoma State University for their valuable contributions towards this project. We also thank Mr. Brent Bell for his technical support.

References

1. Spiro T.G., *Biological Applications of Raman Spectroscopy. Volume 1: Raman Spectra and Conformation of Biological Macromolecules*. John Wiley & Sons, New York, 1987.

2. Yu N.-T. and East E.J. Laser Raman Spectroscopic Studies of Ocular Lens and Its Isolated Protein Fractions. *J Biol Chem*, 1975: 250; 2196-2202.
3. Mizuno A., Tsuji M., Fujii K., Kawauchi K., Ozaki Y. Near-infrared Fourier transform Raman spectroscopic study of cornea and sclera. *Japan J Ophthalmol*, 1994; 38(1): 44-48.
4. Siew DCW, Clover GM, Cooney RP, and Wiggins PM. Micro-Raman Spectroscopic Study of Organ Cultured Corneae. *J Raman Spectrosc* 1995; 26: 3-8.
5. Goheen SC, Lis LJ, and Kauffman JW. Raman Spectroscopy of Intact Feline Corneal Collagen. *Biochim Biophys Acta*, 1978; 536(1): 197-204.
6. Bauer NJC, Wicksted JP, Jongsma FHM, March WF, Hendrikse F, and Motamedi M. Noninvasive Assessment of the Hydration Gradient Across the Cornea Using Confocal Raman Spectroscopy. *Invest. Ophthalmol. Vis. Sci.* 1998; 39(4): 831-835.
7. Frushour B.C. and Koenig J.L. Raman Scattering of Collagen, Gelatin, and Elastin. *Biopolymers* 1975; 14: 379-391.
8. Wicksted JP, Erckens RJ, Motamedi M, and March WF. Raman Spectroscopy Studies of Metabolic Concentrations in Aqueous Solutions and Aqueous Humor Specimens. *Appl Spectrosc* 1995; 49(7): 987-993.
9. Erckens RJ, Motamedi M, Wicksted JP, and March WF. Raman Spectroscopy for Non-Invasive Characterization of Ocular Tissue: Potential for Detection of Biological Molecules. *J. Raman Spectrosc* 1997; 28: 293-299.
10. Sebag J., Nie S., Reiser K., Charles M.A., Yu N.T. Raman spectroscopy of human vitreous in proliferative diabetic retinopathy. *Invest Ophthalmol Vis Sci* 1994; 35(7):2976-80.
11. Huang L., Deng H., Koutalos Y., Ebrey T., et al. A resonance Raman study of the C=C stretch modes in bovine and octopus visual pigments with isotopically labeled retinal chromophores. *Photochem Photobiol* 1997; 66(6):747-54.
12. Yu N.T., Kuck JFR, and Askren CC. Laser Raman Spectroscopy of the Lens *in situ*, measured in an anesthetized rabbit. *Curr Eye Res* 1981/82; 1(10): 615-618.
13. Jongsma F.H.M., Erckens R.J., Wicksted J.P., Bauer N.J.C., et al. Confocal Raman Spectroscopy System For Noncontact Scanning Of Ocular Tissues: an *In Vitro* Study. *Opt Eng* 1997; 36(11): 3193-3199.
14. Bauer NJC, Motamedi M, Wicksted JP, et al. Non-Invasive Assessment of Ocular Pharmacokinetics using Confocal Raman Spectroscopy. *J Oc Pharm Ther* 1999; 15(2): 123-134.
15. Mandell RB, Polse KA, Brand RJ, Vastine D, Demartini D, Flom R. Corneal hydration control in Fuchs' dystrophy. *Invest Ophthalmol Vis Sci* 1989; 30(5), 845-852.
16. Polse KA. Changes in corneal hydration after discontinuing contact lens wear. *Am J Optom Arch Am Ac Optom* 1972; 49(6): 511-516.
17. Herse PR. Corneal hydration control in normal and alloxan-induced diabetic rabbits. *Invest Ophthalmol Vis Sci* 1990, 31(11): 2205-2213.

18. Herse P and Siu A. Short-term Efects of proparacaine on corneal thickness. *Acta Ophthalmol* 1992; 70(6): 740-744.
19. Dougherty PJ, Wellish KL, and Maloney RK. Excimer laser ablation rate and corneal hydration. *Am J Ophthalmol* 1994; 118(2): 169-176.
20. Fields CR, Taylor SM, and Barker FM. Effect of corneal edema upon the smoothness of excimer laser ablation. *Optom Vis Sci* 1994; 71(2): 109-114.
21. American National Standards Institute. Safe Use of Lasers. In: *ANSI Standard Z136.1*, Laser Institute of America, Orlando, 1993; 28-41.

CHAPTER 7

Noncontact assessment of ocular pharmacokinetics using confocal Raman spectroscopy

Noël JC Bauer, Massoud Motamedi, James P Wicksted,
Wayne F March, Carrol AB Webers, Fred Hendrikse

J Ocular Pharm. Ther. 1999; 15(2):123-134

A B S T R A C T

Aim: A laser scanning confocal Raman spectroscopy (CRS) system was applied for the noncontact quantification of the transport of a drug through the rabbit cornea *in vivo*.

Methods: Employing CRS, the changes in the amplitude of a drug-specific Raman signal were assessed over time in the tearfilm and corneal epithelium of the living rabbit eye (n=6), after topical application of 25μL Trusopt 2%™. This allowed for quantification of pharmacokinetic variables. The effect of the drug on corneal hydration was also monitored.

Results: CRS demonstrated adequate sensitivity and reproducibility, for continuous real-time monitoring of the Trusopt concentration. Each concentration-time curve had a bi-phasic trend; the rapid initial phase (t<8 min.) corresponds to the nonproductive losses of Trusopt from the tears (k_{10}=0.24±0.04 min^{-1}), and the slower later phase (t>20 min.) is the result of transfer from the drug from the corneal epithelium to the stroma (k_{23}=0.0047±0.0004 min^{-1}). Drug absorption into the corneal epithelium occurred at a rate of k_{12}=0.034±0.006 min^{-1}. Trusopt caused an acute dehydrating effect, with a maximum decrease in corneal hydration of ~15%, ~60 min. after drug application.

Conclusion: CRS has the specificity, sensitivity, reproducibility and spatial resolution for employment as a potentially valuable tool for the study of ocular pharmacokinetics.

Introduction

Ocular pharmacokinetics studies the absorption, distribution and elimination of ophthalmic drugs as function of concentration and time. These studies are necessary in order to determine the effectiveness of (potential) ocular drugs, and to optimize therapeutic dosing regimens. The assessment of pharmacokinetics of topical ocular drugs has been a challenging issue for researchers in this field.

Ocular tissues or fluids can not be harvested without seriously interfering with the anatomical integrity of the eye, limiting the applicability of *invasive* assessments in the human to sampling of aqueous humor during intraocular surgery, in order to determine the concentration of a preoperatively instilled ocular drug.[1,2] Consequently, we usually rely on animals, in particular the rabbit, as the subjects of choice in pharmacokinetic research.[3] Because of the obvious differences in anatomy and physiology the application of pharmacokinetic findings to the human might not always be possible. Furthermore, time-dependent drug concentration measurements by means of invasive assessment techniques require a large number of rabbits, since one rabbit is used for one time-point. Noncontinuous sampling will only provide statistically reliable data if sufficient animals per time-point are assessed, at sufficient, adequately spaced, time-points. It is not uncommon to use as many as 200 rabbits in a single pharmacokinetic comparison study of two ocular drugs.[4]

Noncontact pharmacokinetic assessment techniques, whilst they are safe to apply in the human eye, could potentially resolve these issues. Currently, however, no adequate noncontact technique is available for application in ocular pharmacokinetics. Although not specifically designed for pharmacokinetic measurements, non-invasive fluorometry of the anterior segment of the eye has various hallmark characteristics sought after in a suitable pharmacometric technique.[5] It is a non-invasive, sensitive, and safe technique, which yields real-time and continuous quantitative information from all ocular media (tear-film, cornea, aqueous humor and the crystalline lens). This technique has been applied to complement pharmacological studies in the eye, by providing information on tissue-specific physiological properties, i.e. cellular permeability, diffusion rates, and flow of tear-film and aqueous humor.[5-7] Furthermore, fluorometry has the potential to assess the contribution of each tissue or cell-layer to ocular drug transport necessary for the validation of current ocular pharmacokinetic models.[3,4,8] However, fluorometry is inherently nonspecific, and can be hampered by the presence of tissue auto-fluorescence. Therefore the development of a non-invasive technique that combines all aforementioned properties could potentially provide for accurate determination of the pharmacokinetic behavior of ophthalmic drugs in the human eye.[8]

The objective of this study was to investigate the feasibility of applying a novel laser scanning confocal Raman spectroscopy (CRS) system for noncontact pharmacokinetic assessments in the living rabbit eye. Raman spectroscopy is an optical technique that allows for biochemical assessments by identifying specific laser-light induced molecular vibrations. This technique has been utilized in the past to characterize the biochemical changes in the ocular lens during its transformation from normal to the cataractous state; see for example Ref. (9). More recently we applied the CRS technique to determine the temporal and spatial distribution of corneal hydration in an *in vivo* animal model.[10] Furthermore, applications of CRS for the noncontact quantitative assessment of biomolecules in aqueous humor specimens and aqueous solutions have been proposed.[11]

Unlike fluorometry, the inherent specificity of Raman spectroscopy (RS) has the potential to differentiate between the biochemical signature of ocular tissues and ocular drugs, and could therefore enable the monitoring of drug concentrations in ocular tissues. Furthermore, the confocal configuration of the proposed CRS system yields adequate spatial resolution in the tissue of interest, with a cross-sectioning capability of 20 μm or more.[10,12] In addition, the CRS system, like fluorometry, has the potential to assess all ocular media in a noncontact manner, and provide quantitative information in a real-time and continuous fashion.[12]

Thus, we utilized CRS to monitor the time-dependent concentration changes of a commonly used topical ocular drug within the anterior region of the cornea (tear-film and corneal epithelium), in an *in vivo* animal model. The drug of choice was Trusopt 2% (dorzolamide HCl 2%, ophthalmic solution, Merck Co., CA), because of its strong Raman signal, and because the pharmacokinetic behavior of this compound has not yet been elucidated completely.[13] Furthermore, we applied CRS to assess the changes in corneal hydration following the application of this drug.

Materials and methods

Instrumentation

The characteristics and performance of our laser scanning confocal Raman spectroscopy (CRS) system for the noncontact biochemical characterization of ocular tissue has been described previously.[12] In short, the key components of the system are a single grating spectrometer (SPEX500M, Spex Industries, Edison, NJ), with CCD-camera for real-time signal detection, an argon laser (514.5 nm), and a long-working distance microscope objective lens (magnifica-

tion 25x, numeric aperture=0.5, focal length=10 mm, Jena, Karl Zeiss, Oberkochen, Germany). The application of this lens not only yielded high light gathering power, but also noncontact probing of all ocular tissues of interest, by virtue of its long working distance of ~13 mm. This entrance lens was applied in a 180° backscatter configuration (analog to an epi-illuminated microscope), and hence utilized for focusing as well as for collecting the Raman scattered light. An optical fiber at the exit site of this Raman spectroscopy system, for transport of the Raman scattered light towards the spectrometer, was placed in confocal alignment with the entrance lens (LDMO). Thus, this fiber acts like a confocal pinhole, and it effectively eliminates light from out-of-focus places, allowing for the assessment of thin layers. Changing the diameter of the fiber will change the probing volume, mainly by changing the integration depth (≥20 μm). Apart from the hydration assessments, all spectra were obtained using a laser power of 50 mW and a 60 s exposure time, in conjunction with a 50 μm fiber, yielding an integration depth of 120 μm, and each spectrum was acquired by focusing the long-working distance microscope objective lens (LDMO) in such a manner that only the precorneal tearfilm and the corneal epithelium were included in the probing volume.

In vitro and *in vivo* studies

To demonstrate the ability of our method to quantify drug concentrations, a commercially available topical ocular drug (Trusopt, dorzolamide HCl 2% ophthalmic solution, Merck, CA), clinically used to reduce aqueous humor formation by inhibition of the enzyme carbonic anhydrase, was used. The drug was diluted with high-performance liquid chromatography-grade water to concentrations ranging from 0.01 to 2% (undiluted), and assessed with the CRS technique *in vitro*. The Raman intensity of a dorzolamide-specific peak at 1420 cm^{-1} was plotted against sample drug concentration (%), and their relationship investigated for linearity.

Under an approved animal protocol that complied with the ARVO Resolution on the Use of Animals in Research, the *in vivo* studies were performed on the eyes of in total 9 female NZW rabbits (3.0-4.0 kg); 3 rabbits were used for assessment of changes in drug concentration versus time at the anterior region of the cornea (n=6 eyes); 6 rabbits (n=9 eyes) were used to assess the changes in corneal hydration as function of time after application of Trusopt. The animals were restrained in a holder, and anesthetized using intramuscular ketamine hydrochloride (25 mg/kg) and xylazine (5 mg/kg).

Before drug application, five Raman spectra were obtained in the Raman shift range from 517-2018 cm^{-1}, with the LDMO properly focused and optically aligned to the cornea of the anesthetized rabbit (*vide supra*), in order to obtain

baseline values for the Raman peak of interest at 1420 cm^{-1}. At time t=0, 25 µL of Trusopt 2% was applied in one eye, and the LDMO was immediately (<3 sec.) and continuously manually (<10 µm) adjusted to keep the focus in place. Raman spectra were obtained at regular intervals from t=0 to t=120 min., yielding ~20-25 Raman spectra per eye during the course of the concentration assessments. An algorithm was used (Matlab, Mathworks, Natick, MA) to calculate from each single spectrum the amplitude of the drug-specific Raman peak of Trusopt at ~1420 cm^{-1} (in count-per-second, CPS) using the spectral information in the low range (517-2018 cm^{-1}). These values were normalized to the background noise and plotted as a function of time.

Initially, the log-linear concentration versus time curve for each eye was analyzed qualitatively, in order to identify the different phases corresponding to the transfer of drugs from one compartment to the other (see Appendix). The data belonging to each phase was then used to calculate the time-dependent pharmacokinetic drug transfer rate constants (in min^{-1}). Various other pharmacokinetic parameters could be derived using these constants. The details on the calculation of pharmacokinetic variables are described in the Appendix.

Corneal hydration was determined using a previously reported method, which entails a laser power of 25 mW, a 3 s exposure time per spectrum, and an 11 µm fiber (50 µm integration depth). Spectra in the higher Raman shift range (~2700-3600 cm^{-1}) yield OH-vibrations (largely caused by the corneal water) and CH-vibrations (mainly caused by structural proteins of collagen), and the Raman intensity ratio OH/CH is directly proportional to the local degree of hydration (mg water / mg dry wt.). Assessment of corneal hydration was obtained by axially scanning the whole thickness of the cornea with 50 µm steps. The integrated results of each axial scan are strongly correlated with total corneal hydration as assessed with lyophilization or pachymetry.[10] Corneal hydration as function of time was assessed in five corneas of four rabbits after topical application of Trusopt 2%, and in another four eyes of two rabbits without drug application, and compared in order to investigate the acute effects of Trusopt on corneal hydration.

Results

Figure 1 displays typical Raman spectra in the lower Raman shift region (truncated to 700-1800 cm^{-1} for clarity) of [A] the original 2% Trusopt, [B] the anterior region of a normal NZW rabbit cornea *in vivo* before drug application, and a similar corneal region *in vivo* at [C] t=1 and [D] t=120 min, respectively, following application of 25 µL of Trusopt 2%. The spectra of Trusopt 2%, and of the living cornea at t=1 min. after drug application, display a strong Raman

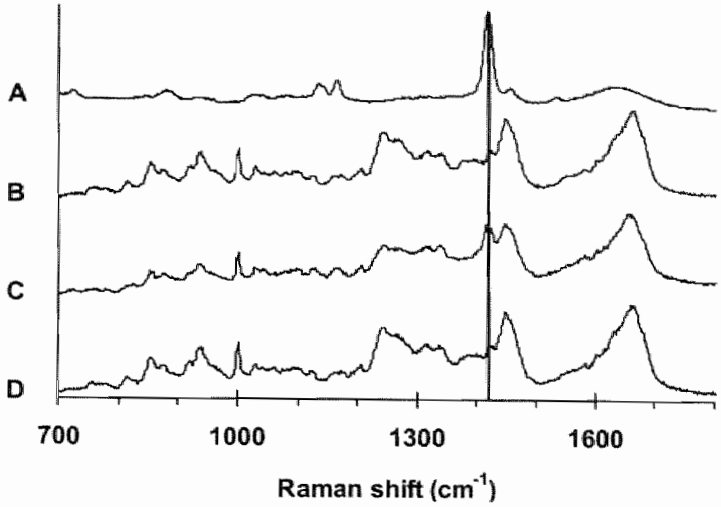

Figure 1. Typical Raman spectra of (A) the original Trusopt 2%, (B) a normal NZW rabbit cornea *in vivo*, and the same cornea at 1 (C) and 120 (D) minutes following application of 25 μL of Trusopt 2% to that eye. Vertical line identifies the Raman shift position (1420 cm^{-1}) attributed to the specific Raman vibration of dorzolamide.

signal at the same Raman shift position of approximately 1398 to 1440 cm^{-1} with a maximum at approximately 1420 cm^{-1} (ring stretch vibration of 2-substituted thiopenes). In the normal cornea a weak signal can be observed at the Raman shift position of approximately 1445 cm^{-1}. The strong Raman signal at 1420 cm^{-1} is caused by the double ring-structures of dorzolamide, and was monitored during the pharmacokinetic measurements. Furthermore, it can be seen in this figure, that the spectra of a normal cornea and the same cornea at t=120 min. after drug application display no significant differences, suggesting that there are no adverse effects of dorzolamide on protein structure and conformation in the corneal stroma.

Figure 2 depicts the intensity of the Raman peak at 1420 cm^{-1} as a function of the concentration of Trusopt in the range 0.01-2.00% as assessed *in vitro*. A strong linear relationship can be seen (R^2=0.999, n=8), proving the validity of the proposed method to assess drug concentrations. The limit of detection with the described experimental conditions used in this study is a Trusopt concentration of approximately 0.02% (200 μg/mL=0.55 mM), but could be significantly lower at longer exposure times or higher light-energy levels. In all cases this sensitivity proved sufficient for assessment of drug concentrations *in vivo* up to 2 hours after drug application.

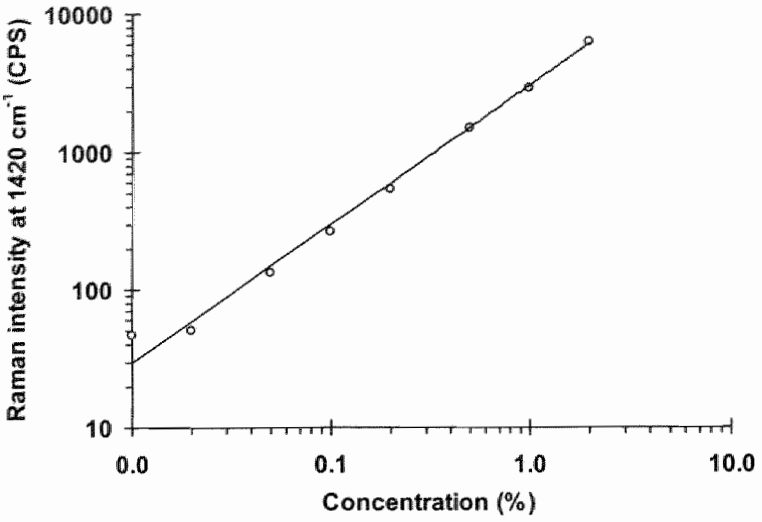

Figure 2. Relationship between Raman intensity (I) and concentration(C) of Trusopt in HPLC-grade water from 0.01 to 2 % (2% is the original solution). In formula: I=2960(±70)C; r=0.9997, p<0.05, n=8.

Figure 3 shows a typical semi-logarithmic plot of the dorzolamide concentration versus time as assessed with the CRS technique after topical application of 25 μL of Trusopt 2% in one eye. It can be seen that the drug concentration versus time follows a bi-phasic trend with a fast first apparent decay rate from t=0 to approximately 7 minutes (A), and a slower second one from approximately 20 minutes onwards (B). These regions were used to calculate k_{10} and k_{23}, respectively (see Appendix). Table 1 summarizes the pharmacokinetic transfer rate constants as assessed using confocal Raman spectroscopy of all 6 eyes. The values for the transfer rate constants are (mean±SD): k_{10}=0.24±0.04, k_{12}=0.034±0.006, and k_{23}=0.0047±0.0004 min^{-1}. From these values it is possible to derive other pharmacokinetic variables (Table 2). The standard deviations (SD) suggest that the proposed method is reproducible, given our small data set, with an average SD for all calculated variables of ~12% (range 9-16%).

Corneal hydration in the 'treated' rabbits (H_T) decreased as a function of time after application of Trusopt 2%, (H_T = -0.0085t + 3.81, r=0.96, p<0.05, n=33) as can be seen from Figure 4. Significant changes in hydration were observed from 30 to 70 minutes. The maximum change in hydration occurred at ~60 minutes after drug deposition and was ~0.55 mg water / mg dry wt. (approximately 15% of H_0). Corneal hydration in the control rabbits (H_C) did not change appreciably over time (H_C = -0.0010t +3.96, r=0.87, p<0.05, n=18).

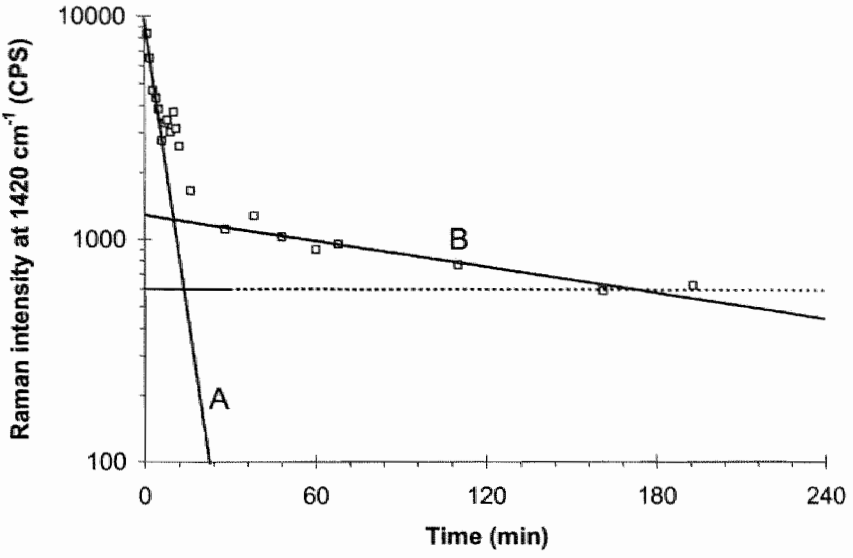

Figure 3. Typical results showing a log-linear graph depicting the amplitude of the Trusopt-specific Raman peak at 1420 cm^{-1} vs. time after application of 25 µL of Trusopt 2% to the eye in the NZW rabbit *in vivo*. (A) and (B) are the curve-fits yielding the pharmacokinetic variables k_{10} and k_{23}, respectively. Broken horizontal line is the Raman intensity *before* drug application, and the data is normalized using this value.

Table 1. Pharmacokinetic transfer rate constants of Trusopt 2% as assessed using laser scanning confocal Raman spectroscopy in the living rabbit cornea (n=6).*

Eye	k_{10} (min^{-1})	*r*	k_{23} (min^{-1})	*r*	k_{12} (min^{-1})
10D	0.30	0.88	0.0050	0.63	0.041
10S	0.24	0.75	0.0047	0.31	0.033
20D	0.23	0.71	NA	NA	NA
20S	NA	NA	0.0052	0.79	NA
30D	0.24	0.98	0.0042	0.94	0.036
30S	0.20	0.98	0.0044	0.82	0.026
Mean±SD	0.24 ± 0.04	-	0.0047±0.0004	-	0.034±0.006

*r is correlation coefficient with $p<0.05$; NA is not available; See Appendix for details.

Table 2. Derived pharmacokinetic variables of Trusopt 2% in the living rabbit cornea (n=6) using the pharmacokinetic transfer rate constants of Table 1.*

Eye	$t_{1/2}$ in tears (min)	$t_{1/2}$ in epith. (min)	Tp_{epi} (min)	K_{epi} (*10^{-5} cm/min)	F (%)
10D	2.0	139	14	2.50	1.6
10S	2.5	147	17	2.35	1.9
20D	3.0	-	-	-	-
20S	-	133	-	2.60	-
30D	2.5	165	17	2.10	1.7
30S	3.1	158	20	2.20	2.2
Mean±SD	2.6±0.4	148±13	17±2	2.35±0.21	1.9±0.2

*See Appendix for details on derivations and description of variables.

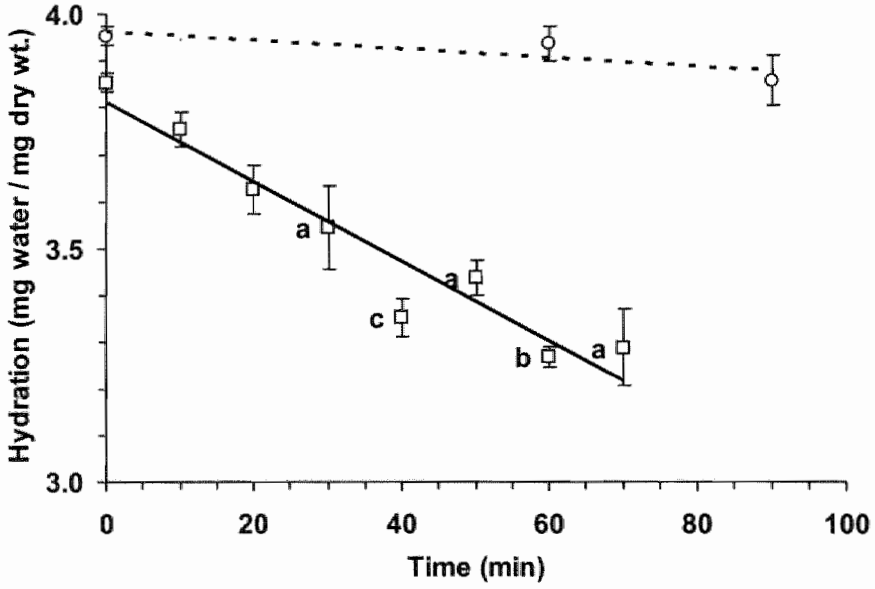

Figure 4. Corneal hydration in the rabbit under *in vivo* conditions as function of time. Solid and dotted lines represent the 'treated' and control rabbits, respectively. P-values for the difference in mean hydration between t=0 and t>0 min. as determined by the Student's t-test in the Trusopt-treated eyes are given by a ($p \leq 0.05$), b ($p \leq 0.005$), and c ($p \leq 0.001$)

Discussion

In this manuscript we present the results on the application of laser scanning confocal Raman spectroscopy (CRS) for ocular pharmacokinetic measurements. This optical technique is believed to have significant advantages over current assessment techniques. The non-contact character of CRS allows for *in vivo* applications and permits multiple assessments of the concentration of a drug in the same sample over time (up to 120 minutes after drug application). This reduces the amount of animals needed to obtain valuable pharmacokinetic information. More importantly, the confocal modality of the proposed Raman spectroscopic technique permits probing of specific tissue layers, allowing determination of drug concentration changes in the different layers of the anterior cornea. A challenging approach to pharmacokinetic drug transport would be to temporally and spatially resolve the distribution of the drug in the cornea after drug deposition, to improve the predictive value of pharmacokinetic models. The feasibility of such a method was shown in an earlier study with regards to corneal hydration.[10] The higher requirements of this type of technique heralds a major increase in signal-to-noise ratio, since both the assessment volume as well as the exposure time need to be decreased significantly for reliable results. Future work by our group in this area is directed towards that goal.

The most significant advantage of CRS over fluorometry is its inherent specificity. This allows for precise analysis of molecular vibrations, and can be utilized to identify ocular drugs by their unique characteristics, thus being able to differentiate drugs from ocular tissues. CRS enables, for the first time, a direct monitoring of the pharmacokinetic drug transport within the eye. The specificity of CRS can also be put to use to study the effects of the drug on the tissue it is being applied to. In theory, tissue-protein changes will exhibit themselves in Raman spectroscopic changes in the lower (signature) region of the Raman spectrum from 517-2018 cm^{-1}. The present study did not find significant spectral changes in this signature region as a result of drug application, as shown by comparing the spectral response of a normal cornea and the same cornea two hours after drug application. However, hydration changes due to application of Trusopt 2% were easily quantified, as presented in Figure 4. The dehydrating effect of Trusopt could be due to an increased level of evaporation on the surface of the cornea, maybe through an increased tear production due to the irritating effect of the drug.

The concentration changes of dorzolamide were measured at the anterior region of the rabbit cornea under *in vivo* conditions. Qualitatively, the log-linear drug-concentration curves followed the bi-phasic trend commonly observed for other topical ocular drugs.[14-16] The first apparent decay rate (from 0 to 7 minutes) is caused by non-productive losses of the drug from the tears, meaning

the amount of drug that is not lost through transfer via the cornea into the aqueous, but by other means, like for example tear overflow, transport via the tear duct, or the scleral or conjunctival circulation. This non-productive loss, here defined as k_{10}, determines the length of presence of the drug in the precorneal tearfilm (normally <10 minutes with ophthalmic solutions). This rate (normally 0.05-0.30 min^{-1}) is higher the more irritating the drug is to the eye, like Trusopt, which can cause stinging. Indeed, with k_{10}=0.24±0.05 min^{-1}, our results indicate that the non-productive drug loss of Trusopt is at the higher end of the aforementioned range. Although the transport of dorzolamide to the site-of-action seems to be mainly through the sclera, a small portion is taken up by the cornea to reach the aqueous humor.[17] The drug transfer from the tears into the epithelium, is not directly visible in the concentration-time curves. This value was derived using k_{10}, and the drug-concentrations at t=0 for both the tears and the epithelium, according to function [2] of the Appendix, and yielded 0.034±0.06 min^{-1}, indicating that dorzolamide is easily taken up by the corneal epithelium, with an absorption coefficient of ~$10.2 \cdot 10^{-3}$ cm/hr. The latter half of the second apparent decay rate is contributed to the transfer of drug out of the epithelium, defined as k_{23}, which was 0.0047±0.0004 min^{-1}, yielding an epithelial permeability of ~$1.4 \cdot 10^{-3}$ cm/hr. This is comparable to the epithelial permeabilities for dexamethasone, pilocarpine, and timolol,[14] but significantly better than previously reported values for transcorneal absorption of other topically active carbonic anhydrase inhibitors.[18] Data taken from a previous study shows that the concentration change of Trusopt in the whole cornea occurs at a rate of ~0.005 min^{-1}.[13] This is comparable to the value found in our study for k_{23}. Since transport of a drug through the whole cornea is governed by the slowest transport rate, the transport of dorzolamide from the epithelium into the stroma can now be identified as the limiting factor for drug transport of dorzolamide through the cornea. This finding suggests that the posterior site of the corneal epithelium is more obstructing to drug transport than the anterior site, and thus that dorzolamide is relatively more lipophilic than hydrophilic, because $k_{12} > k_{23}$. This could be an explanation of the alternate route of transport of dorzolamide through the sclera. For transport via the cornea it can be stated that for Trusopt, as previously stated for pilocarpine, the corneal epithelium acts both as a barrier for transport as well as a depot for sustained release of this compound into the stroma, with an epithelium half-life time of ~148 minutes.[19]

Although all three determined pharmacokinetic transfer rate constants seem to be realistic for this type of topical ocular drug, no further comparison can be made with the literature although the reproducibility of our measurements are high. Apart from the mentioned study by Sugrue, no ocular pharmacokinetic rate constants are published for Trusopt 2%.[13]

Apart from direct drug monitoring in the eye another interesting application of RS would be to assess more directly the drug-tissue interactions, like binding of a carbo-anhydrase inhibitor to its receptor, which has been possible with resonance RS using an ultra-violet light source, by correlating spectral line shifting with drug-receptor complex formation.[20] Furthermore, since metabolites and the original drug would display differences in Raman signature, these metabolites could be detected, and with it the identification of metabolic activity in the tissue of interest. Over time and at various positions within the cornea, the Raman shift position of dorzolamide did not change significantly, suggesting that either our technique is not sensitive enough for these kinds of assessments or that no drug-tissue interaction or metabolic activity is taking place. In the light of previous pharmacological studies, we have to assume that the sensitivity of our technique is not adequate.

Since Raman scattering is inherently weak the sensitivity of the Raman scattering will be determined by the amount of light energy, the wavelength used (the shorter the wavelength the higher the Raman scattering), the sensitivity of the detector, and the Raman cross-section of the molecular vibrations to be studied (stronger bonds exhibit a higher Raman scattering). In this study, we compromised between sensitivity and safety and opted for an Argon laser at a relatively high power setting of 50 mW and long exposure times (60 sec.). Future clinical application using laser scanning confocal Raman spectroscopy as a diagnostic tool has to be preceded by significant improvements in the safety. With the introduction of more sensitive detectors preferably in the infra-red spectrum these apparent disadvantages will definitely decrease, as the exposure times can be decreased, and longer, less damaging wavelengths can be chosen, increasing the (clinical) applicability and safety of CRS for possible use in the human situation.[21] Furthermore, a more sensitive analysis technique could be used to extract more useful information from the individual Raman spectra. This could be performed using the so-called Partial Least Squares technique, currently being developed in our lab for purpose of pharmacokinetic measurements.

The fact that the drug in question should have a detectable Raman signal poses another disadvantage. However, in the light of the potential use of this technique it would theoretically be possible to label drugs with a specific Raman active compound, or design drugs with an incorporated Raman active bond.[22] Thus, the mentioned disadvantages are not absolute per se. We have shown in this study that the non-contact optical technique of CRS is a powerful biochemical analytical tool, which has the potential to be applied for pharmacokinetic measurements.

In conclusion, we believe that this study has shown that the potential of a novel non-contact technique based on Raman spectroscopy could be utilized

for the study of ocular pharmacokinetics, allowing for continuous assessment of the concentration of a topical eye drug at different regions within the cornea under *in vivo* conditions. CRS has inherent beneficial characteristics potentially applicable to study drug-tissue interactions, whether it be adverse effects on the tissue in question, metabolic processes, or monitoring direct drug-receptor binding.

Acknowledgments

This work was sponsored in part by a Research to Prevent Blindness unrestricted grant, and a grant from the Department of Energy (DOE-FG03-95ER61971).

References

1. Uterman D., Matz, K., Meyer, K. Gentamicinspiegel in Kammerwasser des Menschen nach parenteralen, subkonjunktivaler und lokaler Applikation. *Klin. Monatsbl. Augenheilk*, 171:579, 1977.
2. Donnenfeld E.D., Perry, H.D., Snyder, R.W., Moadel, K., Elsky, M., Jones, H. Intracorneal, Aqeous Humor, and Vitreous Humor Penetration of Topical and Oral Ofloxacin. *Arch. Ophthalmol.*, 115:173-176, 1997.
3. Urtti A., Salminen, A. Animal Pharmacokinetic Studies. *In* Ophthalmic Drug Delivery Systems, Mitra A.K. ed., Marcel Dekker, Inc., New York, 1993, p. 121-136.
4. Schoenwald R.D. Ocular drug delivery: Pharmacokinetic considerations. *Clin. Pharmacokinet.*, 18(4):255-269, 1990.
5. Brubaker R.F., Maurice, D.M., McLaren, J.W. FLuorometry of the Anterior Segment. *In* Noninvasive Diagnostic Techniques in Ophthalmology, Masters B.R. ed., Springer-Verlag, New York, 1990, p. 248-280.
6. Egan C.A., Hodge, D.O., McLaren, J.W., Bourne, W.M. Effect of Dorzolamide on Corneal Endothelial Function in Normal Human Eyes. *Invest. Ophthalmol. Vis. Sci*, 39(1):23-29, 1998.
7. Adler C.A., Maurice, D.M., Paterson, T.M. The effect of viscosity of the vehicle on the penetration of fluorescein into the human eye. *Exp. Eye. Res.*, 11:34, 1971.
8. Lee V.H.L., Robinson, J.R. Review: Topical Ocular Drug Delivery: Recent Developments and Future Challenges. *J. Oc. Pharm.*, 2(1):67-108, 1986.
10. Dai S., Qi, L., Bai, C., Ni, T., and Deng, X. Laser Raman spectroscopy study on experimental galactose-induced cataract. *Yen Ko Hsueh Pao* [Eye Science], 11(3):143-146, 1995.

11. Bauer N.J.C., Wicksted, J.P., Jongsma, F.H.M., March, W.F., Hendrikse, F., and Motamedi, M. Non-Invasive Assessment of the Hydration Gradient Across the Cornea using Confocal Raman Spectroscopy. *Invest. Ophthalmol. Vis. Sci.*, 39(4):831-835, 1998.
12. Erckens R.J., Wicksted, J.P., March, W.F., and Motamedi, M. Raman Spectroscopy for Non-Invasive Characterization of Ocular Tissue: Potential for Detection of Biological Molecules. *J. Ram. Spectros.*, 28:293-299, 1997.
13. Jongsma F.H.M., Erckens, R.J., Wicksted, J.P., Bauer, N.J.C., Hendrikse, F., March, W.F., and Motamedi, M. Confocal Raman Spectroscopy System for Non-Contact Scanning of Ocular Tissues: an *in vitro* study. *Optical Engineering*, 36(11):3193-3199, 1997.
14. Sugrue M.F. The Preclinical Pharmacology of Dorzolamide Hydrochloride, a Topical Carbonic Anhydrase Inhibitor [review]. *J. Oc. Pharm. Ther.*, 12(3): 363-376, 1996.
15. Mishima S. Clinical Pharmacokinetics of the Eye; Proctor Lecture. *Invest. Ophthalmol. Vis. Sci*, 21:504-541, 1981.
16. Nagataki S., Mishima, S. Pharmacokinetics of Instilled Drugs in the Human Eye. *Int. Ophthalmol. Clinics*, 20(3):33-49, 1980.
17. Schoenwald R.D. Ocular pharmacokinetics/Pharmacodynamics. *In* Ophthalmic Drug Delivery Systems, Mitra A.K. ed Marcel Dekker, Inc., New York, 1993, p. 83-110.
18. Schoenwald R.D., Deshpande, G.S., Rethwisch, D.G., Barfknecht, C.F. Penetration into the anterior chamber via the conjunctival/scleral pathway. *J. Ocular Pharmacol.*, 13:41-59, 1997.
19. Sharir M., Pierce Jr., W.M., Chen, D., Zimmerman, T.J. Pharmacokinetics, adic-base balance and intraocular pressure effects of ethyloxaloylasolamide-A novel topically active carbonic anhydrase inhibitor. *Exp. Eye Res.*, 58(1):107-116, 1994.
20. Sieg J.W., Robinson, J.R. Mechanistic studies on transcorneal permeation of pilocarpine. *J. Pharm. Sci.*, 65:1816-1822, 1976.
21. Kumar K., and Carey, P.R. The Resonance Raman Spectra and Excitation Profiles of some 4-sulfamylazobenzenes. *Can J. Chem.*, 55:1444-1453, 1977.
22. Baraga J.J., Feld, M.S., Rava, R.P. Rapid Near-Infrared Raman Spectroscopy of Human Tissue with a Spectrograph and CCD detector. *Appl. Spectrosc.*, 46(2):187-190, 1992.
23. Sijtsema N.M., Duindam, J.J., Puppels, G.J., Otto, C., and Greve, J. Imaging with Extrinsic Raman Labels. *Appl. Spectrosc.*, 50(5):545-551, 1996.
24. Cavanagh H.D., Petroll, W.M., and Jester, J.V. Confocal Microscopy: Uses in Measurement of Cellular Structure and Function. *In* Progress in Retinal and Eye Research, Elsevier Science Ltd., London, 1995, p. 527-565.

Appendix

The diagram below shows the pharmacokinetic model that was used in the present study:

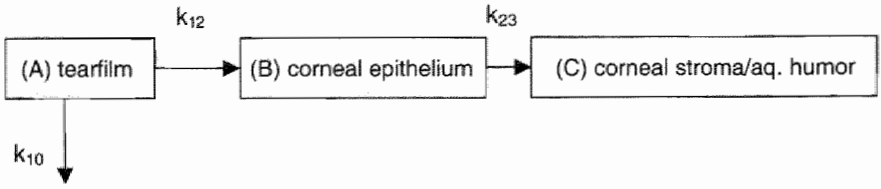

A confocal Raman spectroscopic technique was used to assess the changes in drug concentration in the pre-corneal tears and corneal epithelium of the rabbit cornea *in vivo*. The site of focus (with an axial length of 110 μm) includes the tearfilm (~41-46 μm)[23], and corneal epithelium (~40 μm), but not the corneal stroma/aqueous humor, and is constantly kept at the interface between the two layers. A three compartment model is adopted, to best describe the transfer of drug from the site of focus (see Scheme above).[4, 14, 16] The first compartment is (A) the tearfilm, the second is (B) the corneal epithelium, and the third is the (C) corneal stroma/aqueous humor. Thus, the change in drug concentration as a function of time can be described with three pharmacokinetic transfer rate constants, describing the non-productive losses from the tearfilm (k_{10}), the transfer of drug from the tears into the epithelium (k_{12}), and the transfer of drug from the epithelium into the pharmacokinetically equivalent compartment of the corneal stroma and aqueous humor (k_{23}). These compartments are equal because the thin lipophilic endothelium seems to play an insignificant role for the corneal permeability of hydrophilic ocular drugs[8]. The early part (<10 min.) of the concentration-time curve only describes the non-productive losses of drug from the tears k_{10}, and not the transfer of drugs from tears into the epithelium k_{12}, since the latter has no net effect on the Raman intensity of the drug-specific signal, because both layers are assessed simultaneously with our methods. Thus, k_{12} cannot be determined directly, but can be derived however (see below).

Assuming first-order kinetics, k_{10} can be calculated by fitting a single exponential, according to [1] to this part of the concentration-time curve,

$$C(t)=C(0)e^{-kt}, \text{ (in counts-per-second, CPS)} \quad [1]$$

with C(0) being the tearfilm drug-concentration at t=0, and *k* being the numerical value for k_{10} (in min^{-1}).

The constant k_{23} is calculated by fitting a single exponential according to [1] to the terminal log-linear phase of the concentration-time curve; with C(0) being the extrapolated drug-concentration in the epithelium at t=0, and *k* being the numerical value for k_{23}.
The transfer constant k_{12} can not be measured directly, as said before. However, both intercepts C(0) and k_{10} can be used to derive k_{12}, since

$$k_{12}=k_{10} \cdot [C(0)_{epi} / C(0)_{tear}], \text{ (in } min^{-1}\text{); Ref. (14)} \quad [2]$$

Other pharmacokinetic variables which can be derived for the tissue of interest using k_{10}, k_{12}, and k_{23} are (Ref. 14):

- the half-life times of the drug in each compartment,

$$t_{1/2} = \ln(2)/k, \text{ (in min)} \quad [3]$$

with *k* being any of the three transfer rate constants,

- the time to peak in the corneal epithelium,

$$TP_{epi}= \ln(k_{10} / k_{23})/(k_{10} - k_{23}), \text{ (in min)} \quad [4]$$

- the permeability of the epithelial barrier,

$$K_{epi} = (k_{23} \cdot V / Q) = (k_{23} \cdot T), \text{ (in cm/min)} \quad [5]$$

with V, Q, and T the volume, the surface area, and the average thickness ($=5 \cdot 10^{-3}$ cm) of the epithelial layer, respectively,

- and, the fraction absorbed into the cornea,

$$F = (1- [k_{10} / (k_{10} + k_{23})]) \cdot 100\% = [k_{23} / (k_{23} + k_{10})] \cdot 100\%, \text{ (in \%)}. \quad [6]$$

CHAPTER 8

Remote temperature measurements in the eye using confocal Raman spectroscopy

Noël JC Bauer, Wayne F March, Fred Hendrikse, Massoud Motamedi

Submitted

A B S T R A C T

Aim: The application of a suitable technique for remote temperature measurements in biological tissues could be of significance in monitoring its physiological state. For example, temperature measurements in the eye could yield the monitoring of various causes of ocular hyperthermia (inflammation, or induced by laser or ultrasound). We sought to determine the feasibility of Raman spectroscopy (RS) for remote temperature measurements within the aqueous humor of the rabbit eye *in vivo*.

Methods: Using a Confocal Raman Spectroscopy (CRS) system (250 mJ argon light at 514.5 nm) high signal-to-noise ratio Raman spectra from 2580-3800 cm^{-1} were recorded in HPLC-grade water (13-48°C; calibrated thermocouple) and the aqueous humor of the rabbit eye under *in vivo* and *ex vivo* conditions (14-34 °C; calibrated intra-ocular thermocouple).

Results: The ratio between the integrated Raman intensities of two temperature dependent OH-vibrational regions (OH2/OH1) in the spectra of water showed high linearity with the prevailing temperature (T °C), both in pure water (0.0049(±1.2%)T+0.4522(±0.5%), R^2=0.99, n=50, p<0.05) as well as in the rabbit aqueous humor (0.0036(±2.8%) T+0.4966(±0.6%), R^2=0.98, n=162, p<0.05) with a high degree of reproducibility and sensitivity (~0.2-0.7 °C).

Conclusion: Raman spectroscopy can be used for sensitive temperature assessments in the aqueous humor of the rabbit eye under *in vivo* conditions.

Introduction

Raman spectroscopy (RS) is a powerful optical technique for the biochemical characterization of biological media.[1] Furthermore RS can also be applied for temperature assessments, since Raman scattering is per definition a temperature dependent process. A well established method for thermometry using RS entails the assessment of the Stokes/anti-Stokes Raman intensity ratio.[2] Because the anti-Stokes lines are usually extremely weak at physiological temperatures the applicability of this method in living biological tissues is limited. Another previously reported method consists of assessing the temperature-dependent changes in the shape of the Raman spectrum of water,[3,4] and has been applied for the remote temperature assessments of sub-surface ocean-waters[5] and biological tissues.[6] The latter could have significant applications in biology and medicine, since most biological tissues are embedded in water.

The focus of our research is mainly aimed at the application of RS in ocular tissues. Thus, we have investigated the feasibility of RS for temperature measurements in the eye. This is of clinical significance because it could possibly yield the evaluation of the temperature reducing effect of ophthalmic anti-inflammatory drugs,[7,8] and the monitoring of therapeutic interventions involving potentially hazardous increases in intra-ocular temperature. The latter could be an issue during phaco-emulsification of the ocular lens,[9] laser photo-refractive surgery of the cornea,[10] or localized heating of the eye during chemotherapy of intra-ocular tumors.[11] In addition, currently used steady-state temperature or heat-transfer models of the eye could be validated through the accurate determination of local variations in temperature within the eye.[11,12] However, no suitable technique is available for these kinds of assessments. Invasive methods such as using thermocouples are generally too intrusive for application in the eye and are unpractical for spatially resolved temperature measurements. The non-invasive detection of infra-red radiation from the eye does usually not permit direct intra-ocular temperature assessments, because of the strong water absorption of this kind of radiation. This technique has been used in the past though to measure corneal temperature as a predictor for the pharmacological potential of ocular anti-inflammatory drugs.[8]

We previously reported on a non-contact confocal Raman spectroscopy (CRS) system specifically designed for the rapid and sensitive characterization of biochemical properties of ocular tissues *in vivo*.[13] Apart from the application of CRS for pharmacokinetic measurements in the eye,[14] we assessed the spatial and temporal distribution of corneal hydration in anesthetized rabbits.[15] Furthermore, we successfully recorded the first *in vivo* Raman spectra of human corneas and were able to detect changes in corneal hydration due to the application of a topical dehydrating agent.[16]

The non-contact character of the CRS technique and the ability to assess small volumes of material could also yield the possibility to apply this technique for remote temperature measurements within the eye. Thus, with this project we sought to determine the feasibility of CRS for temperature measurements in aqueous solutions and the aqueous humor of the rabbit eye under *in vivo* circumstances.

Materials and Methods

We used a non-contact confocal Raman spectroscopy (CRS) system, of which a detailed description and the overall performance have been described elsewhere[13], for Raman spectroscopic assessments of aqueous solutions and aqueous humor of rabbit eyes under *in vivo* and *in vitro* circumstances at various temperatures. For calibration purposes HPLC-grade water was heated to ~50°C, transferred to a quartz cuvette and left to cool to ~30°C while monitoring the temperature with a calibrated thermocouple as the standard. Raman spectra in the Raman shift range from 2580 to 3780 cm^{-1} were recorded at regular intervals using 25 mW of Argon-laser light and exposure times of 10 s.

In addition we tested if the Raman spectral features of water would change due to the applied laser energy. Consequently, Raman spectra were recorded in HPLC-grade water at a constant temperature of ~23°C at irradiation powers ranging from 5 to 150 mW and exposure times ranging from 1 to 120 s.

Under an Institutional Review Board approved animal protocol that complied with the ARVO Resolution on the Use of Animals in Research, the animal studies were performed on 16 eyes of in total 9 NZW rabbits (~3.5 kg). Prior to Raman spectroscopic assessments the rabbits were anesthetized with Ketamine and Xylazine and were restrained in a holder to reduce movement artifacts. For reference temperature measurements we used either a rectal thermoprobe alone (n=13 eyes), or in conjunction with a needle-thermocouple (n=3 eyes) which was positioned in the aqueous humor of the eye. In order to obtain a wide range of intra-ocular temperatures, the aqueous humor of the rabbit eyes were probed *in vivo* at different core-temperatures with or without applying additional whole body heating with a heating pad (~40-41°C), after euthanasia with the eye cooling down *in-situ*, and during warming up of a cold-stored (15°C; 1hr.) enucleated eye *in vitro*. All experiments were performed at room temperatures of ~20°C.

Initially, the Raman spectra of HPLC-grade water were analyzed qualitatively, in order to find temperature dependent Raman spectral features. Consequently, the most valid, sensitive, and reproducible Raman spectral feature was

utilized to predict the temperature in aqueous solutions and the aqueous humor of the rabbit eyes.

Results

Figure 1A shows typical Raman spectra in the range from 2580 to 3780 cm^{-1} of HPLC-grade water at various temperatures. It can be seen that the Raman spectral features of water change as a function of temperature, since the regions from ~3000-3400 and ~3500-3650 cm^{-1} show marked differences in intensity and shape with changing temperature. However, these changes are rather subtle and can be visualized more clearly when plotting the change in Raman intensity per degree change in temperature ($\Delta I/\Delta T$) as a function of the Raman shift, as depicted in Figure 1B. With increasing temperature, the region labeled OH1 (2878-3430 cm^{-1}) decreases in intensity while the region OH2 (3430-3729 cm^{-1}) increases in intensity. These changes are in the order of 0.5% of the maximum photon counts at ~3190 and 3550 cm^{-1} per °C change in temperature. The occurrence of an isoskedastic point at ~3430 cm^{-1} corresponds well with the literature.[17] Both data taken from the HPLC-water *in vitro* and the rabbit aqueous humor *in vivo* yield comparable results, as can be seen from the dashed and solid curves in Figure 1B, respectively, suggesting a consistency under both circumstances in the relationship between the changes in the Raman spectral features of water and the temperature.

In order to find the most suitable Raman spectroscopic predictor (RP) for the temperature in an aqueous sample, eight Raman spectroscopic features were tested for their reproducibility, sensitivity, and validity, by evaluating the relationship $RP=A(\pm SE_A)T+B(\pm SE_B)$, where A and B were respectively the slope and the intercept of the curve-fit between water temperature (T in °C) and the Raman spectroscopic predictor. The standard errors SE_A and SE_B were used as a measure for the reproducibility, while the correlation coefficient R^2 could be used as a measure for the accuracy. The results are described in Table 1. As can be seen, the best predictor for water temperature using Raman spectral information was the integrated Raman intensity ratio IR(3430-3729)/ IR(2878-3430) with the lowest SE_A and SE_B, and the highest R^2. The relationship between this predictor (OH2/OH1) and the water temperature of HPLC-grade water (T) from 30-46°C is depicted in Figure 2. In formula: $OH2/OH1= 0.0049 (\pm 1.2\%)T+0.4522(\pm 0.5\%)$, $R^2=0.99$, $n=50$, $p<0.05$. This particular ratio was used for the for the remainder of the experiments.

The influence of the laser beam on the Raman spectral features of water revealed no appreciable change in the integrated Raman intensity ratio OH2/OH1 due to the applied laser power or exposure time. Analyzing similar

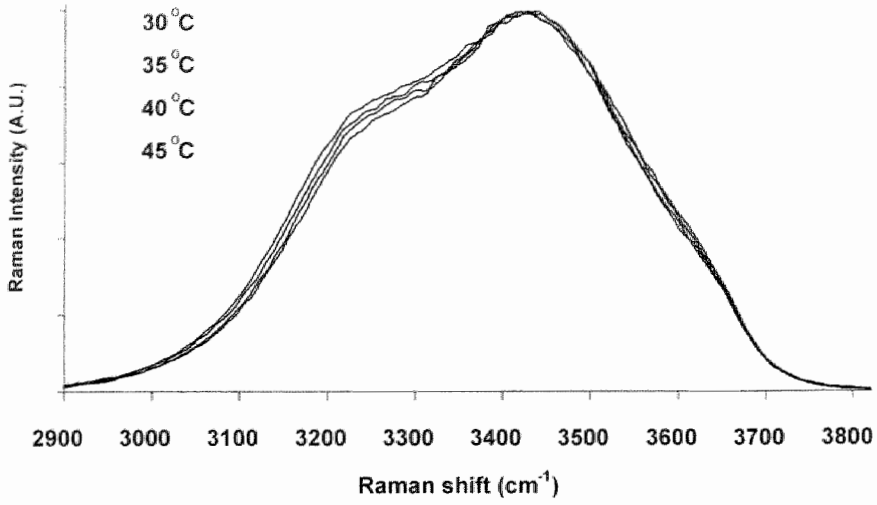

Figure 1A. Raman spectra of HPLC-grade water in quartz cuvette at different temperatures (calibrated thermocouple).

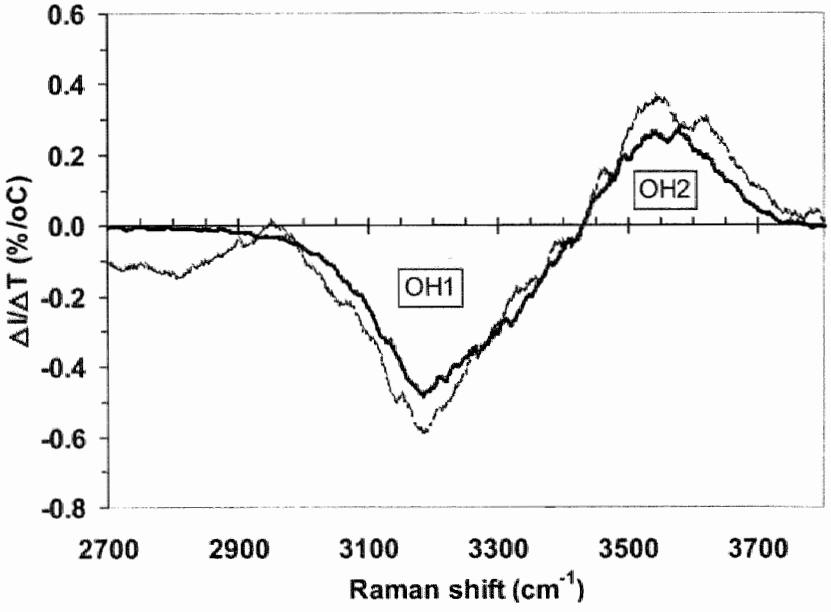

Figure 1B. Ratio of the change in Raman intensity (ΔI) in the spectrum of water vs. the change in temperature (ΔT) as a function of Raman shift position within HPLC-grade water (bold line) and the rabbit aqueous humor (dashed line).

Table 1. Raman spectroscopic predictors of water temperature.

	RP=A(±SE_a)T+B(±SE_b);with T = water temperature (°C)				
Raman spectroscopic predictor (RP)*	A	SE_a(%)	B	SE_b(%)	R^2
I(3184)	-0.47	0.01(2.5)	74	0.45(0.6)	0.9720
I(3558)	0.25	0.01(5.0)	47	0.48(1.0)	0.8916
I(3558)/I(3184)	0.014	0.0003(1.9)	0.53	0.01(1.9)	0.9832
IR(2878-3430)	-96	3.0(3.1)	25170	118(0.5)	0.9551
IR(3430-3729)	43	1.7(3.9)	12075	65(0.5)	0.9311
IR(3430-3729)/ IR(2878-3430)	0.0049	6E-5(1.2)	0.4522	0.0023(0.5)	0.9928
I(3558)-I(3184)	0.72	0.014(1.9)	-25	0.5(2.1)	0.9825
IR(3430-3729)- IR(2878-3430)	140	2.1(1.5)	-13100	84(0.6)	0.9887

*I = Raman peak intensity; IR = integrated Raman intensity.

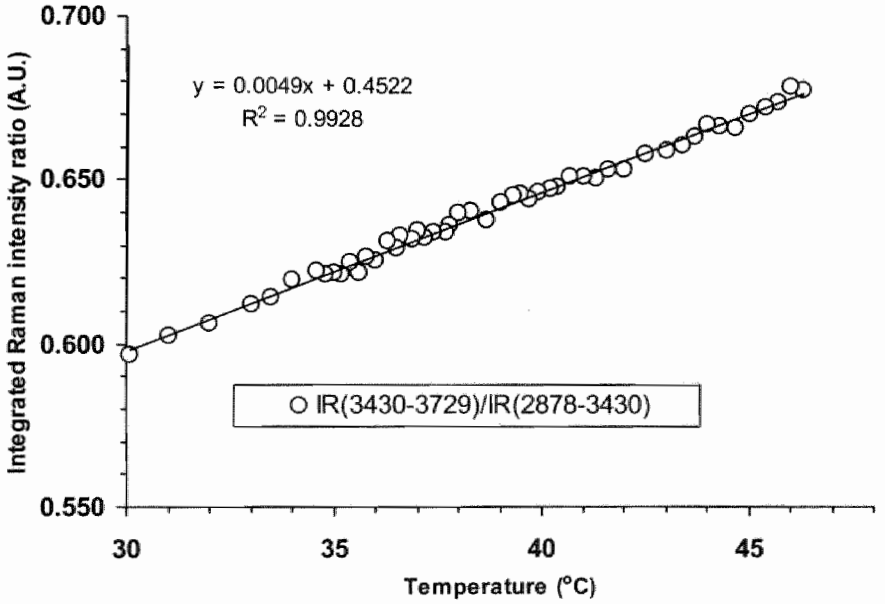

Figure 2. Integrated Raman intensity ratio of OH-peak regions 2878-3430 and 3430-3729 cm^{-1} as a function of water temperature.

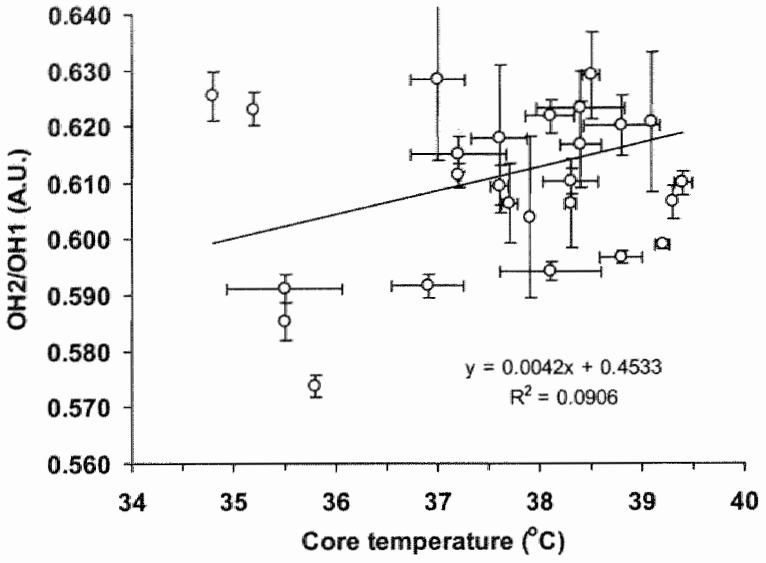

Figure 3. Relationship between Raman intensity ratio OH2/OH1 in the aqueous humor (n=358 assessments) and the core temperature of the rabbit (n=16 eyes).

signal-to-noise ratio spectra of HPLC-grade water at ~23 °C showed a ratio OH2/OH1 of 0.5670±0.0016, corresponding to a calculated temperature of 23.4±0.1 °C and a standard error of ~0.3%.

In Figure 3 the results are shown on the assessment of the integrated Raman intensity ratio OH2/OH1 in the aqueous humor of all eyes as a function of the rabbit core temperature. It can be seen that the relation core temperature vs. ratio OH2/OH1 in the aqueous humor resembles the values found in the *in vitro* water experiments with OH2/OH1 = 0.0042T+0.4533 ≈ 0.0049T+ 0.4522, although the correlation is rather weak (R^2=0.09).

The results on the non-contact Raman spectroscopic assessment of the aqueous humor temperature (range 14 to 34 °C) using the intra-ocular thermocouple as a standard are shown in Figure 4. A strong linear relationship was found between the measured aqueous humor temperature and the Raman intensity ratio OH2/OH1, with OH2/OH1 = 0.0036(±0.0001)T+ 0.4966 (±0.0030) (R^2=0.9763, n=162). The slope of this relationship differed slightly from the results obtained from the *in vitro* water experiments. However, the *in vivo* assessments agreed well with the HPLC-grade experiment (dashed line in Figure 4). In anesthetized rabbits at a steady-state core temperature of 38.9±0.7°C, the *measured* aqueous humor temperature was 33.5±0.2°C.

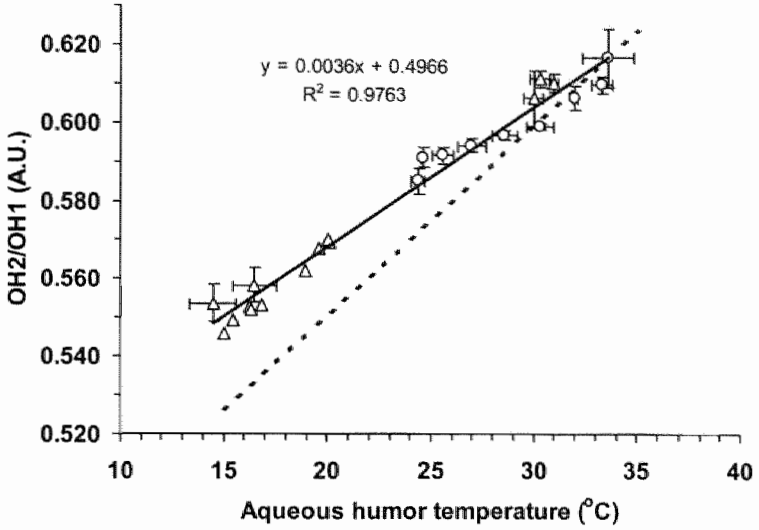

Figure 4. Relationship between the Raman intensity ratio OH2/OH1 (n=162) and the aqueous humor temperature of rabbit eye A (squares: *in vivo* circles: *ex vivo*) and eye B (diamonds: *in vivo*, triangles: *ex vivo*). Dashed line is the similar relationship in HPLC-grade water *in vitro* (see Fig. 2).

Non-contact Raman spectroscopic assessment of the aqueous humor revealed an integrated Raman intensity ratio OH2/OH1 of 0.613±0.005 (n=65 assessments), corresponding to a *calculated* temperature of 32.8±0.3°C (using the HPLC-grade water data for calibration). No statistical significant difference between the *measured* and the *calculated* intraocular temperature could be assessed. In comparison, in anesthetized rabbits without the intraocular thermoprobe at a steady-state core-temperature of 37.9±0.6°C, an integrated Raman intensity ratio OH2/OH1 of 0.617±0.009 was found (n=199 assessments), corresponding to a *calculated* temperature of 33.6±0.13 utilizing the HPLC-grade water finds for calibration.

Discussion

We have used confocal Raman spectroscopy (CRS) to determine the temperature-dependent changes in the Raman spectra of aqueous solutions and the aqueous humor of the rabbit eye at various temperatures in order to test the feasibility of CRS to assess the intra-ocular temperature.

A highly linear relationship was found between the Raman intensity ratio OH2/OH1 and the temperature of the aqueous humor of rabbit eyes over a temperature range of 14 to 34°C with a high degree of reproducibility as measured by the standard error of the slope of this relationship of ~1.2%. The sensitivity of the proposed thermometric application of CRS is solely a characteristic of the signal-to-noise ratio of the recorded spectra and is determined by the incident light energy used and the shot noise of the CCD camera. The aforementioned standard error corresponds to a standard deviation of ~8%. Thus, a difference in integrated Raman intensity ratio of ~16% corresponding to a temperature difference of ~0.2 °C is easily resolved at the experimental conditions used in this study. In the *in vivo* studies a sensitivity of ~0.7 °C was calculated. It seems that our method is more sensitive than previously reported temperature measurements using RS.[4] This could be attributed to the high signal-to-noise ratio Raman spectra which we can obtain with our confocal system, but more importantly the fact that the whole Raman spectral characteristics of water can be recorded in one spectrum.

A slight difference in the Raman intensity ratio OH2/OH1 vs. temperature relationship was observed between the animal and the HPLC-grade water experiments, although both relationships were highly linear. Since the *in vivo* animal results agreed favorably with the HPLC-grade water experiments, additional variables in the *in vitro* situation besides the temperature could have influenced the changes in the shape of the Raman spectrum of water. The occurrence of the applied euthanasia agent in the aqueous humor and the fact that the blood-aqueous barrier breaks down after euthanasia of the rabbits with a consequent leakage of proteins into the aqueous humor, could possibly have resulted in the occurrence of interfering fluorescence or otherwise altered the background properties of the spectra, possibly explaining the difference in slope of the OH2/OH1 ratio vs. temperature relationship between the *in vitro* and *in vivo* results. However, we did show that the proposed method was easily applicable in the *in vivo* situation, and only utilized ocular tissues *in vitro* to obtain a wide range of intra-ocular temperatures in cases where whole body heating *in vivo* did not suffice. Thus we found that the intra-ocular aqueous humor temperature of anesthetized rabbits at steady-state core temperatures within the normal physiological range and a room-temperature of 20°C is ~33.5°C as assessed using non-contact confocal Raman spectroscopy.

In conclusion, the Raman spectrum of water is subject to changes as a result of changing temperatures. This implicates that care should be taken when comparing Raman spectra of biological tissues containing water, i.e. that either the temperature is kept constant or the Raman spectra are corrected for the temperature dependent changes. More importantly, since most biological tissues consist at least in part of water, confocal Raman spectroscopy might possibly be

used to non-invasively assess the temperature of these tissues. This pilot study showed that confocal Raman spectroscopy can be applied for remote temperature measurements within the aqueous humor of the rabbit eye under *in vivo* circumstances with a high degree of sensitivity, specificity, and reproducibility.

References

1. Carey PR. Biochemical Applications of Raman and Resonance Raman spectroscopies. In Horecker B, Kaplan NO, Marmur J, and Scheraga HA Eds., *Molecular Biology: An International Series of Monographs and Textbooks*. Academic Press Inc., New York (1982).
2. Malyj M and Griffiths J.E. Stokes/Anti-Stokes Raman Vibrational Temperatures: Reference Materials, Standard Lamps, and Spectrophotometric Calibrations. *Applied Spectroscopy* 37(4): 315-333 (1983).
3. Walrafen GE. *J. Chem. Phys.* 47: 114 (1967).
4. Vehring R and Schweiger G. Optical Determination of the Temperature of Transparent Microparticles. *Applied Spectroscopy* 46(1): 25-27 (1992).
5. Leonard DA, Caputo B and Hoge FE. Remote sensing of subsurface water temperature by Raman scattering. *Applied Optics* 18(11): 1732-1745 (1979).
6. Baranska H and Labudzinska. *Applied Spectroscopy* 41: 1068 (1987).
7. Fujishima H, Toda I, Yagi Y, and Tsubota K. Quantitative evaluation of postsurgical inflammation by infrared radiation thermometer and laser flare-cell meter. *J Cataract Refract Surg* 20: 451-454 (1994).
8. Tanaka M, Hasegawa T, Matsushita M, Miichi H, and Hayashi S. Quantitative Evaluation of Ocular Anti-Inflammatory Drugs Based on Measurements of Corneal Temperature in Rabbits: Dexamethason and Glycyrrhizin. *Ophthalmic Research* 19: 213-220 (1987).
9. Berger JW, Talamo JH, LaMarche KJ et al. Temperature measurements during phacoemulsification and erbium:YAG laser phacoablation in model systems. *J Cataract Refract Surg* 22: 372-378 (1996).
10. Betney S, Morgan PB, Doyle SJ, and Efron N. Corneal Temperature Changes During Photorefractive Keratectomy. *Cornea* 16(2): 158-161 (1997).
11. Lagendijk JJW. A mathematical model to calculate temperature distributions in human and rabbit eyes during hyperthermic treatment. *Phys. Med. Biol.* 27(11): 1301-1311 (1982).
12. Scott JA. A finite element model of heat transport in the human eye. *Phys. Med. Biol.* 33(2): 227-241 (1988).
13. Jongsma F.H.M., Erckens R.J., Wicksted J.P., Bauer N.J.C., et al. Confocal Raman Spectroscopy System For Noncontact Scanning Of Ocular Tissues - an *In Vitro* Study. *Optical Engineering* 36(11):3193-3199 (1997).

14. Bauer NJC, Motamedi M, Wicksted JP, March WF, Webers CAB, and Hendrikse F. Non-Invasive Assessment of Ocular Pharmacokinetics using Confocal Raman Spectroscopy. *J Ocular Pharm Ther* 15(2): 123-134 (1999).
15. Bauer NJC, Wicksted JP, Jongsma FHM, March WF, Hendrikse F, and Motamedi M. Noninvasive Assessment of the Hydration Gradient Across the Cornea Using Confocal Raman Spectroscopy. *Invest. Ophthalmol. Vis. Sci.* 39(4): 831-835 (1998).
16. Bauer NJC, Hendrikse F, and March WF. *in vivo* Confocal Raman Spectroscopy of the Human Cornea. *Cornea* 18: 483-488 (1999).
17. Walrafen GE, Hokmabadi MS and Wang WH. *J Chem Phys* 85: 6964 (1986).
18. Huizinga A, Bot CC, de Mul FFm, Vrensen GFJM, and Greve J. Local Variation in Absolute Water Content of Human and Rabbit Eye Lenses Measured by Raman Microspectroscopy. *Exp Eye Res* 48: 487-496 (1989).
19. Aliotta F, Fontana MP, Maisano G, Migliardo P, and Wanderlingh F. Coexistence of structures in electrolytic solutions investigated by Raman scattering. *Optica Acta* 27(7): 931-938 (1980).

Summary and Conclusions

Raman spectroscopy (RS) is a powerful optical technique for biochemical assessments, based on the phenomenon that a fraction of the incident monochromatic light is scattered with a different frequency due to the interaction of light with matter, on the molecular vibrational level. A Raman spectrum depicts these frequency changes in the form of discrete and specific Raman lines. Each of these lines can be assigned to specific molecular bonds, and Raman spectroscopic analysis yields biochemical characterization of the sample in question, from simple molecules such as water to complex proteins, or tissues. Although RS has been applied in the past in various fields of biology and medicine, *in vivo* application of this technique in the field of ophthalmology has been limited. The **aim of this thesis** was to investigate the potential applications of RS for non-contact biochemical assessments of (intra)ocular tissues and fluids of the intact eye under *in vivo* circumstances, utilizing a novel confocal Raman spectroscopy system.

Chapter 1 hypothesizes that the successful *in vivo* application of Raman spectroscopy in ophthalmology is of clinical significance since numerous ocular as well as systemic diseases and disorders express themselves through changes in the biochemical properties of ocular tissues and fluids, which could potentially be diagnosed and/or monitored applying the proposed technique. Against this background a general introduction into the theoretical, practical and optical aspects, including safety, of the application of Raman spectroscopy in ophthalmology is given, and the aim of this thesis is presented (see above).

Chapter 2 gives an in-depth description of the principles and practice of applied Raman spectroscopy in biology and medicine in general, and ophthalmology in specific. Furthermore, the characteristics of a suitable Raman spectroscopy system as a diagnostic tool for biochemical assessments in the eye under *in vivo* circumstances are outlined.

Chapter 3 presents the description and performance of the confocal Raman spectroscopy system which was applied in the studies contained in this thesis. The light source of this optical system is provided by an Argon laser or a Helium-Neon laser. A beam-expander yields a collimated beam of light with a diameter matching the back aperture of the focusing optics, which is a high numerical aperture (NA=0.5) long working distance (13 mm) microscope objective lens (LDMO). This LDMO is used both for focusing the incident light onto the sample as well as collecting the backscattered light. A holographic type beam-splitter deflects only the Raman backscattered light towards a camera lens, which focuses the Raman light onto a fiber-optic. This fiber acts as the pinhole

in this confocal alignment (see Chapter 1, Figure 1), and transports the Raman light into a spectrometer, where it is dispersed and consequently detected by a highly sensitive back-thinned CCD-detector, which digitizes this signal so that it can be stored in a computer and displayed on a screen. The key performance characteristics of this system are (1) its free working distance of 13 mm, allowing non-contact assessment of the tear-film, the cornea, the aqueous humor, the lens, and the vitreous humor; (2) its confocal alignment, yielding optical sectioning capabilities of 'optical' tissue slices as thin as 20 μm, while minimizing the detection of light from out-of-focus places in the same tissue or nearby other tissues, effectively increasing the signal-to-noise ratio; (3) its sensitivity, through the highly efficient use of the LDMO, as well as the application of a sensitive CCD-detector; and (4) its adequate temporal resolution for rapid spectral acquisitions. Additionally, through telecentric alignment of the focusing optics the LDMO can be moved along its optical axis without changing its back focal distance, allowing dynamic probing of static objects. Applying this optical system, discrete and specific Raman spectra were obtained from the cornea, the aqueous humor and the lens, typically utilizing 25 mW of laser light at exposure times as short as 1 sec.

It is concluded that this confocal Raman spectroscopy system might offer a novel optical sectioning technique for rapid non-contact biochemical characterization of various (intra)ocular tissues.

Chapter 4 describes the general working area in ophthalmology for which the confocal Raman spectroscopy system is thought to be most suitable. Furthermore, this chapter provides an insight into our ongoing efforts of establishing potential applications of confocal Raman spectroscopy in ophthalmology. Apart from the projects described in more detail elsewhere in this thesis, some pilot studies are mentioned such as the detection of biomolecules in the aqueous humor (i.e. glucose and phenylalanine), the assessment of biochemical changes in procured corneal buttons, and the biochemical characterization of a more or less common fibrovascular proliferative ailment, i.e. a pterygium.

Chapter 5 presents the results on the application of confocal Raman spectroscopy for the assessment of the hydration gradient across the cornea *in vivo*. The confocal properties of the proposed technique yielded the optical sectioning capability by which biochemical assessments could be performed of tissue slices significantly smaller than the full thickness of the cornea. Utilizing a specific Raman intensity ratio between two Raman spectral lines, the hydration was assessed of phantom media and rabbit corneas *in vivo*, with a high degree of sensitivity and reproducibility. The water content of rabbit corneas showed a significant increase from anterior to posterior, in line with our current understanding regarding the non-homogeneous distribution of corneal hydration. Furthermore, the characterization of the axial corneal hydration provided a reli-

able estimation of total corneal hydration as compared with conventional measurements using pachymetry and lyophilization. We concluded that the proposed confocal Raman spectroscopy technique has the potential to assess the extent and distribution of the corneal water content *in-vivo* with a high degree of sensitivity and reproducibility.

Chapter 6 describes the first ever application of this type of Raman spectroscopy in human subjects. The aim was to investigate the feasibility of confocal Raman spectroscopy for the assessment of corneal hydration in two legally blind subjects. Raman spectra from the anterior 100-150 μm of the cornea were recorded over a period of time before and after topical application of a mild dehydrating drug. The results showed that high signal-to-noise ratio spectra were obtained using as little as 15 mJ of laser light energy. Furthermore, changes in corneal hydration as a result of the dehydrating agent could be observed. We concluded that with adequate improvements in the safety the proposed technique could potentially be applied clinically as a tool for the non-contact assessment of corneal hydration in the human situation.

In **Chapter 7** the aim was to apply confocal Raman spectroscopy for the quantification of the transport of a topically applied ocular drug through the rabbit cornea under *in vivo* circumstances. The amplitude of a drug-specific Raman signal was assessed in the tearfilm and the corneal epithelium as a function of time after instillation of a single drop of dorzolamide 2% to the eyes of 6 anesthetized rabbits. A three-compartment pharmacokinetic model was used to describe the drug transport from the tearfilm (compartment 1) via the corneal epithelial layer (compartment 2) into the corneal stroma (compartment 3). Pharmacokinetic transfer rate constants (k) for the drug transport from one compartment to the other could be calculated by fitting the pharmacokinetic equations belonging to the three-compartment model of drug-transport to the data obtained from the Raman spectroscopic assessments. The drug-concentration versus time curve in each eye had a bi-phasic trend, with a rapid initial decrease in drug-concentration corresponding to the non-productive losses from the tears (k_{10}=0.24±0.04 min^{-1}), and a significantly slower later phase as a result of the transfer of drug from the corneal epithelium to the corneal stroma (k_{23}=0.0047±0.0004 min^{-1}). The rate of drug uptake from the tears into the corneal epithelium could also be established (k_{12}=0.034±0.006 min^{-1}). The standard deviations of these pharmacokinetic variables suggested good reproducibility. Furthermore, Raman spectroscopy is inherently specific, a strong advantage over currently used fluorometric assessments of ocular pharmacokinetics. In combination with the non-contact probing, the adequate sensitivity and spatial resolution, we concluded that confocal Raman spectroscopy has the potential to be employed as a valuable tool for the study of ocular pharmacokinetics in a non-contact manner.

In **Chapter 8** we sought to determine the feasibility of confocal Raman spectroscopy for remote temperature measurements within the aqueous humor of the rabbit eye under *in vivo* circumstances. We used the temperature-dependent changes in the Raman spectral features of water. As it turned out the amplitude of one OH-vibrational mode decreased while another OH-vibrational mode of water increased with an increase in temperature. The ratio between the Raman intensity of these two OH-vibrational modes showed a strong linear correlation with the prevailing temperature as measured with a Golden Standard (needle thermocouple), both in HPLC-grade water (R^2=0.99) as well as in the rabbit aqueous humor (R^2=0.98) with a high degree of reproducibility and a sensitivity of ~0.5°C. We concluded that, since the Raman spectral features of water and probably also other biochemicals are dependent on the prevailing temperature, care should be taken to keep the temperature constant during comparative Raman spectroscopic studies. Furthermore, it was proven that confocal Raman spectroscopy can be utilized for sensitive temperature measurements in the aqueous humor of the rabbit eye under *in vivo* conditions and in a non-contact manner.

In **summary**, this thesis describes the potential applications of confocal Raman spectroscopy for the biochemical characterization of various ocular tissues and fluids *in vivo*. At present this technique is perfected and optimized and can be successfully applied for *in vivo* animal research. Whether this novel optical technique will find its way into the clinical practice of ophthalmology depends on various factors. First and foremost is the safety issue as explained in Chapter 1. In general, the use of longer wavelengths is advocated in order to prevent fluorescence which can obscure the Raman signal. However, the confocal technique which we have applied has proven to be adequate in this perspective when using the 514.5 nm argon laser. The ANSI report on the Safe Use of Lasers does not show any wavelength dependency in ocular hazard in the 400-700 nm range. Since the Raman intensity is in direct proportion to the frequency of the incident light to the fourth power, the Raman yield is ~2.5x higher when using the argon laser at 514.5 nm as opposed to the helium-neon laser at 632.8 nm. Moreover, the sensitivity of the CCD-camera is 2x higher in the same Raman frequency shift region by using the argon laser as compared with the helium-neon laser. Thus, the Raman yield is ~5x higher when using the argon laser then when using the helium-neon laser. In the future, the use of even shorter wavelength could be considered. A reliable source in this respect would be the helium-cadmium laser (425 nm), yielding 2x higher Raman signals as opposed to the argon laser. True non-invasive application of Raman spectroscopy in the eye using a laser is only possible when the light load is either significantly reduced to below 1 mW/cm^2 or light exposure to the retina is prevented altogether. This last option has our utmost attention, since this will

permit utilizing higher laser light energies safely, yielding high signal-to-noise ratio spectra without chemical or thermal damage to the ocular tissues. Secondly, it needs to be established whether the proposed method is adequately practical in use in a clinical setting. Until now, spectral analysis is performed manually which is extremely time-consuming. First, each spectrum has to be pre-processed by determining the valuable signals from the background noise (shot-noise of the CCD camera, auto-fluorescence). Secondly, multiple Raman peaks in each single spectrum have to be assigned to a specific molecular bond. Only then, qualitative and (under certain circumstances) quantitative data analysis is possible. Computerized spectral analysis could certainly increase the practical application of Raman spectroscopy but whether this is possible still needs to be established. Thirdly, at this point the operation of the experimental setup demands much time in the form of aligning, calibration, and stabilization, which certainly leaves room for improvement in the future. Lastly, the added value of this optical technique has to be established with regards to the currently used non-invasive diagnostic tools in ophthalmology. Since the confocal Raman spectroscopy system described in this thesis in fact combines the advantages of confocal microscopy with a powerful chemical analytical technique in a highly efficient manner, it was possible to investigate ocular tissues and fluids in a totally new manner. Instant information on the biochemical composition of transparent ocular tissues and fluids can now be obtained rapidly in a non-contact manner from almost any depth within the eye under *in vivo* conditions. Furthermore, the proposed optical technique is adequately flexibility to allow for either time-dependent or spatially-resolved biochemical assessments, or a combination of both, in practically every ocular tissue or fluid.

Future efforts should be directed towards optimization of the proposed technique with regards to safety, practicality and operational procedures, to enable the application of Raman spectroscopy in the human eye *in vivo*. Only when safety is guaranteed we can open the way for investigating the true clinical potential of confocal Raman spectroscopy in ophthalmology.

Samenvatting en Conclusies

Raman spectroscopie (RS) is een krachtige optische techniek voor biochemische bepalingen, gebaseerd op het fenomeen dat een fractie van het opvallend licht wordt verstrooid met een andere frequentie, als gevolg van een interactie van het licht met de materie op moleculair nivo. Een Raman spectrum toont deze frequentie veranderingen in de vorm van discrete en specifieke Raman lijnen. Elke lijn kan toegewezen worden aan een specifieke moleculaire verbinding, waarna met behulp van Raman spectroscopische analyse stoffen biochemisch gekarakteriseerd kunnen worden, uiteenlopend van simpele moleculen zoals water tot complexe eiwitten en weefsels. Ondanks dat RS in het verleden werd toegepast in verschillende biologische en medische disciplines, zijn er weinig *in vivo* toepassingen beschreven van deze techniek in de oogheelkunde. Het **doel van dit proefschrift** was dan ook om de mogelijke toepassingen van RS te onderzoeken voor contactloze biochemische bepalingen van (intra)oculaire weefsels en vloeistoffen van het intacte oog onder *in vivo* omstandigheden, gebruikmakend van een nieuw confocaal Raman spectroscopie systeem.

In **Hoofdstuk 1** wordt de hypothese geponeerd dat de succesvolle *in vivo* toepassing van Raman spectroscopie in de oogheelkunde van klinisch significant belang is, omdat talrijke oogheelkundige alsook systemische afwijkingen tot uiting komen in veranderingen van de biochemische eigenschappen van oculaire weefsels en vloeistoffen, welke eventueel gediagnostiseerd dan wel vervolgd zouden kunnen worden met behulp van deze techniek. Tegen deze achtergrond wordt een algemene inleiding in de theoretische, praktische en optische aspecten (inclusief de veiligheid) van de toepassing van Raman spectroscopie in de oogheelkunde gegeven, en het doel van het proefschrift wordt gepresenteerd (zie boven).

Hoofdstuk 2 geeft een uitgebreide beschrijving van de principes van toegepaste Raman spectroscopie in de biologie en geneeskunde in het algemeen en oogheelkunde in het bijzonder. Verder worden de eisen voor een bruikbaar Raman spectroscopisch systeem gedefinieerd, om deze techniek als diagnostisch hulpmiddel te kunnen gebruiken voor biochemische bepalingen in het oog onder *in vivo* omstandigheden.

Hoofdstuk 3 beschrijft de mogelijkheden van het confocale Raman spectroscopie systeem welke gebruikt werd in de studies die in dit proefschrift beschreven zijn. De lichtbron van dit optische systeem is een Argon laser dan wel een Helium-Neon laser. De smalle laserbundel wordt verbreedt tot een evenwijdige bundel met een diameter die overeenkomt met de achterste apertuur van het focusserende microscoop-objectief (LDMO), welke een hoge

numerieke apertuur heeft (NA=0.5) en een lange vrije-werk afstand (13 mm). Deze LDMO wordt zowel gebruikt om het laserlicht op het object te focusseren alsook om het teruggekaatste licht weer op te vangen. Een holografische deelspiegel zorgt ervoor dat alleen het Raman licht wordt geleid naar een camera-lens, welke op zijn beurt het Raman licht weer op een fiber focusseert. Deze fiber dient als het confocale 'pinhole' (zie Hoofdstuk 1, Figuur 1), en transporteert het licht verder naar een spectrometer, waar het licht afhankelijk van de kleur wordt afgebogen en vervolgens gedetecteerd door een zeer gevoelige CCD-camera. Deze digitaliseert het signaal zodat het op een computer opgeslagen en op een beeldscherm afgebeeld kan worden. De sterke punten van dit systeem zijn (1) de vrije-werk afstand van 13 mm, waardoor op een contactloze wijze de traanfilm, het hoornvlies, het kamerwater, de lens en het glasachtig lichaam gekarakteriseerd kunnen worden; (2) de confocale opstelling van de optische onderdelen, welke het mogelijk maakt optische coupes te maken van minstens 20 µm dikte, terwijl de detectie van strooilicht van het weefsel of omliggende weefsels wordt geminimaliseerd, en zodoende de signaal-ruisverhouding vergroot; (3) de hoge gevoeligheid, door efficiënt gebruik te maken van het microscoop objectief alsook de toepassing van een hoogwaardige CCD-detector; en (4) de adequate resolutie in tijd, voor snelle spectrale data acquisitie. Tevens maakt de telecentrische uitlijning het mogelijk de LDMO te transleren over de optische as van het systeem zonder verandering in de achterste brandpuntsafstand, zodat het mogelijk is statische objecten dynamisch te meten. Met de toepassing van dit optische systeem werden discrete en specifieke Raman spectra verkregen van het hoornvlies, het kamerwater, en de intraoculaire lens, gebruik makend van 25 mW laserlicht en een 1 s. expositie-tijd. Er wordt geconcludeerd dat dit confocale Raman spectroscopie systeem een nieuwe techniek is die door middel van optische coupes, op een snelle manier (intra)oculaire weefsels en vloeistoffen biochemisch kan karakteriseren.

Hoofdstuk 4 beschrijft het algemene werkterrein in de oogheelkundige discipline waarvoor confocale Raman spectroscopie met name geschikt wordt geacht. Tevens geeft dit manuscript enig inzicht in de voortgaande queeste naar de mogelijke toepassingen van confocale Raman spectroscopie in de oogheelkunde. Naast de projecten die in meer detail terugkomen als aparte hoofdstukken in dit proefschrift, worden enkele pilot-studies genoemd zoals het detecteren van biomoleculen in het kamerwater (bijv. glucose en fenylalanine), het bepalen van biochemische veranderingen in donorcorneas, en de biochemische analyse van een min of meer vaak voorkomende fibrovasculaire aandoening van het oog, het pterygium.

Hoofdstuk 5 presenteert de resultaten van de toepassing van confocale Raman spectroscopie voor de bepaling van de water gradiënt in de cornea *in vivo*. De confocaliteit leende zich bij uitstek voor het maken van optische weefsel coupes welke significant dunner waren dan de gehele dikte van het hoornvlies. Gebruik makend van een bepaalde Raman intensiteitsratio tussen

twee Raman spectrale lijnen kon de watergraad van een test medium en het hoornvlies van het konijn, *in vivo* en met een hoge mate aan gevoeligheid en reproduceerbaarheid bepaald worden. Het watergehalte van het konijne-hoornvlies wordt hoger naarmate men meer van anterieur naar posterieur gaat, wat in overeenstemming is met onze huidige opvatting omtrent de niet-homogene verdeling van de cornea hydratie. Tevens kon met behulp van de bepaling van de axiale watergraad een juiste schatting gemaakt worden van de totale cornea hydratie, als we dat vergeleken met conventionele methoden zoals pachymetrie en vriesdrogen. Wij concludeerden dat het voorgestelde confocale Raman spectroscopie systeem in potentie de hoogte en de verdeling van de cornea hydratie kan bepalen onder *in vivo* omstandigheden, met een hoge mate aan sensitiviteit en reproduceerbaarheid.

Hoofdstuk 6 beschrijft de allereerste keer dat deze vorm van Raman spectroscopie is toegepast op proefpersonen. Het doel van de studie was te onderzoeken of het mogelijk was met confocale Raman spectroscopie de cornea hydratie te bepalen in twee zogenaamde 'legally blind' personen. Er werden Raman spectra genomen van het anterieure 100-150 µm deel van de cornea over een bepaalde tijd voor en na topicale toediening van een milde dehydrerende oogdruppel. De resultaten lieten zien dat Raman spectra vervaardigd konden worden met een hoge signaal-ruis verhouding gebruik makend van slechts 15 mJ laser licht. Tevens konden veranderingen in de cornea hydratie worden aangetoond als gevolg van toediening van de dehydrerende oogdruppel. Wij concludeerden hieruit dat met adequate verbeteringen in de veiligheid de voorgestelde techniek mogelijk gebruikt kan worden in een klinische setting om contactloos de cornea hydratie te bepalen in de humane situatie.

Het doel van het onderzoek beschreven in **Hoofdstuk 7** was de toepassing van confocale Raman spectroscopie voor de kwantificatie van het transport van een topicaal toegediende oogdruppel in de konijne-cornea onder *in vivo* omstandigheden. De amplitude van een farmacon-specifiek Raman signaal werd bepaald in de traanfilm en het cornea-epitheel als functie van de tijd na het indruppelen van een enkele druppel dorzolamide 2% in de ogen van 6 konijnen onder algehele anesthesie. Een drie-compartimenten model werd gebruikt om het transport van het farmacon te beschrijven vanuit de traanfilm (compartiment 1) via het cornea epitheel (compartiment 2) naar het corneale stroma (compartiment 3). Farmacokinetische snelheids-constanten (k) voor het transport van het ene compartiment naar het andere konden worden berekend door met farmacokinetische formules, behorend bij het drie-compartimenten model, het farmacon transport te modelleren aan de hand van de data van de Raman spectroscopische bepalingen. De concentratie vs. tijd curven van ieder oog hadden elk een bi-fasisch verloop, met een snelle eerste daling van de farmacon-concentratie als gevolg van niet-productieve verliezen uit de traanfilm (k_{10}=0.24±0.04 min^{-1}), en een significant langzamere fase als gevolg van het farmacon-transport vanuit het cornea-epitheel naar het cornea-stroma

(k_{23}=0.0047±0.0004 min^{-1}). Tevens kon de opname van farmacon vanuit de tranen naar het cornea-epitheel bepaald worden (k_{12}=0.034±0.006 min^{-1}). De standaard deviaties van deze farmacokinetische variabelen suggereren een goede reproduceerbaarheid. Tevens is Raman spectroscopie inherent specifiek, wat een groot voordeel is over de thans gebruikte fluorometrische bepalingen van de oculaire farmacokinetiek. Samen met het contactloos bepalen, de adequate gevoeligheid en de spatiele resolutie, leidde dit tot onze conclusie dat confocale Raman spectroscopie mogelijk gebruikt zou kunnen worden als een waardevolle contactloze techniek voor oculair farmacokinetische bepalingen.

In **Hoofdstuk 8** trachtten we te bepalen of het mogelijk was om met behulp van confocale Raman spectroscopie contactloos de temperatuur te bepalen in het kamerwater van het konijne-oog onder *in vivo* omstandigheden. We gebruikten daarbij de temperatuur-afhankelijke veranderingen in het Raman spectrum van water. Het bleek dat de amplitude van een van de OH-signalen verkleinde terwijl de amplitude van een ander OH-signaal juist vergrootte. De ratio tussen de Raman intensiteiten van deze twee OH-signalen vertoonde een sterke lineaire correlatie met de temperatuur zoals gemeten met de Gouden Standaard (naald thermo-koppel), zowel in HPLC-zuiver water (R^2=0.99) alsook in het kamerwater van de konijne-ogen (R^2=0.98) met een hoge mate aan reproduceerbaarheid en een sensitiviteit van ~0.5°C. Wij concludeerden, gezien de temperatuur-afhankelijkheid van de Raman signalen van water en waarschijnlijk ook van andere biomoleculen, dat er tijdens vergelijkende Raman spectroscopische studies op gelet moet worden dat de temperatuur constant gehouden wordt. Tevens werd geconcludeerd dat confocale Raman spectroscopie toegepast kan worden voor sensitieve en contactloze temperatuur bepalingen in het kamerwater van konijne-ogen onder *in vivo* omstandigheden.

Samenvattend beschrijft dit proefschrift de potentiële toepassingen van confocale Raman spectroscopie voor biochemische bepalingen van verschillende oculaire weefsels en vloeistoffen. Op dit moment is deze techniek geoptimaliseerd voor en kan succesvol toegepast worden in *in vivo* proefdier studies. Het hangt van verschillende factoren af of deze nieuwe optische techniek zijn weg zal vinden in de klinische praktijk van de oogheelkunde. Allereerst en meest belangrijke factor is de veiligheid, zoals reeds beschreven in Hoofdstuk 1. In het algemeen wordt het gebruik van langere golflengten aanbevolen om zo de detectie van fluorescentie, welke het Raman signaal kan maskeren, te verminderen. Desalniettemin hebben we kunnen aantonen dat confocale Raman spectroscopie in dit opzicht adequaat kan worden toegepast gebruik makend van de 514.5 nm argon laser. Het ANSI rapport aangaande de 'Safe Use of Lasers' toont geen verband tussen oogheelkundig gevaar en de golflengte van zichtbaar licht tussen de 400 en 700 nm. Omdat de Raman intensiteit direct afhangt van de frequentie van het gebruikte laser licht tot de vierde macht, zal bijvoorbeeld deze intensiteit 2.5 maal hoger uitvallen bij gebruik van een argon laser (514.5 nm) vergeleken met een helium-neon laser (632.8 nm) met

eenzelfde vermogen. Tevens is de gevoeligheid van de CCD-camera 2 maal hoger in de zelfde Raman 'shift' regio als de argon laser gebruikt wordt in plaats van de helium-neon laser. In de toekomst zou zelfs het gebruik van nog kortere golflengten overwogen kunnen worden. In dit perspectief zou de helium-cadmium laser (425 nm) een betrouwbare lichtbron kunnen zijn, welke een 2 maal hoger Raman signaal zou geven dan de argon laser. Echte niet-invasieve toepassing van confocale Raman spectroscopie is slechts mogelijk als de retinale blootstelling aan laserlicht significant gereduceerd wordt tot minder dan $1 mW/cm^2$ of wanneer blootstelling van de retina aan het directe laserlicht geheel wordt vermeden. Deze laatste optie heeft onze volledige aandacht, omdat dit ons in staat zou stellen om op een veilige manier hogere licht energieën te gebruiken, welke spectra met een hoge signaal-ruis verhouding zouden opleveren zonder thermale of chemische schade aan de oculaire weefsels. Ten tweede moet vastgesteld worden of de voorgestelde techniek praktisch genoeg is voor gebruik in de klinische setting. Nu wordt de spectraal analyse nog grotendeels manueel uitgevoerd wat extreem tijdrovend is. Ten eerste moet elk spectrum voorbewerkt worden teneinde de waardevolle signalen van de achtergrond signalen ('shot-noise' van de CCD-camera, auto-fluorescentie) te scheiden. Dan moeten de afzonderlijke Raman pieken in elk spectrum toegewezen worden aan specifieke moleculaire verbindingen. Pas dan is kwalitatieve en (onder bepaalde omstandigheden) kwantitatieve data analyse mogelijk. Computer-ondersteunde data analyse zou hier zeker uitkomst kunnen bieden, maar of dit mogelijk is moet nog onderzocht worden. Ten derde vergen de operationele handelingen van de experimentele opstelling, zoals het uitlijnen, de kalibratie en de stabilisatie, nog veel tijd, wat zeker nog ruimte tot verbetering overlaat. Tenslotte zal de toegevoegde waarde van deze optische techniek afgewogen moeten worden tegen de reeds in gebruik zijnde conventionele niet-invasieve technieken in de oogheelkunde. Omdat het hier beschreven confocale Raman spectroscopie systeem de voordelen bundelt van confocale microscopie met een krachtige biochemisch analytische techniek in een hoogst efficiënte manier, was het mogelijk oculaire weefsels op een geheel nieuwe manier te onderzoeken. Directe informatie betreffende de biochemische compositie van transparante oculaire weefsels en vloeistoffen kan nu verkregen worden op een contactloze manier op bijna elke diepte in het oog onder *in vivo* omstandigheden. Tevens is de voorgestelde techniek uitermate flexibel zodat zowel tijd-afhankelijke alsook plaats-afhankelijke biochemische bepalingen gedaan kunnen worden, of een combinatie van beiden, in bijna elke oculair weefsel of vloeistof.

In de toekomst zal de voorgestelde techniek geoptimaliseerd moeten worden met het oog op de veiligheid, het practisch nut, en de operationele procedures, zodat de toepassing van Raman spectroscopie in het humane oog onder *in vivo* omstandigheden mogelijk gemaakt kan worden. Pas als de veiligheid is gegarandeerd zullen we de weg kunnen openen om het werkelijke klinische potentieel van confocale Raman spectroscopie in de oogheelkunde te kunnen onderzoeken.

Dankwoord

Bij dezen wil ik iedereen die een vooraanstaande rol heeft gespeeld bij het totstandkomen van dit proefschrift bedanken. Bedenkend wie ik vooral niet moet vergeten, kijk ik terug naar hoe het allemaal ook alweer begonnen en gelopen is. Daar ik aan het eind van mijn co-schappen mijn zinnen had gezet om later als oogarts door het leven te gaan, wilde ik als voorbereiding daarop een keuze-wetenschapsstage oogheelkunde gaan doen. Dus belde ik eind 1994 met de afdeling oogheelkunde van het AZM in Maastricht. In een vloeiende veel-regelige volzin legde ik de stage-begeleidster mw. drs. M.R. Beintema mijn bedoelingen uit. Margot, ik kan me nog levendig herinneren hoe jij zei: "Zo, da's pas met de deur in huis vallen". Jij was erg enthousiast en zorgde ervoor dat ik meteen aan de slag kon met een interessant project in het lab van Frans Jongsma, waarvoor dank. Samen met dr Paul Derhaag werd een begin gemaakt aan een onderzoek waarin ik veel van mijn beta-kwaliteiten kwijt kon. De stage werd afgesloten met de scriptie "Computer-aided analysis of video images on morphometrical changes of the microcirculation of the bulbar conjunctiva in type I diabetics". Al met al zouden deze onderzoeks-perikelen de aanzet zijn tot iets groters. Het bleek namelijk dat er een promotie-onderzoeks-plaats in Texas beschikbaar zou komen, en of ik daar eens over zou willen nadenken. Met een mogelijke promotie en een opleidingsplaats oogheelkunde in Maastricht in het vooruitzicht was de keuze niet zo moeilijk.

Mijn promotor en heden tevens mijn opleider prof. dr F. Hendrikse gunde mij het vertrouwen om dit promotie-onderzoek tot een goed einde te brengen. Professor Hendrikse, de gesprekken die wij in de loop van de afgelopen jaren aangaande het verloop en de uiteindelijke afronding van dit promotie-onderzoek hebben gehad, waren telkens weer een stimulans voor mij om de gestelde doelen in de afgesproken tijd te halen. Ik wil u bedanken voor de mogelijkheden welke deze promotie mij geboden heeft, op research en ander gebied, voor de aanmoedigende en stimulerende begeleiding tijdens de afrondingsfase, en voor het kritisch beoordelen van de manuscripten in dit proefschrift.

Een volgend persoon die een zo grote rol heeft gespeeld bij het totstandkomen van dit proefschrift, is (nu ondertussen zelf gepromoveerd) dr F.H.M. Jongsma. Frans, ik heb jouw hulp voor, tijdens en na mijn onderzoeksjaren in Galveston zeer gewaardeerd. Ontelbare uren zijn we bezig geweest het confocale Raman spectroscopie systeem te verbeteren, ideeën uit te werken, experimenten te verrichten, manuscripten voor te bereiden etc. Jou schijnbaar oneindige hoeveelheid kennis van zaken in de optica en jouw evenzeer onver-

moeibare enthousiasme en inzet zijn van onschatbare waarde geweest in dezen. Niet in de laatste plaats ben jij ten slotte 'uitvinder' van dit apparaat. De tijd welke we samen aan dit project hebben gewerkt zijn voor mij onvergetelijk geweest. Tevens heb jij als geen ander mijn proefschrift tot in de puntjes gelezen en bekritiseerd. Frans, ik hoop dat we nog lang zullen kunnen samenwerken, wel of niet aan een Raman spectroscopie project.

Drs R.J. Erckens, mijn voorganger in Galveston, wil ik hier natuurlijk ook niet onvermeld laten. Roel, jij maakte me wegwijs in het hele Raman-gebeuren, en leerde me de fijne kneepjes van het ingewikkelde apparaat, om het te laten doen wat ik wilde. Tevens vormden jouw inspanningen de grondslag van dit onderzoek. Ik bedank je voor de talrijke uren welke we nog samen hebben kunnen werken, en de tijd erna.

The research presented in this thesis was performed at the Biomedical Laser and Spectroscopy Program of the Department of Ophthalmology at the University of Texas Medical Branch, Galveston, Texas, under guidance of Professor and Chairman Dr W.F. March and Dr M. Motamedi, to whom I both feel greatly indebted.

Dr March, as my promotor I would like to thank you for giving me the opportunity to work with you and your colleagues. Your never ending amount of enthusiasm in ophthalmic scientific research in general and the Raman-project in specific were contagious, to say the least. You always had and kept faith in the project, and always came up with new ideas and visions. Through you I personally met some of the most interesting people in the field of Ophthalmology of which Dr Theo Seiler, Dr Nussenblatt, and Dr John Marshal, have stayed fresh in my memory. You always proudly showed your guests the lab, giving me the opportunity to explain what we were doing, but which also meant a nice break from the daily routine. I would also like to thank some of your staff by name, who have made small or large contributions toward this thesis: Dr Judith Brown and Dr Stefan Trocme (corneal viability study and human donor corneas), Richard (photography), Rosemary Moore (pathology), Dr Charlise Gundersson (pharmacology work), and Dr Erik van Kuijk (pterygium study).

Massoud, as director of the Biomedical Laser and Spectroscopy Program and a very diverse researcher, and now as my co-promotor, you taught me the fine art of writing scientific publications, for which I am grateful. After long hours of working on a paper, writing and re-writing it, thinking this latest version would certainly be okay, it finally came to your attention. Most of the times still more modifications were made, and the whole process was repeated. You always claimed that you never had a paper rejected, just because by the time you submitted it, it was just perfect for that particular journal. And indeed. Most of the times your predictions were correct, and the papers got accepted the

first time. I would also like to thank you for the possibilities you gave me in enlarging my knowledge in optics and lasers in your lab, where so much interesting research was and is still going on.

I am greatly indebted to Dr J.P. Wicksted. Jim, your immense knowledge in optics, lasers, and (Raman)spectroscopy were an invaluable asset to this project. I thank you for all the effort and time you invested in this project. We had the most interesting discussions about our work, and through you I learned a lot concerning the principles, physics and practice of Raman spectroscopy. It was a pleasure to work with you during your stays in Galveston over the summer. Elaine and I will also never forget the great time we had at your home in Stillwater.

Brent Bell, I thank you for your technical assistance and the blood, sweat and tears you spilled to get that darn machine going when it was broken. Marcel Goetz I thank for teaching me the ins and outs of the Matlab-program, which helped me a great deal in creating my own custom-made spectral analysis programs. Marcel, unfortunately the time we spent together on the project was short but nonetheless intense. I hope you have found you niche in San Francisco.

Mijn co-promoter dr ir G.J. Puppels dank ik voor het kritisch doorlezen van mijn proefschrift. Gerwin-Jan, bedankt voor de inspanningen welke je je hebt getroost om een aantal hoofdstukken in mijn proefschrift duidelijker, correcter en leesbaarder te maken.

De leden van de beoordelingscommissie prof. dr H.A.J. Struijker-Boudier, prof. dr W. Th. Hermens, prof. dr A. Persoons, prof. dr F. Spaans, en dr ir D. Sterenborg dank ik voor het beoordelen van dit proefschrift.

Een woord van dank is tevens op zijn plaats voor mijn huidige collega's van de afdeling oogheelkunde van het AZM Maastricht, waaronder de stafartsen, polimedewerkers, en niet in de laatste plaats mijn collegae arts-assistenten, voor hun steun en hulp tijdens de afrondingsfase van mijn promotie.

Tevens dank ik de firma Alcon, voor de financiële ondersteuning bij de publicatie van dit proefschrift.

And last but by no means least, I thank my lovely wife Elaine. Dearest Elaine, you have always said that behind every successful man there is an even more successful wife. Well, I guess I have to agree with you, since without your support, patience, and encouragement especially in this year past, I would have never made it. You succeeded in pulling me through, and I love you for helping me through thick and thin. We did it!

Curriculum Vitae

Noël Jozef Catharinus Bauer werd geboren te Heerlen op 11 November 1968. In 1987 werd met goed gevolg het eindexamen Gymnasium β behaald aan het Bisschoppelijk College Schöndeln te Roermond. Vanaf 1987 studeerde hij geneeskunde aan de Rijksuniversiteit Limburg te Maastricht, welke in 1995 werd voltooid met het behalen van het basisartsexamen. Aansluitend werd het onderzoek in het kader van deze dissertatie verricht aan de University of Texas Medical Branch at Galveston, Texas, van 1995 tot 1998, onder begeleiding van Prof. dr Wayne F. March, dr Massoud Motamedi en prof. dr Fred Hendrikse. Sedert augustus 1998 is de auteur werkzaam als arts-assistent in opleiding tot oogarts bij de afdeling oogheelkunde van het Academisch Ziekenhuis Maastricht (opleider prof. dr F. Hendrikse).

Hij is getrouwd met Elaine Wilson en heeft een zoon, Brandon.

Publications

NJC Bauer, WF March, JP Wicksted, F. Hendrikse, FHM Jongsma, M. Motamedi. "*In vivo* confocal Raman spectroscopy of the human eye." *ARVO Abstract Invest. Ophthalmol. Vis. Sci.* 1996; 37(3): S753.

RJ Erckens, NJC Bauer, WF March, FHM Jongsma, F. Hendrikse, M. Motamedi. "Non-invasive *in vivo* assessment of corneal dehydration in the rabbit using confocal Raman spectroscopy." *ARVO Abstract Invest. Ophthalmol. Vis. Sci.* 1996; 37(3): S360.

NJC Bauer, WF March, F. Hendrikse. "Confocale Raman spectroscopie van de humane cornea." Nederlands Oogheelkundig Gezelschap, Breda, 1996.

RJ Erckens, FHM Jongsma, NJC Bauer, JP Wicksted, M. Motamedi, F. Hendrikse, WF March. "Het detecteren van intraoculaire siliconen olie met Raman spectroscopie in een *in vivo* model." Nederlands Oogheelkundig Gezelschap, Breda, 1996.

NJC Bauer, MJ Goetz, FHM Jongsma, WF March, M. Motamedi. "*In vivo* confocal Raman spectroscopy of ocular tissue". 14th Annual Meeting on Biomedical Engineering (1996). University of Houston, Texas, USA.

FHM Jongsma, RJ Erckens, JP Wicksted, NJC Bauer, F Hendrikse, WF March, M Motamedi. "Confocal Raman spectroscopy system for non-contact scanning of ocular tissues; an *in vitro* study". *Optical Engineering* 1997; 36(11): 3193-3199.

NJC Bauer, SJ Koons, JP Wicksted, FHM Jongsma, F. Hendrikse, M. Motamedi, WF March. "Non-invasive assessment of the axial hydration gradient after corneal abrasion of the rabbit eye". *ARVO Abstract Invest. Ophthalmol. Vis. Sci.* 1997; 38(4): S535.

NJC Bauer, S.J. Koons, JP Wicksted, FHM Jongsma, M. Motamedi, WF March, F. Hendrikse. "Kwantitatieve bepaling van de hydratie van het anterieure stroma in *in vivo* konijne corneas na de-epithelialisatie". Nederlands Oogheelkundig Gezelschap, Groningen, 1997.

NJC Bauer, JP Wicksted, FHM Jongsma, WF March, F. Hendrikse, M Motamedi. "Non-invasive assessment of the hydration gradient across the cornea using scanning confocal Raman spectroscopy". *Invest. Ophthalmol. Vis. Sci.* 1998; 39(4): 831-835.

NJC Bauer, M. Motamedi, JP Wicksted, WF March, F. Hendrikse. "Confocale Raman Spectroscopie voor Farmacokinetische Bepalingen in het Oog". Nederlands Oogheelkundig Gezelschap, Maastricht, 1998.

NJC Bauer, M. Motamedi, JP Wicksted, F. Hendrikse, WF. March. "Non-invasive ocular pharmacokinetics via Raman spectroscopy". *ARVO Abstract. Invest. Ophthalmol. Vis. Sci.* 1998; 39(5):

NJC Bauer, M. Motamedi, JP Wicksted, F. Hendrikse, WF. March. "Confocal Raman Spectroscopy For the Non-Invasive Assessment of Ocular Pharmacokinetics". 16th Annual Meeting on Biomedical Engineering (1998). University of Houston, Texas, USA.

NJC Bauer, M Motamedi, JP Wicksted, WF March, CAB Webers, F Hendrikse. "Non-Invasive Assessment of Ocular Pharmacokinetics using Confocal Raman Spectroscopy". *J Ocular Pharm. Ther.* 1999; 15(2): 123-134.

NJC Bauer, F. Hendrikse, WF. March. *"In vivo* Confocal Raman Spectroscopy of the Human Cornea". *Cornea* 1999; 18: 483-488.

JP Wicksted, NJC Bauer, RJ Erckens, FHM Jongsma, EE Smit-Kepel, M Motamedi, Wayne F March. "Noninvasive Assessment of Ocular Tissue using Confocal Raman Spectroscopy". The International Society for Optical Engineering. *Biomedical Applications of Raman Spectroscopy*. SPIE January 1999; vol. 3608: pp. 111-122.

NJC Bauer. Potential Applications of Confocal Raman Spectroscopy in Ophthalmology. Thesis. University of Maastricht, The Netherlands, December 1999.